A FEEDBACK MODEL FOR THE EVALUATION OF THE ADAPTIVE CHANGES TO TEMPORAL MUSCLE ACTIVATION PATTERNS FOLLOWING POSTURAL DISTURBANCE

A Dissertation
Presented to
The Academic Faculty

by

Torrence David Jesse Welch

In Partial Fulfillment
of the Requirements for the Degree
Doctor of Philosophy in the
Wallace H. Coulter Department of Biomedical Engineering

Georgia Institute of Technology
August 2008

A FEEDBACK MODEL FOR THE EVALUATION OF THE ADAPTIVE CHANGES TO TEMPORAL MUSCLE ACTIVATION PATTERNS FOLLOWING POSTURAL DISTURBANCE

Approved by:

Dr. Lena H. Ting, Advisor
Department of Biomedical Engineering
Georgia Institute of Technology / Emory University

Dr. Eric H. Schumacher
School of Psychology
Georgia Institute of Technology

Dr. Young-Hui Chang
School of Applied Physiology
Georgia Institute of Technology

Dr. Kurt A. Thoroughman
Department of Biomedical Engineering
Washington University in St. Louis

Dr. T. Richard Nichols
School of Applied Physiology
Georgia Institute of Technology

Date Approved: June 19, 2008

To those with the courage but not the means to pursue their dreams
Ingenium res adversae nudare solent, celare secundae

ACKNOWLEDGEMENTS

There are many people that have been instrumental to my successes thus far. I would be remiss not to take this opportunity to express my gratitude for their undying support and encouragement through the long and difficult journey toward my achievements, both in academia and in life.

I would first like to thank several members of my family, without whom I would not be who I am today. First, my mother, Carol Welch, for all the sacrifices she has made to put me in the position to achieve each and every one of my goals. And to my father, Carlyle Welch, who has taught me the value of hard work, how to be both a strong and loving man, and not to take life so seriously. Together, their never-ending love and pride in me has been a constant source of motivation for which I am infinitely grateful. Also, to my grandparents, Susie and Thomas Perkins, who have played a very important role in molding me into a strong yet humble man. I am lucky to have been able to share so much of my life with such loving and supportive grandparents and am glad to still have you both in my corner. To my aunt Doris Perkins and uncles Wayne and Kelvin Perkins for always being there for me, whether it was with a hug and smile, a hand-me-down game to test my wit, or a timely check in the mail (got to love those!). I would also like to thank my young nephew, Chance Dabney, who has taught me so many life lessons at such a young age. His youthful energy and richness in spirit and love has been a renewed source of inspiration to me. I only hope that he will enjoy the same support and nurturing that I was given, so that he can have the opportunity to fulfill his dreams and live to his full potential. Thanks to Zach Stovall, a dear friend of nearly 10 years, and his parents

Charlene and Jack Stovall, who have served as my second family. Your interest and pride in my successes have been a wonderful gift to me and I am glad to have you in my life. I would also like to thank our family friend, Bill Slaughter, for his financial support during the early years of my college training. Without his kind gift to our family, I would not have been able to pursue my education at such an excellent institution as Tulane University.

There are so many colleagues whose insight and brilliance have served to guide and inspire my work over the past five years. First, I thank my wonderful advisor, Lena Ting, for all of her guidance, both academic and personal. Your intelligence is awe-inspiring and you have really made a difference in the way that I think about and view the world around me. I appreciate the individualized care that you have given me, as I developed as a scientist, engineer, and thinker. You have taught me many lessons that I will carry throughout my lifetime and for that I am forever grateful. To my thesis committee members: Young-Hui Chang, Richard Nichols, Eric Schumacher, and Kurt Thoroughman, for their critical evaluation and intellectual support of my work – it has been an honor to work with you all. To Charles Isbell, who has been a mentor and friend. Thanks for the lessons you have taught and the insights you have given me regarding the academic process. In addition to these, your merciless beatings at racquetball have taught me invaluable lessons in humility. To Gelsy Torres-Oviedo, who has served as a peer mentor to me throughout my graduate career: it has really been a delight to grow as a scientist with you and to share in both my frustrations and excitements by your side. I have truly missed your smiling face and sharing "fiesta fingers" with you this last year of my graduate studies. I am so very proud of your growth and successes as a scientist and

wish you all of the best in your very promising future in academia. I would also like to thank Keith van Antwerp, who has served as both a colleague and friend throughout my studies: you may never know how much you have changed my outlook on life, my achievements, and my potential for greatness. I thank you for serving as a source of personal inspiration to me and wish you the best of luck and success in your graduate career.

I would like to thank Daniel Lockhart for his role in developing the feedback control model that has been at the center of my PhD work. I was always quite impressed with the intelligence you shared with us during our two years together. It is unfortunate that we were not able to continue our academic relationship, as I had looked forward to working together as a team on the work I present here in this dissertation. I would also like to thank my undergraduate assistants: Ravi Parikh, for his help in developing some critical pieces of kinematics software for my analyses; and C'iana Barker, for her help in determining the onset of muscle activation in countless numbers of EMG waveforms. Finally, I would like to thank the many members of the Neuromechanics Lab, past and present, for their academic support and friendship: Nate Bunderson, Stacie Chvatal, Alex Koenig, Lucas McKay, Kyla Ross, Seyed Safavynia, Jevin Scrivens, Kartik Sundar, Subina Surendran, Yi-Ying Tsai, Hari Trivedi, and Jasper Yen. Also, the members of the Laboratory for Neuroengineering at Georgia Tech and my classmates in the Department of Biomedical Engineering at Georgia Tech and Emory. I have enjoyed working with you all and cannot wait to see the amazing things that you will all contribute to the worlds of science and engineering.

With the stresses of school and the pressures and frustrations of scientific research, I am thankful to have had so many amazing friends by my side to ease my mind and keep me sufficiently entertained. To my Tulane crew: Sarah Blascovich, Eric Bond, Ron Bucca, Barrett Conrad, Heather Dubois, Jason Ford, Mike Glick, Lauren Halloran, Caroline Hecker, Steve Karlsgodt, Darren McCarley, Pete McGee, Rich Miller, Job Patterson, Ross Pine, Phil Romero, Ashley Schneider, Bill Serotta, John Suarez, Andrew Wascom, and the many others. My times with all of you have been irreplaceable. Thanks for sharing the best years of my life with me. All of your accomplishments continue to astonish me and I cannot wait to share in our successes together. To my past roommates, Scott Robinson and Neal Weinrich, for keeping the first four years of graduate school interesting while we lived together; you guys hold a special place in my heart and have really made some of my harder times here much easier to bear. You had to put up with a lot of crap from me over the years. For that and everything you continue to do for me, I am truly grateful. To my current roommates: Brock Wester and Blaine Zern. Brock, your tireless work ethic, go-get-em attitude, and willingness to do anything for anyone make you a truly amazing person. I know you will be successful in anything you do and I wish you the best. Blaine, thanks for never cutting me any slack; whether it was your intent or not, you have motivated me more than you can know. To Anjali Shah, who has been a great source of support and friendship: keep pressing on towards freedom! And to the many other friends I have met in Atlanta – Randy Ankeny, AJ Bernardi, Marisa Bramlett, Andres Bratt-Leal, Rich Carpenedo, Sean Coyer, Eric Deutsch, Craig Duvall, Paul Evans, Maria Forline, Seth Gazes, Tiffany Geyer, Angie Gulino, Claire Honeycutt, Reese Jones, Jeremy Lim, Angela Lin, Katie Maeillaro, Spencer Olsen, Christina O'Neal, Michael

Romeo, Sarah Pollack, Andrew Smith, Erin Spinner, Brooks and Paige Stout, Sean Sullivan, Miyu Toyoshima, and the many others: thanks for making my days of graduate school fun and exciting. I treasure the friendships that I enjoy with all of you and hope they last a lifetime.

And finally, I would like to thank my close friend of 17 years, Ebony Spikes. You know me so very well, often better than I know myself. Through our ups and downs, I know that you truly care for me, and I for you, and your support for me has been unfailing. You have always been honest with me, even when I was less than true to myself, and for that I am ever so grateful. Thanks for all the love and prayers you have sent my way over the years – they have truly made the difference! You are truly the most intelligent and caring person I have ever met and I cannot wait to see the greatness that is in store for you.

TABLE OF CONTENTS

LIST OF TABLES

Page

LIST OF FIGURES

Page

SUMMARY

Humans perform complex sensorimotor tasks, such as walking on uneven terrain, in a seemingly effortless manner. However, even simple voluntary tasks, like lifting the arm to shake hands, require intricate adjustments to maintain balance. With experience, humans learn to produce the appropriate patterns of muscle activity necessary to maintain balance during everyday activities, as well as highly specialized motor tasks. Here, I investigated the neural feedback mechanisms controlling the formation of the muscle activity used during balance tasks.

I hypothesized that humans use feedback from on-going balance perturbations to establish their muscular responses. Specifically, I investigated center-of-mass (CoM) kinematics as a control signal for the formation of these muscle activation patterns. Using an inverted pendulum model under delayed feedback control, I both reconstructed the temporal EMG patterns measured during experimental perturbations and predicted the optimal EMG patterns for responding to the same perturbations. By modulating four feedback parameters, this feedback law accounted for 91% of the variability in all experimentally-recorded EMG patterns – regardless of the mechanical action of the muscle or the response strategy chosen by the subject.

To investigate the changes in postural control during motor learning, I used this feedback model to characterize responses while naïve subjects adapted to repetitive unidirectional and reversing perturbations. By adjusting feedback gains related to CoM velocity and displacement, subjects adapted their muscle activity to improve control over the CoM for both perturbation types. Though subjects were unable to use anticipatory

strategies to reduce muscle onset latency or to mute inappropriate responses to reversing perturbations, more subtle feedforward adjustments to feedback-mediated postural responses were evident. With experience, subjects adapted their postural responses toward the optimal solution.

The results of this work, when combined with on-going studies of muscle synergies, will provide a powerful tool for investigating the consequences that result from the changes in spatiotemporal muscle activity associated with aging, neurological dysfunction, musculoskeletal injury, and specialized training programs. This quantitative knowledge is critical to the development of diagnostic tools for balance and movement disorders, as well as for the design of effective interventional therapies, bipedal robots, and neural prostheses.

CHAPTER 1

INTRODUCTION

The execution of most motor tasks requires the intricate control of muscles throughout the body to maintain the proper balance and postural configuration. During postural tasks, the spatial and temporal patterns of muscle activation change instantaneously when the biomechanical constraints are altered, for instance when the size of the base of support is reduced (Horak and Nashner 1986) or when the use of hands is allowed (Jeka and Lackner 1994). However, when adapting to a novel environment, such as standing on a moving platform, a slower change over time of these muscle activation patterns is observed (Horak 1996). How does the nervous system orchestrate this exquisite muscular coordination? What signals are used to detect the ongoing changes in the postural environment? How does the nervous system fine-tune its strategy to maintain postural stability with experience or training?

When a balance perturbation is incurred, as in a support-surface translation where the floor is moved beneath the feet, an automatic postural response (APR) is evoked to maintain the center-of-mass (CoM) within the limits of the base of support. During this response, the body sways in the opposite direction of the perturbation. This postural sway can be confined to occur about the ankle joint alone (the 'ankle' strategy), as in mild perturbations, or about the hip (the 'hip' strategy) in response to more challenging perturbations (Horak and Nashner 1986). These two extreme patterns of postural sway form the boundaries of a continuum of 'mixed' strategies used to recover balance following perturbation (Alexandrov et al. 2001a; Runge et al. 1999). These strategies are

also associated with characteristic patterns of muscle activity, where mechanically-relevant muscles throughout the body are activated in a distal-to-proximal fashion to return the body to an upright and stable configuration.

While muscle activity associated with the APR has been characterized extensively in cats and humans, the neuromechanical basis of its temporal formation remains largely unclear. The muscle activation pattern typical of the APR has been described as consisting of an initial burst of activity followed by an extended plateau region of tonic activity (Diener et al. 1988). In humans, ankle muscle activity associated with the APR occurs at a latency of approximately 100 ms. This timing suggests that, rather than being the result of a spinal reflex, higher-level processing may be involved in the formation of the muscle activation pattern (Diener et al. 1984). However, the onset of initial muscle activity occurs before voluntary control over the response can be feasibly exerted.

Several studies indicate that these reactive muscle activation patterns are related to the characteristics of the applied perturbation, suggesting that task-related feedback may be used to form this muscle activity. For example, the amplitude of the initial burst of muscle activity correlates with perturbation velocity, while the tonic plateau region activity scaled with the total displacement of the perturbation (Diener et al. 1988). Further, antagonist muscles produce consistent muscle activity in response to the decelerating impulse that is similar in timing to that invoked in the agonist by the initial impulse of a postural perturbation (Bothner and Jensen 2001; Carpenter et al. 2005; McIlroy and Maki 1994; Runge et al. 1999); muscle activity between these two impulses is highly variable (Bothner and Jensen 2001). The kinematics of the CoM follow those of platform motion during experimental perturbations, suggesting that the body may track

CoM motion as a feedback signal for adjusting muscle responses to perturbations. However, the individual effects of the perturbation dynamics have often been obscured by the covariation of acceleration and velocity in perturbation paradigms (Maki and Ostrovski 1993a; Szturm and Fallang 1998), possibly resulting from the use of controllers in which only the displacement waveform is specified (Brown et al. 2001). Therefore, in order to test specific hypotheses regarding the use of feedback during postural control, precise control over perturbation dynamics is required to allow the independent specification and modulation of the perturbation characteristics.

Human subjects use both feedback and feedforward mechanisms to help mitigate balance disturbances. Previous studies in cats suggest that delayed feedback of CoM kinematics can robustly reproduce temporal patterns of muscle activation in response to a variety of balance disturbances (Lockhart and Ting 2007). Consistent with this idea, interactions between CoM position, velocity, and acceleration appear to influence temporal patterns of muscle activity in humans through feedback. Both initial leaning about the ankles and natural postural sway prior to perturbation affect the onset and level of muscle activation in ways not predicted by the modification of stretch reflexes by peripheral conditions (Horak and Moore 1993; Park et al. 2005; Tokuno et al. 2006). The resulting effect is a feedforward stiffening of the ankle joint that allows elastic properties of the muscles and gravitational torques to better contribute to resisting disturbances (Shinha and Maki 1996).

Studies of voluntary arm reaching movements also illustrate the interplay between feedback and feedforward mechanisms in the adaptation of voluntary movements. The central nervous system uses internal models of the body's interaction with the external

environment to plan movement trajectories and predict the forces that it will encounter during these movements (Flanagan and Wing 1997; Gandolfo et al. 1996; Lackner and Dizio 1994; Miall et al. 1993; Shadmehr and Mussa-Ivaldi 1994). However, when a novel environment is encountered, this internal model must be updated to account for changes necessary to perform consistent and accurate movements. Subjects use feedback to reduce errors in ongoing movements, however feedback alone is insufficient to eliminate these errors altogether (Hwang and Shadmehr 2005). In addition to these online feedback strategies, subjects use an estimate of errors from previous trials to modify the initial trajectory of the next movement attempt in a feedforward manner (Thoroughman and Shadmehr 1999). These feedforward strategies are thereby included within the internal model, updating subsequent movement plans and the expected sensory information during task performance. This short term learning is more complete when changes in environmental feedback are gradual as opposed to a large, sudden change (Kagerer et al. 1997), and the updates in the mapping between visual and motor representations of space are not easily overridden by conscious effort (Cunningham and Welch 1994).

However, the adaptation of muscle activation during involuntary and reactionary responses, such as the automatic postural response, has not been explored extensively. Initial studies in postural response adaptation have looked at changes to muscle activity in response to repetitive perturbations (Chong et al. 1999; Hansen et al. 1988; Horak et al. 1989; Keshner et al. 1987; Timmann and Horak 1997). These studies indicate a decrease in response magnitude with successive trials, which has been attributed to changes in central set (Horak 1996), consistent with the adjustment of feedback parameters that relate to muscle activity formation. Several feedforward strategies have also been

observed in the response to repetitive perturbations, where subjects make attempts to mitigate the destabilizing effects of expected perturbations by using bracing strategies to prepare for perturbations (Blouin et al. 2003) or making anticipatory adjustments to muscle activity (Carpenter et al. 2005; Horak et al. 1989). A quantitative understanding of the interactions between these feedback and feedforward strategies during the adaptation of the automatic postural response will provide valuable insight into the mechanisms used for postural control and motor control in general.

Through the integration of computer simulations and experimental data analysis, I investigated the neuromechanical control framework used to create the temporal patterns of muscle activation for postural control and how these mechanisms adapt to changing task conditions. In **Chapters 2 and 3**, I identify a feedback loop for human postural control based on delayed feedback of CoM kinematics and demonstrate its robustness to a variety of perturbation dynamics. In **Chapter 4**, I quantify the time course of the adaptation of CoM kinematics and temporal muscle activation patterns during repetitive perturbations. I then use a feedback model of human postural control to describe the changes to the postural control mechanism that are responsible for the adaptive changes to muscle activity.

CHAPTER 2

A FEEDBACK MODEL FOR HUMAN POSTURAL CONTROL

This chapter was originally published as a Report in the *Journal of Neurophysiology*:

Welch TDJ and Ting LH. A feedback model predicts muscle activity during human postural responses to support surface translations. *J Neurophysiol* 99: 1032-1038, 2008.

Abstract

Although feedback models have been used to simulate body motions in human postural control, it is not known whether muscle activation patterns during postural responses can also be explained by a feedback control process. We investigated whether a simple feedback law could explain temporal patterns of muscle activation in response to support-surface translations in human subjects. Previously, we used a single-link inverted-pendulum model with a delayed feedback controller to reproduce temporal patterns of muscle activity during postural responses in cats (Lockhart and Ting 2007). We scaled this model to human dimensions and determined whether it could reproduce human muscle activity during forward and backward support-surface perturbations. Through optimization, we found three feedback gains (on pendulum acceleration, velocity, and displacement) and a common time delay that allowed the model to best match measured electromyographic (EMG) signals. For each muscle and each subject, the entire time courses of EMG signals during postural responses were well-reconstructed

in muscles throughout the lower body and resembled an optimal solution. In ankle muscles, >75% of the EMG variability was accounted for by model reconstructions. Surprisingly, >67% of the EMG variability was also accounted for in knee, hip, and pelvis muscles, even though motion at these joints was minimal. Although not explicitly required by our optimization, pendulum kinematics were well-matched to subject center-of-mass (CoM) kinematics. Together, these results suggest that a common set of feedback signals related to task-level control of CoM motion is used in the temporal formation of muscle activity during postural control.

Introduction

We recently demonstrated that the entire time course of muscle activity following postural perturbations to standing balance in cats could be reproduced using simple feedback model of postural control (Lockhart and Ting 2007). A single-link inverted pendulum model with a delayed-feedback controller reproduced the characteristic temporal patterns of muscle activation throughout the cat hindlimb. Temporal patterns of muscle activation were generated through a combination of center of mass (CoM) acceleration, velocity, and displacement waveforms. These results suggest that a common set of variables related to the task goal of controlling body CoM motion are used to coordinate the activation of proximal and distal muscles during balance control. The goal of this study was to determine whether the same sensorimotor transformation could also be used to describe the temporal patterns of muscle activation observed in human postural responses.

Typically, feedback models of human postural control have reproduced joint torques and segmental motions of the body, but not muscle activity. Using single- or

multi-link inverted pendulum models, they demonstrate that a set of time-invariant feedback gains can explain joint kinematics during either quiet standing or postural responses to perturbations (Alexandrov et al. 2001a; Bortolami et al. 2003; Kiemel et al. 2002; Kuo 1995; Park et al. 2004; Peterka 2000; Runge et al. 1995; van der Kooij et al. 1999). Because feedback loops at each joint are used to generate stabilizing joint torques, these models cannot uniquely specify temporal patterns of muscle activation. Muscles must be explicitly included because the low-pass dynamics of the body introduce redundancy in the temporal domain, whereby different temporal patterns of muscle activation can produce similar kinematic outputs (Gottlieb et al. 1995; Lockhart and Ting 2007).

Evidence suggests that muscle activity during human postural responses is dependent upon acceleration, velocity, and displacement signals, as previously demonstrated in cats. In response to support-surface translations, temporal patterns of muscle activity in humans and cats have a similar rapid initial rise followed by a longer, sustained plateau region (Macpherson et al. 1989). In cats, this waveform is due to CoM acceleration, velocity, and displacement feedback (Lockhart and Ting 2007). Consistent with this feedback model, muscle activity in human postural responses have been shown to be modified by perturbation velocity and total excursion (Diener et al. 1988), smoothness of the initial perturbation trajectory or acceleration, (Brown et al. 2001; Siegmund et al. 2002; Szturm and Fallang 1998), and the deceleration impulse at the end of the perturbation (Bothner and Jensen 2001; Carpenter et al. 2005; McIlroy and Maki 1994).

We hypothesized that the activity of multiple muscles during human postural responses to perturbation is generated by a common delayed-feedback law based on CoM motion. As a first step, we scaled the single inverted-pendulum feedback model used in Lockhart and Ting (2007) to human dimensions (similar to Peterka 2000) and examined whether this model was capable of reconstructing temporal patterns of muscle activation in proximal and distal muscles. We examined forward and backward support-surface perturbations to standing balance that elicited "ankle strategy" responses (Horak and Nashner 1986). We demonstrate that a delayed feedback law on CoM acceleration, velocity, and displacement can reconstruct temporal patterns of both muscle activity and CoM kinematics during postural responses to support surface translations.

Methods

Seven healthy subjects (5 male, 2 female) from the Georgia Institute of Technology student population, aged 19.4±1.4 years (mean±s.d.), participated in the study. The experimental protocol was approved by both the Georgia Institute of Technology and Emory University Internal Review Boards. Subjects stood on two force plates installed on a moveable platform that translated in the horizontal plane. Subjects were instructed to cross their arms at chest-level, look straight ahead, and react naturally to the support-surface perturbations. A set of 20 acclimatization perturbations were followed by a set of 170 randomized forward and backward perturbations of varying peak velocity and acceleration. To test the feasibility of our model in this study, we analyzed responses to forward and backward perturbations of 12 cm total excursion, 25 cm/s peak velocity, and 0.3g peak acceleration. For each subject, five trials from each direction

were collected and averaged. A minimum of 5 minutes seated rest was enforced between each set of 60 perturbations to reduce muscle fatigue.

Platform acceleration and position, and surface EMG from eleven muscles in the legs and trunk were collected at 1080 Hz, synchronized with body segment kinematics collected at 120 Hz (Figure 2.1A). Platform signals were low-pass filtered at 30 Hz (3^{rd} order zero-lag Butterworth filter). EMGs were collected from the following muscles on the right side of the body: TA, tibialis anterior; MG, medial gastrocnemius; SOL, soleus; VLAT, vastus lateralis; RFEM, rectus femoris; SEMB, semimembranosus; SEMT, semitendinosus; BFLH, long head of biceps femoris; BFSH, short head of biceps femoris; ES, erector spinae; RA, rectus abdominis. Raw EMG signals were high-pass filtered at 35 Hz (3^{rd} order zero-lag Butterworth filter), demeaned, half-wave rectified, and low-pass filtered at 40 Hz (1^{st} order zero-lag Butterworth filter). EMG signals were then normalized to the maximum EMG observed in each muscle over all conditions for each subject. Body segment kinematics were derived from a custom bilateral Helen Hayes 25-marker set that included head-arms-trunk (HAT), thigh, and shank-foot segments. Center of mass motion was calculated from kinematic data as a weighted sum of segmental masses (Winter 2005).

Reconstruction of EMG Using a Feedback Control Model

We determined whether our feedback model could reproduce the time course of EMG signals in each subject. The model consisted of a single-link inverted pendulum, with a point mass *m* (equivalent to each subject's mass) and length *h,* (equal to the height of each subject's CoM during quiet standing) (Figure 2.1B). Disturbance torques calculated from experimentally-recorded platform accelerations were applied at the ankle

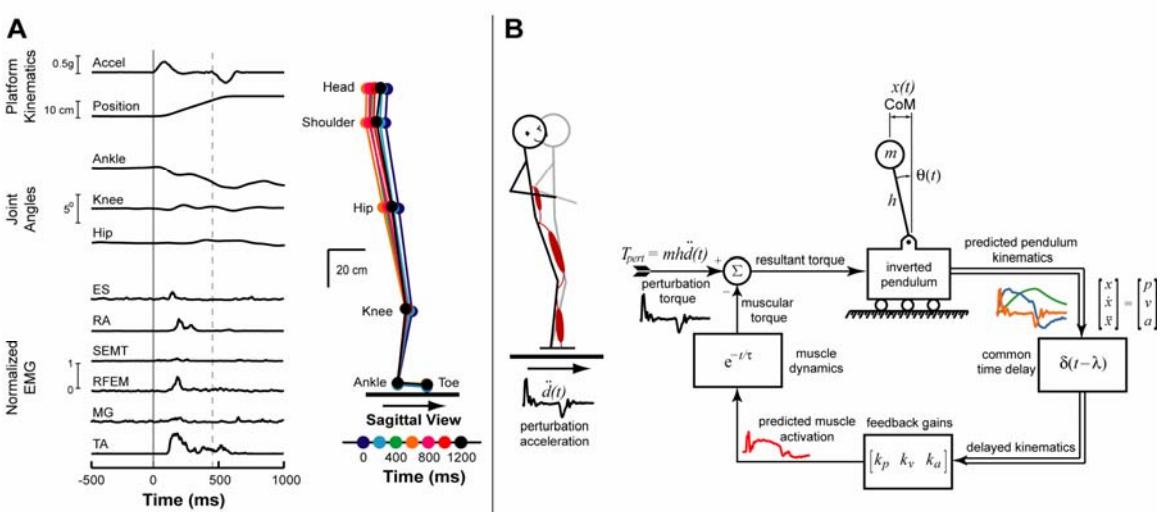

Figure 2.1 Example postural response, modeled as an inverted pendulum under delayed-feedback control. A) In response to a forward support-surface perturbation, the primary joint motion occurred at the ankle joint. Muscles throughout the body were activated in a coordinated fashion to counteract the disturbance (left). The original postural configuration was typically restored within one second of perturbation onset (right). **B)** The standing human was modeled as an inverted pendulum that was perturbed with a torque based on recorded platform acceleration [$\ddot{d}(t)$]. To generate the reconstructed EMG activity, pendulum displacement, velocity, and acceleration (p, v, a) were subject to a common time delay (λ) and feedback gains on each channel (k_p, k_v, k_a). The reconstructed EMG signal was then passed through a first-order muscle model to generate the response torque to counteract the perturbation.

to model the effect of support-surface perturbations (Lockhart and Ting 2007; Peterka 2000). Delayed feedback of horizontal CoM trajectories [displacement, *p(t)*; velocity, *v(t)*; and acceleration, *a(t)*] were used to stabilize the inverted pendulum (Figure 2.1B). EMG reconstructions (EMG_p) were taken as the output of the feedback controller, which was a linear combination of the weighted horizontal CoM kinematic trajectories at a common neural transmission delay (λ):

$$EMG_p = k_p p(t-\lambda) + k_v v(t-\lambda) + k_a a(t-\lambda). \quad (1)$$

Each EMG reconstruction was half-wave rectified and converted to a muscle torque using a first-order muscle model with a 40 ms time constant (He et al. 1991; Lockhart and Ting 2007).

For each muscle in each subject, the feedback gains (k_p, k_v, k_a) and delay (λ) that best matched the EMG reconstruction to the measured EMG signal were found. We used an optimization (MATLAB, *fmincon.m*) to find the values of k_i and λ using the following cost function:

$$\min_{K \in G} \left\{ J = E\left(\int_0^{t_{end}} \left[{e_m}^T \mu_s e_m + \max\left(\mu_m \left| e_m \right| \right) \right] dt \right) + We_x\left(t_{end} \right) \right\}. \quad (2)$$

The first term penalized the error between the reconstructed and measured EMG signal over time as represented by the vector e_m with weight μ_s. The second term penalized the maximum deviation between the reconstructed and measured EMG signals at any single point in time with weight μ_m. The final term penalized the final state of the inverted pendulum if it differed from that of the experimental subject (*i.e.*, upright configuration) with weight *W*. Note that this differs from the formulation of Lockhart and Ting (2007) in that only the EMG pattern, and not the CoM kinematics, was matched. Feedback gains were restricted to have values between 0 and 100, and the delay was restricted to between 60 and 250 ms. We assessed the goodness of fit between reconstructed and measured EMG signals using both the coefficient of determination (r^2) and the uncentered Pearson's coefficient of determination (variability accounted for; VAF).

Recorded and reconstructed EMG patterns were compared to those predicted by an optimal control model (Lockhart and Ting 2007). Using a controller design similar to that of the linear quadratic regulator (He et al. 1991), this delayed quadratic regulator (DQR) model determined gains for CoM kinematic feedback channels, without *a priori* knowledge of recorded EMG, through the use of a quadratic cost function and time-

delayed feedback. Feedback gains on delayed CoM kinematics (k_i) were optimized using the following cost function:

$$\min_{K \in G} \left\{ J = E\left[\int_0^{t_{end}} \left(x^T Q x + \rho u \right) dt + \Omega x\left(t_{end}\right) \right] \right\}. \quad (3)$$

The first term penalized deviations from zero of the pendulum position, velocity, and acceleration (where $x = \begin{bmatrix} p & v & a \end{bmatrix}^T$) with weights $Q = \begin{bmatrix} 0.05 & 50 & 1 \end{bmatrix}$. The second term penalized EMG activation level (u) with weight ρ = 20, requiring the minimum possible level of muscle activation to achieve the postural task. The final term penalized final pendulum configurations that were not upright with weight Ω. Because the optimization process consistently selected the minimum allowable feedback delay, this delay was set to 100 ms for all subjects to allow the calculation of an intersubject average of the optimal postural control solution and to facilitate qualitative comparisons with recorded and reconstructed EMG patterns.

Results

Temporal patterns of muscle activity throughout the leg in both forward and backward perturbations were reconstructed by our feedback model in all subjects. Reconstructed EMG activity in ankle muscles TA and MG were well-matched to measured EMG activity in forward and backward perturbations, respectively (VAF > 0.75; Figures 2.2A-B). Notable variations in the temporal patterns of muscle activity were observed across subjects; these variations were accounted for by differences in feedback gains (Figure 2.3D). Still, ankle muscle activity in all subjects resembled the optimal control solution although an exact match was not achieved by any subject (cf. Figures 2A-B, DQR Prediction; TA: $r^2 = 0.53 \pm 0.16$, VAF = 0.73 ± 0.09; MG: $r^2 = 0.45$

± 0.13, VAF = 0.68 ± 0.08). Although the ankle strategy responses evoked produced little knee or hip motion (Figure 2.1A), muscle activity in biomechanically-relevant proximal muscles was also well-described by the feedback model (VAF > 0.67 across all muscles and subjects; Figure 2.2C). The time course of experimentally-recorded CoM kinematic trajectories were similar to the motion of the inverted pendulum model controlled by the reconstructed EMG pattern (Figure 2.3C). This was surprising because we only explicitly required the temporal EMG patterns, and not kinematics, to match the experimentally-recorded data, suggesting that the kinematics of the body are indeed encoded in the pattern of muscle activation used by the nervous system for postural control.

A decomposition of the reconstructed EMG into contributions from each feedback component demonstrates that the initial burst region was predominated by acceleration feedback, while velocity and displacement feedback contribute to the plateau region of muscle activity (Figure 2.3B). Acceleration feedback from the deceleration of the platform also contributed to the termination of muscle activity (solid gray, Figure 2.3B). The mechanical dynamics of the pendulum defined the temporal separation of the various feedback contributions; addition of independent delays for each channel had no significant effect on the model reconstructions [TA: $\Delta r^2 = 0.00$ ($p = 0.80$), $\Delta VAF = 0.01$ ($p = 0.31$); MG: $\Delta r^2 = 0.05$ ($p = 0.11$), $\Delta VAF = 0.02$ ($p = 0.10$)].

Acceleration feedback was required to reconstruct EMG activity using physiological delays. When acceleration feedback was removed, delays shorter than the 55-ms latency of the stretch response during postural perturbations (Diener et al. 1984) were required (intersubject range=10−60 ms; Figure 2.3D). Without acceleration feedback, the early EMG activity in the initial burst and plateau regions, including the

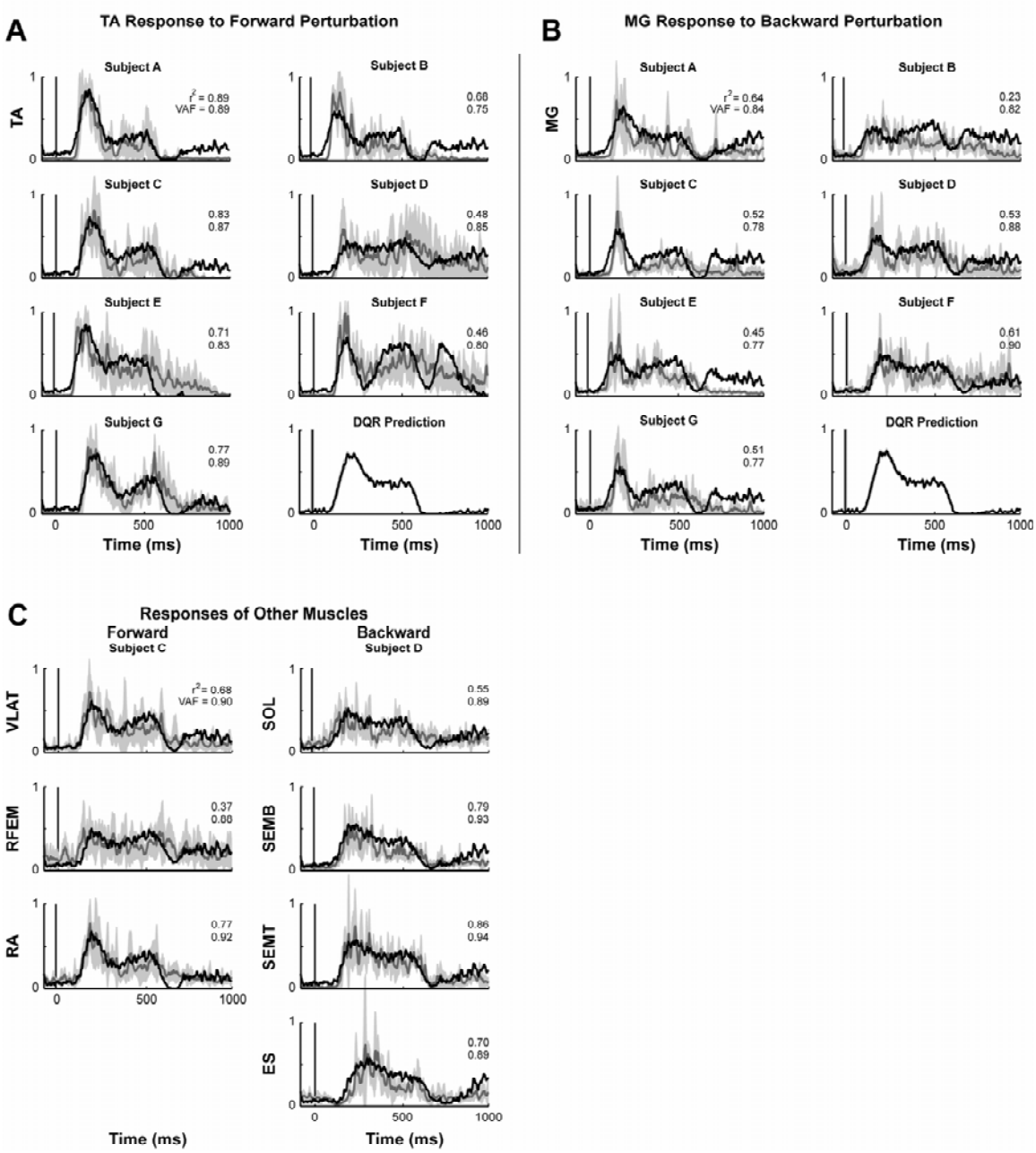

Figure 2.2 Averaged time courses of recorded (solid gray) and reconstructed (solid black) EMGs during postural responses. Gray shaded regions indicate one standard deviation from the mean recorded EMG for each muscle across five trials. **A)** TA EMG signals in response to forward perturbations across all subjects are presented with the average optimal control solution (DQR Prediction). Significant variations in the temporal patterns of TA EMGs were observed across subjects; however, each response resembled the optimal DQR prediction. The feedback model was able to reproduce these variations with >75% VAF by choosing a slightly different set of feedback gains and delay for each subject. **B)** Similarly, MG EMG signals in response to backward perturbations were reconstructed with >77% VAF across all subjects and resembled the DQR prediction. **C)** Additionally, EMG signals from knee, hip, and pelvis muscle that were active during either forward or backward perturbations were also reproduced with >67% VAF across all subjects.

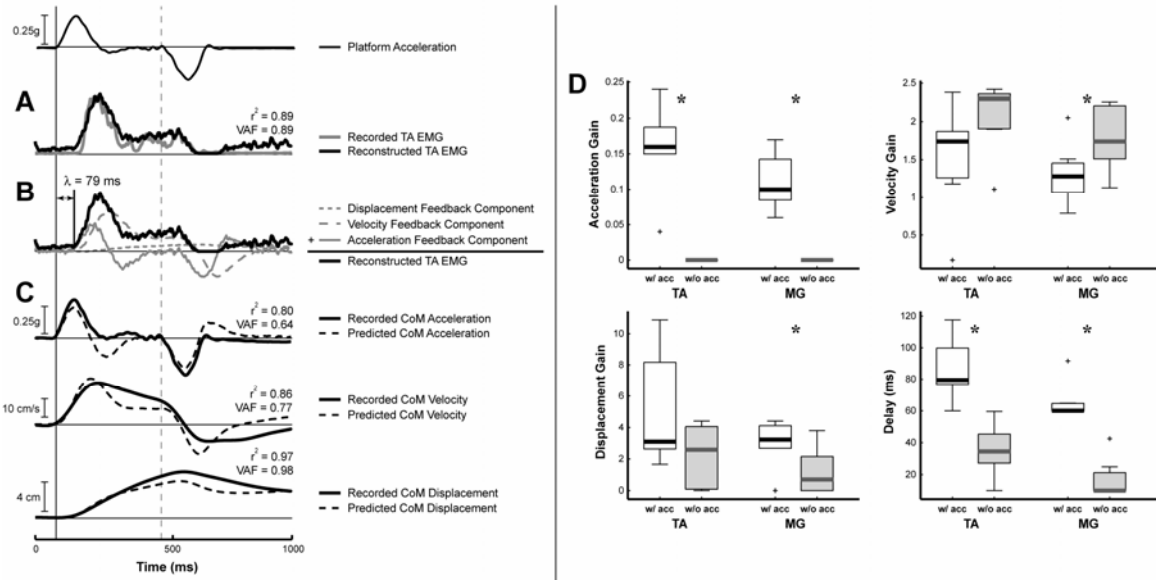

Figure 2.3 Contributions of each feedback component to the time course of EMG depend upon muscle- and subject-specific feedback gains. A) Recorded (gray) and reconstructed (black) TA EMG signals for Subject A. **B)** Decomposition of the reconstructed EMG signal (black) into individual feedback components from acceleration feedback (gray line), velocity feedback (gray dashed line), and displacement feedback (gray dotted line). Acceleration feedback contributes to the rapid initial rise in EMG activity. Velocity and displacement feedback contribute to later activity during the plateau region. **C)** Recorded (solid line) and predicted (dashed line) CoM acceleration, velocity, and displacement trajectories are also similar. This was surprising, because our optimization only explicitly required temporal patterns of EMG signals to be matched between the model and experiment. These results suggest that CoM kinematics are indeed used by the nervous system in generating EMG signals. The time course of each feedback component's contribution to the reconstructed EMG is determined by these CoM kinematic trajectories after a delay (λ). The mechanical dynamics of the pendulum thus define the temporal separation of the contributions from each feedback channel, illustrated in **B**. The amplitude of the contributions from each feedback channel depends upon the magnitude of the feedback gains, which varies across muscles and subjects. **D)** Variations in feedback gains for TA and MG muscles across subjects (white boxes) when acceleration feedback was included. Boxes delimit the middle 50% of the data, with the center indicating the median value (thick black line). Whiskers delimit the full range of the data, excluding outliers (indicated with a +). When acceleration feedback was removed from the model (gray boxes), the remaining model parameters changed (* represents significant difference at $p<0.05$), resulting in modest or insignificant changes in goodness-of-fit. However, the range of the delays required to reproduce the EMG signals without acceleration feedback was reduced to durations shorter than the 55-ms short-latency stretch response during postural perturbations, and were therefore not physiological.

initial slope of the response, were under-predicted (data not shown). Further, the goodness-of-fit between reconstructed and recorded EMGs was reduced in TA [$\Delta r^2 = -0.14$ ($p = 7\times10^{-4}$); $\Delta VAF = -0.07$ ($p = 0.006$)], but not MG [$\Delta r^2 = -0.05$ ($p = 0.42$); $\Delta VAF = -0.03$ ($p = 0.13$)]. In both cases, however, the reconstructed EMGs without acceleration feedback were often insufficient to maintain the pendulum in an upright configuration (data not shown).

Discussion

Our results demonstrate that the neural mechanisms generating temporal patterns of muscle activity for postural control in humans can be described by a feedback transformation from body kinematics to EMG. For ankle-strategy responses, an inverted pendulum model of human posture reproduced muscle- and subject-specific muscle activation patterns throughout the lower body using delayed feedback of acceleration, velocity, and displacement of the pendulum. The pendulum motion also matched recorded CoM kinematics, although not explicitly required by the optimization. Our simulation therefore provides a mechanistic model that functionally validated the sensorimotor transformation between CoM motion and muscle activity. These results suggest that a common set of feedback signals related to the task-level control of CoM motion are indeed used in the temporal formation of muscle activity during postural control.

The nervous system may take advantage of the naturally-occurring physical relationships between acceleration, velocity, and displacement to provide feedback control of the CoM without need for feedforward control mechanisms. Previous studies have observed a positive, phase-leading correlation between muscle activity during quiet

stance and CoM motion, suggesting the use of predictive, feedforward control (Fitzpatrick et al. 1996; Fitzpatrick et al. 1992; Gatev et al. 1999). The phase-lead characteristics of acceleration feedback may serve to explain this observation in the context of feedback control. In our model, the contribution of acceleration feedback is fully reflected in the muscular response before significant displacement-related information becomes available. Moreover, the acceleration component of the reconstructed muscular response leads CoM displacement, but occurs after the CoM acceleration induced by the perturbation. The phase lead of acceleration feedback with respect to CoM displacement in our simulations was approximately 135 ms, consistent with the 100–250 ms phase lead observed experimentally for high frequency postural sway (Fitzpatrick et al. 1992). The early burst of muscle activity during postural responses to perturbation, here shown to arise from acceleration feedback, has previously been attributed to a feedforward component (Diener et al. 1988). Consistent with our model, however, the middle portion of the response varies with changes in perturbation velocity, while the late response is affected by changes in perturbation displacement (Diener et al. 1988).

Several other studies provide support for acceleration feedback in postural control. Postural responses have been shown to scale with perturbation acceleration in the neck muscles of seated subjects (Siegmund 2004; Siegmund et al. 2002) and in perturbations to arm movements (Soechting and Lacquaniti 1988). In standing posture, muscle onset latency and total ankle moment are also affected by perturbation acceleration (Brown et al. 2001; Siegmund et al. 2002; Szturm and Fallang 1998). Further, the rate of muscle activity onset during perturbations to treadmill walking has

also been related to perturbation acceleration (Dietz et al. 1987). Several studies during standing postural responses suggest that the termination of the postural response results from feedback on the deceleration impulse (Bothner and Jensen 2001; Carpenter et al. 2005; McIlroy and Maki 1994). Consistent with this finding, in our model, termination of the postural response can also be attributed to the delayed effects of the deceleration impulse (Figure 2.3A).

Our study supports the idea that a small set of variables related to task-level goals are used to coordinate multiple muscles throughout the body during postural control and other movements. Activity in muscles crossing the hip, knee, and ankle joints all exhibited temporal patterns that were explained by combinations of the CoM motion as modeled by an inverted pendulum. Although the hip and knee joints did not undergo appreciable joint angle changes (Figure 2.1A), proximal muscle activity may be necessary to minimize joint motions from interaction torques generated by ankle muscle activity (van Antwerp et al. 2007; Zajac and Gordon 1989). Therefore, whenever the ankle muscles are activated, the proximal muscles must also be activated to maintain the postural configuration. We propose that a muscle synergy defining consistent spatial patterns of multiple muscle activity for ankle-strategy responses (Torres-Oviedo and Ting 2007) may be temporally regulated by feedback signals. The spatiotemporal patterns of muscle activation for postural control could thus be specified by defining a constant set of gains on CoM acceleration, velocity, and displacement for each muscle.

While we have demonstrated the feasibility of task-level feedback in explaining ankle strategy responses to support surface translations, more complex biomechanical models may be necessary to represent the full range of responses—ankle, hip, and mixed

strategies—in the postural control suite (Alexandrov et al. 2001b; Horak and Nashner 1986; Runge et al. 1999). This is especially pertinent for modeling muscular responses to backward translations, as well as to support surface rotations and upper-body perturbations, where hip-strategy responses produce significant joint motions and muscle activation about the proximal joints (Jo and Massaquoi 2004; Runge et al. 1999). Because the hip-strategy response has a distinct muscle synergy pattern that can be decomposed from a mixed response (Torres-Oviedo and Ting 2007), it is possible that the hip-strategy response is also regulated by a task-level feedback controller that is independent of the ankle-strategy controller.

Comparisons of experimentally-recorded EMG with an optimal control solution suggest that the postural responses of our human subjects, while similar to the optimal solution, may not have completely achieved the optimal feedback pattern for responding to support-surface translations during the course of our experiment. In contrast, cats subjected to a similar perturbation protocol exhibited EMG patterns that matched the optimal solution as predicted by the DQR model (Lockhart and Ting 2007). The cats underwent a rigorous training regimen in which they learned to stand on the perturbation platform over the course of several weeks or months (cf. Macpherson et al. 1987). Our human subjects, however, were completely naïve to postural perturbation studies and each completed the experimental protocol in less than one hour. We hypothesize that, during their training regimen, the cats may have slowly adapted their muscular responses toward the optimal control solution for the task. We therefore predict that, with training, human muscle activity during postural responses may more closely match the optimal feedback pattern predicted by our DQR model. Alternately, it may be possible that each

human subject used a different set of optimality criteria, which could be modeled by varying the weights in the cost function (Qu et al. 2007), or changing the components of the cost function altogether.

Our feedback model may provide a low-dimensional framework for understanding variability in muscle activation patterns during postural control (Ting 2007). Extensive intersubject variability in temporal patterns of muscle activity may be accounted for by varying only three feedback gains (Figure 2.2 A-B). Rather than performing a point-by-point adjustment of neural activity over time, the CNS may adjust gains to each feedback channel. This differential weighting of feedback channels may explain changes in muscle responses due to habituation and changes in central set (Horak et al. 1989). For example, when the interval between acceleration and deceleration of translation perturbations is short and predictable, subjects anticipate the deceleration timing (Carpenter et al. 2005; McIlroy and Maki 1994). The advance in the timing of response termination might occur due to changes in CoM velocity and displacement feedback gains, which alter the time at which the acceleration feedback triggers the offset of EMG activity.

CHAPTER 3

A FEEDBACK MODEL EXPLAINS THE SCALING OF HUMAN POSTURAL RESPONSES

This chapter is in preparation for submission to the *Journal of Neurophysiology*:

Welch TDJ and Ting LH. A feedback model explains the differential scaling of human postural responses to perturbation acceleration and velocity (in prep).

Abstract

While the neural basis of balance control remains unknown, previous studies suggest that a feedback law on center-of-mass (CoM) kinematics is used in the temporal patterning of muscle activity during human postural responses. We hypothesized that this feedback law can robustly describe the changes to muscle activity that occur with changing perturbation characteristics. The CoM motion of subjects was experimentally modulated using anterior-posterior support-surface translations of varying peak acceleration and velocity. EMG was examined for several muscles of the trunk and lower limbs to identify the effects of perturbation characteristics on the time course of muscle activity. Using an inverted pendulum model under optimal feedback control, we predicted the effects of perturbation characteristics on optimal EMG response patterns. Consistent with optimal model predictions, the initial burst of muscle activity scaled linearly with peak acceleration, while the tonic 'plateau' region scaled with peak velocity. Because EMG for all subjects/conditions did not exactly match the optimal solution, two

data-matching models were used to further evaluate the robustness of the feedback law. The first model used the predicted kinematics of an inverted pendulum model to reconstruct recorded EMG. The second model directly reconstructed EMG using recorded CoM kinematics. By adjusting four parameters related to CoM kinematics, these models successfully reconstructed experimentally-recorded EMG, accounting for 91% variability in all EMG patterns across subjects, muscles, and conditions. These results suggest that the CNS uses an invariant feedback law to develop the entire time course of muscle activity for a variety of postural disturbances.

Introduction

The mechanisms responsible for the formation of muscle activity for postural control and the modification of these muscular patterns with changing task conditions are not well understood. Few studies have examined the entire time course of temporal patterns of muscle activation. Previous work has primarily focused on descriptive measures, such as mean electromyogram (EMG) level over fixed time windows and EMG onset/offset latencies, to quantify the changes in muscular responses due to perturbation. A theoretical framework for investigating the temporal generation of muscle activity patterns during postural responses and the variability in these patterns across subjects and trials would facilitate an understanding of the neural mechanisms mediating the observed variations in postural responses and provide clues regarding the transformation from sensory information to motor output during postural tasks. Such a framework would also allow the development of testable hypotheses regarding how EMG patterns should change under different experimental conditions (*e.g.*, variations in perturbation characteristics, adaptation/learning, and neuromuscular impairment).

We recently demonstrated that a feedback law could quantitatively describe the sensorimotor transformation between perturbation characteristics and muscle activation patterns in normal and sensory-loss cats (Lockhart and Ting 2007), as well as in healthy human adults (Welch and Ting 2008). When applied to a single-link inverted pendulum model, the temporal patterns of EMG during ankle strategy responses were reconstructed as the weighted sum of center of mass (CoM) acceleration, velocity, and displacement waveforms with a common time delay. By modulating four feedback parameters, we successfully reconstructed a wide variety of muscle activation patterns, both between subjects and muscles. Further, without explicit specification, the model accurately predicted the temporal characteristics of CoM acceleration, velocity, and displacement, which arise due to the combined effects of the perturbation itself and the neural feedback mechanism.

This feedback law predicts that changes in CoM kinematics during perturbation would modulate specific, localized changes in muscle activity during the time course of the postural response. Model simulations suggested that the initial burst of EMG and the termination of the muscular response were predominated by feedback of CoM acceleration, while velocity and displacement feedback acted upon the extended activity of the plateau region. Therefore, the model predicts that altering the perturbation acceleration waveform should directly modulate the shape of the initial burst and the duration of the postural response. Similarly, altering perturbation velocity should affect the magnitude of later activity during the plateau region of the response.

The perturbation-dependent changes in the temporal features of muscle activation patterns previously described during postural disturbances are consistent with these

model predictions. For example, the initial EMG burst amplitude scales with perturbation velocity, while the tonic "plateau" region scales with perturbation displacement (Diener et al. 1988); these authors did not control or explore the effects of perturbation acceleration on muscle responses. However, EMG amplitudes also depend on the smoothness of the initial perturbation trajectory (Brown et al. 2001; Siegmund et al. 2002; Szturm and Fallang 1998) and the deceleration impulse at the end of the perturbation (Bothner and Jensen 2001), which determines the timing of the termination of the postural response (Carpenter et al. 2005; McIlroy and Maki 1994). This evidence suggests that ongoing feedback regarding the perturbation may be used to shape the temporal formation of muscle activity during responses to postural perturbations.

Do humans optimally use the available feedback regarding on-going perturbations to shape the muscle activity used to recover their balance? While muscle activity in highly-trained feline subjects matched an optimal feedback solution for postural control (Lockhart and Ting 2007), we recently showed that EMG in naïve human subjects merely resembled the optimal muscle activation pattern for ankle strategy postural responses (Welch and Ting 2008). The cats underwent a rigorous, reward-based training regimen over the course of several weeks that involved withstanding perturbations with varying characteristics in several directions; however, our human subjects were only subjected to an hour of perturbations of varying characteristics in two directions. We suspect that this intensive training period may have allowed sufficient time for cats to optimize the feedback mechanisms used during postural control, while the time of exposure was too short for humans to adopt a similar optimal feedback control strategy. Alternatively, humans may use a different set of optimal criteria for postural control or may weigh these

criteria differently based on their level of balance ability and personal experiences. Nevertheless, a more comprehensive investigation of human postural responses is warranted to determine whether these muscular response patterns reflect optimal feedback control.

Several omissions from previously-published works confound the ability to draw specific conclusions regarding the use of acceleration and velocity feedback for the temporal formation of muscle activity during postural control. Many authors did not report information regarding platform or CoM accelerations during their experimental sessions. In addition, many studies were performed using perturbation paradigms that exhibit significant correlation between the acceleration and velocity waveforms of the platform motion. Because our feedback model predicts that acceleration and velocity information have temporally separate effects on muscle activity, the independent manipulation of the acceleration and velocity characteristics used within the perturbation paradigm is necessary to thoroughly examine these feedback pathways and their contributions to muscle activity during postural control.

The goal of this paper was to test whether our CoM feedback law for the generation of temporal patterns of muscle activity during human postural control could account for changes in perturbation characteristics using an invariant feedback structure with constant feedback gains. We explicitly tested the effects of altering the temporal patterns of CoM kinematic trajectories (sensory input) on the evoked temporal patterns of muscle activity (motor output) and compared them to model predictions. To that end, we designed a custom perturbation platform in which the displacement, velocity, and acceleration of support surface translations can be specified and varied independently.

This careful decoupling of velocity and acceleration allowed the examination of the individual effects of these perturbation characteristics on the temporal patterns of muscle activity during the entire postural response. By comparing the recorded EMG to patterns of muscle activity predicted by an optimal feedback control model, we confirmed that the postural control of our naïve human subjects resembles but does not exactly follow an optimal feedback strategy. We therefore used two additional delayed feedback control models that match model predictions to recorded EMG data to demonstrate that the experimentally-measured effects of altering perturbation acceleration and velocity are consistent with those predicted by an invariant feedback law on CoM kinematics with constant feedback gains. These results suggest that feedback related to task-level variables may be encoded within the muscle activity patterns elicited in response to support surface translations.

Methods

Seven healthy subjects (5 male, 2 female), ages 19.4 ± 1.4 years (mean ± SD), were recruited from the Georgia Institute of Technology student population to participate in an experimental protocol that was approved by both the Georgia Institute of Technology and Emory University Internal Review Boards. All subjects signed an informed consent form before participating. Subjects stood with weight evenly distributed upon two force plates installed on a moveable platform that could translate in the horizontal plane. Subjects focused vision to a scenic view 4.6 meters away and were instructed to cross their arms at chest-level and react naturally to the support surface perturbations.

Experimental Protocol

In order to vary the acceleration and velocity characteristics of subject motion independently, we designed two types of 12-cm anterior-posterior support surface translations (Figures 3.1B-C). The first type (constant acceleration) maintained constant peak acceleration, while peak velocity was varied between perturbations. In the second type (constant velocity), peak acceleration was varied, keeping peak velocity constant. The independence of acceleration and velocity was achieved through careful controller design; using a standard industrial controller to specify acceleration changes resulted in coupled variations in peak acceleration and velocity, as well as positional overshoot (Figure 3.1A). Perturbation characteristics spanned a range of velocities (5 cm/s steps between 25 and 40 cm/s) and accelerations (0.1g steps between 0.1 and 0.6g) that were varied independently in both forward and backward directions for a total of 34 perturbation types. After a set of 20 acclimatization trials at an intermediate perturbation level (35 cm/s at 0.4g) in both directions, five replicates of each perturbation condition were administered in random order for a total of 170 perturbations per subject. Intertrial time varied randomly between 5 and 15 seconds. A minimum of 5 minutes seated rest was enforced between each set of 60 perturbations to reduce muscle fatigue. Only those trials in which subjects were able to maintain balance without stepping were included in further analyses. Results from one experimental condition (25 cm/s at 0.3g) have been previously published (Welch and Ting 2008).

Data Collection

Platform acceleration and position, and surface EMG from fifteen muscles in the legs and trunk were collected at 1080 Hz, synchronized with body segment kinematics

collected at 120 Hz (Figure 3.2). Platform signals were low-pass filtered at 30 Hz (3rd order zero-lag Butterworth filter). Platform velocity was calculated by numerical differentiation of the filtered platform position. EMGs were collected from the following muscles: TA, tibialis anterior (bilateral); MG, medial gastrocnemius (bilateral); SOL, soleus; VLAT, vastus lateralis; RFEM, rectus femoris; SEMB, semimembranosus; SEMT, semitendinosus; BFLH, long head of biceps femoris; BFSH, short head of biceps femoris; ES, erector spinae (bilateral); RA, rectus abdominis (bilateral). Muscles collected bilaterally are reported herein using the suffixes '–R' and '–L' to indicate right and left legs, respectively. All other EMG signals were collected from the right leg only. Raw EMG signals were high-pass filtered at 35 Hz (3rd order zero-lag Butterworth filter), demeaned, half-wave rectified, and low-pass filtered at 40 Hz (1st order zero-lag Butterworth filter). EMG signals were then normalized to the maximum EMG observed in each muscle over all conditions for each subject. Body segment kinematics were derived from a custom bilateral Helen Hayes 25-marker set that included head-arms-trunk (HAT), thigh, and shank-foot segments. Center of mass motion was calculated from kinematic data as a weighted sum of segmental masses (Winter 2005).

Data Analysis

Empirical Identification of Perturbation Effects on Muscle Activity

Changes in muscle activity due to the manipulation of perturbation characteristics were determined by examining mean muscle activity during specific time bins (Brown et al. 2001; Diener et al. 1988; Maki and Ostrovski 1993b). Recorded EMG following postural disturbance was examined during two consecutive 150-ms time periods following muscle onset — the initial burst (IB) and plateau region (PR) (Figure 3.2). To

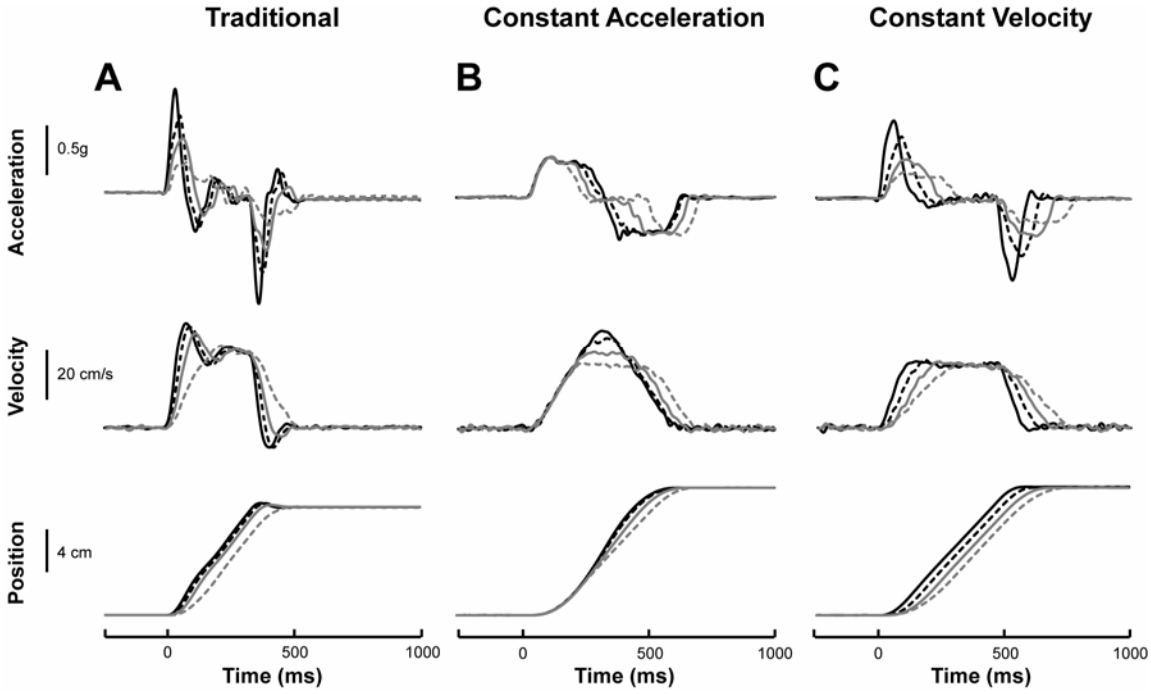

Figure 3.1 Optimized platform paradigm performance. A) While many traditional platform paradigms have been characterized by the covariation of peak velocity and acceleration as well as underdamped performance, our custom platform allowed the individual specification and variation of displacement, velocity, and acceleration under a strict control scheme. **B)** Our platform allowed the variation of velocity while maintaining peak acceleration and **C)** the variation of acceleration while maintaining peak velocity. Total platform displacement was not affected by either mode of dynamic variation and no positional overshoot was observed in this optimized paradigm.

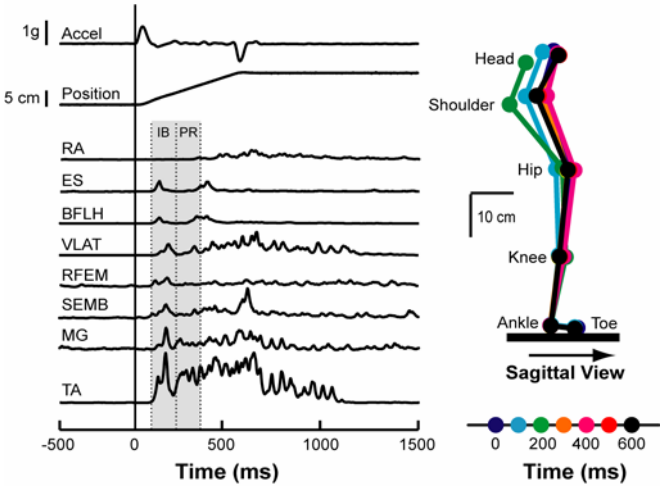

Figure 3.2 Representative response to a forward support surface translation. To a postural disturbance, muscles were activated in a coordinated fashion to produce forces to counteract the perturbation (*left*). This coordinated muscle activity served to rectify posture to an upright position, usually within one second of the perturbation onset (*right*). The shaded areas on EMG traces represent the initial burst (IB) and plateau region (PR) periods of muscle activity.

increase temporal resolution, each period was further subdivided to create a total of four 75-ms periods following muscle onset (APR1 – 4), where IB is formed by APR1 and APR2, while PR is formed by APR3 and APR4. Mean EMG levels during each time period were calculated for each muscle and normalized to the maximum EMG observed in that muscle over all conditions for each subject. To examine the scaling of muscle responses with perturbation characteristics, we performed three-way ANOVA (velocity × acceleration × subject) on the mean EMG data during each period. For those muscles significantly affected by perturbation characteristics, we computed the slopes of the scaling relationships by performing linear regression analysis of mean EMG to peak platform acceleration and velocity. ANOVA results were evaluated at a significance level of $\alpha = 0.05$, adjusted with a Bonferroni correction for multiple comparisons ($\alpha = 0.0125$; $n = 4$). All averaged data are presented herein as mean ± SD.

Prediction and Reconstruction of Muscle Activity Using CoM Feedback Law

The DQR Optimal Feedback Control Model

We compared localized changes in EMG during perturbations of varying motion characteristics to optimal control solutions to these same perturbations derived from a previously-described delayed quadratic regulator, or DQR model (Lockhart and Ting 2007; Welch and Ting 2008). Experimental subjects were modeled individually as single-link inverted pendulums that were perturbed with disturbance torque trajectories calculated from experimentally-recorded platform accelerations (Figure 3.3A). A feedback controller was used to stabilize each inverted pendulum using delayed feedback of CoM displacement (p), velocity (v), and acceleration (a). From these feedback

channels, an EMG prediction (EMG_p) was calculated as the linear combination of the weighted horizontal CoM kinematic trajectories at a common neural transmission delay:

$$EMG_p = k_p p(t-\lambda) + k_v v(t-\lambda) + k_a a(t-\lambda). \quad (1)$$

Each EMG prediction was half-wave rectified and converted to a muscle torque, using a first-order muscle model, to counteract the disturbance torque. For each recorded muscle and perturbation condition, a feedback delay (λ) and three feedback gains (k_i) were optimized in MATLAB (*fmincon.m*) based on optimal criteria aimed to minimize total muscle activation and kinematic deviation of the pendulum from the initial upright configuration, without regard to experimentally-recorded data:

$$\min_{K \in G} \left\{ J = E\left[\int_0^{t_{end}} \left(x^T Q x + \rho u \right) dt + \Omega x(t_{end}) \right] \right\}. \quad (2)$$

The first term penalized deviations of the state variable $x = \begin{bmatrix} p & v & a \end{bmatrix}^T$ from zero with weights Q. The second term required the minimum possible level of muscle activation to achieve the postural task by penalizing EMG activation level (u) with weight ρ. The final term penalized non-zero final pendulum states with weight Ω. Feedback parameters (K) were restricted such that $0 < k_i < 100$ and $60 < \lambda < 250$.

The TSyID Feedback Control Model

We used a previously-described delayed feedback control model (temporal systems identification, or TSyID model) to reconstruct the entire time course of EMG recorded during experimental manipulations (Welch and Ting 2008). The TSyID model used the same inverted pendulum model as described for the DQR model (Figure 3.3A), with a different cost function, based on matching experimental data, to determine feedback parameters. For each recorded muscle and perturbation condition, a feedback

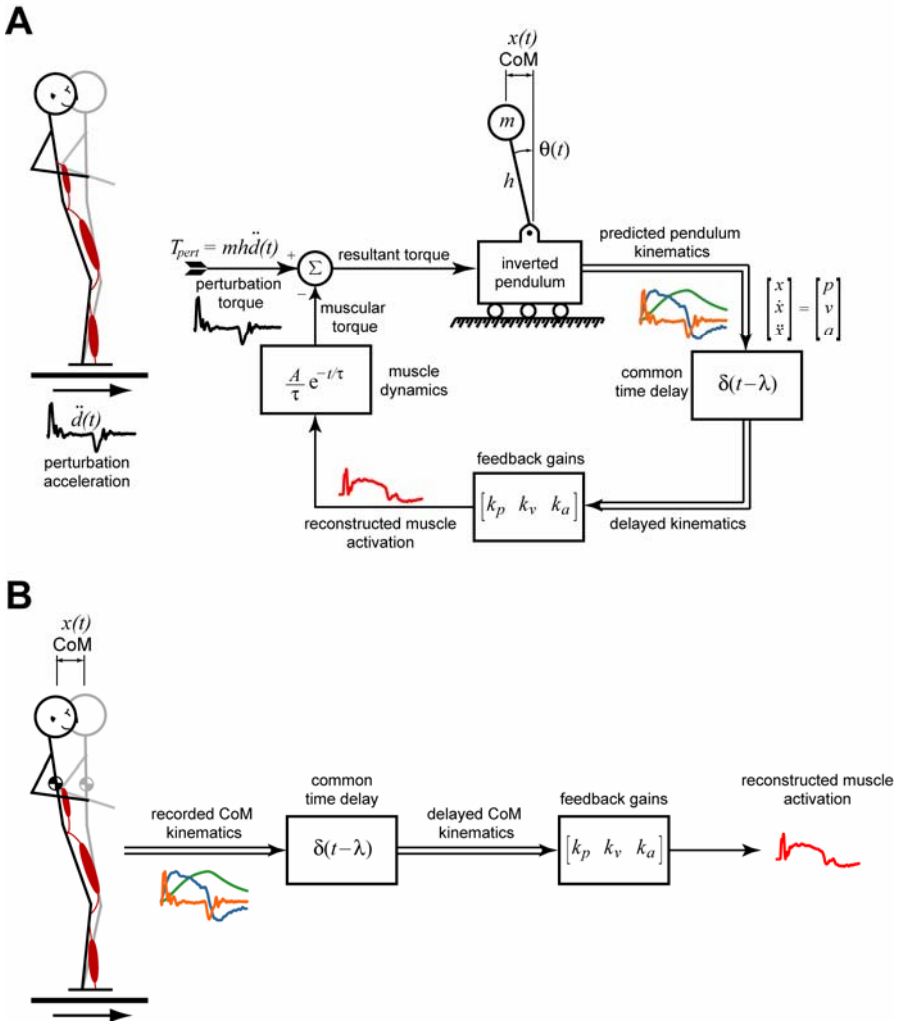

Figure 3.3 Feedback models for postural control. A) For both the delayed quadratic regulator (DQR) and temporal systems identification (TSyID) models, the standing human was modeled as an inverted pendulum that was perturbed using recorded perturbation acceleration trajectories. The model predicted pendulum kinematics and optimized feedback gains and a common time delay on horizontal pendulum acceleration, velocity, and displacement trajectories. The delayed, weighted kinematic feedback signals were summed to predict EMG patterns and a first-order muscle model predicted the resulting muscle torque to counteract the perturbation. The time constant of the muscle model was defined τ = 40 ms and the muscle model gain was $A = 4mh$ [=] kg·m^2/s, where m is the mass (in kg) of the subject and h is the height of the subjects CoM (in m). The DQR optimization was designed to choose feedback gains that minimized kinematic variation and muscle activity. The TSyID optimization chose feedback gains that minimized the square and maximum error between model reconstructions and recorded EMG. **B)** In the jigsaw model, recorded CoM kinematics from experimental subjects were used directly to reconstruct EMG patterns. EMG was reconstructed as the linear combination of the recorded kinematic signals (CoM acceleration, velocity, and displacement) at a common time delay. The jigsaw optimization chose the feedback gains and time delay that minimized square and maximum error between model reconstructions and recorded EMG.

delay (λ) and three feedback gains (k_i) were optimized in MATLAB (*fmincon.m*) using a cost function that minimized the error between the model reconstructions and normalized experimentally-recorded EMG, while ensuring the stability of the inverted pendulum:

$$\min_{K \in G} \left\langle J = E\left\{ \int_0^{t_{end}} \left[{e_m}^T \mu_s e_m + \max\left(\mu_m |e_m|\right) \right] dt \right\} + We_x\left(t_{end}\right) \right\rangle. \quad (3)$$

The first term penalized the error between the reconstructed and measured EMG signal over time as represented by the vector e_m with weight μ_s. The second term penalized the maximum deviation between the reconstructed and measured EMG signals at any single point in time with weight μ_m. The final term penalized non-zero final states of the inverted pendulum $x = \begin{bmatrix} p & v \end{bmatrix}^T$ with weight W, promoting a final pendulum configuration resembling quiet upright stance.

The Jigsaw Feedback Control Model

In the jigsaw model, we used the CoM kinematics recorded during experimental sessions to directly reconstruct the entire time course of recorded EMG patterns. This model does not use an inverted pendulum to predict kinematics, but rather uses the exact motion of the CoM that corresponded to the recorded EMG activity in experimental subjects (Figure 3.3B). For each recorded muscle and perturbation condition, a feedback delay (λ) and three feedback gains (k_i) were optimized in MATLAB (*fmincon.m*) using a cost function that minimized the error between reconstructed and recorded EMG patterns:

$$\min_{K \in G} \left\{ J = E \int_0^{t_{end}} \left[{e_m}^T \mu_s e_m + \max\left(\mu_m |e_m|\right) \right] dt \right\}. \quad (4)$$

Note that the cost function for the jigsaw model is identical to that used during TSyID simulations (see Eq. 3), but excludes the final term related to upright pendulum configuration at the end of the simulation.

Evaluation of the Feedback Parameters Selected by Feedback Models

To examine the consistency of this feedback law across perturbation conditions, we compared the feedback parameters that were chosen by each model across acceleration and velocity levels. Each model optimization resulted in a unique set of three feedback gains and one time delay for each subject, condition, and muscle. For each model and subject, we assessed the goodness of fit between predicted and recorded EMG signals using both the coefficient of determination (r^2) and the uncentered coefficient of determination (variability accounted for; VAF). Next, we performed three-way ANOVA (velocity × acceleration × subject) on each feedback parameter, at a significance level of $\alpha = 0.05$, to determine whether these feedback parameters remained constant or changed with the velocity and acceleration of perturbation. We finally performed regression analysis of mean feedback parameters with respect to peak velocity and acceleration to reveal any significant scaling relationships.

To investigate the temporal effects of varying perturbation characteristics on muscle activity, we generated a set of EMG predictions using the inverted-pendulum model with constant feedback gains. The subject-specific feedback gains and delay derived from the TSyID-reconstructed EMG of an intermediate perturbation condition (35 cm/s at 0.4g) were used to generate EMG predictions to all experimentally-recorded perturbations. These simulation results were compared across acceleration and velocity levels to determine how each individual feedback channel affected muscle activity. In

addition, goodness of fit between recorded EMG and constant-gain EMG predictions was evaluated for each muscle to determine whether a feedback law with constant gains was sufficient to account for the observed variations in muscle activity with perturbation characteristics.

Results

Using a delayed feedback model, we identified a feedback law for human postural control that predicts the effects of perturbation characteristics on the time course of the muscular response to support surface translations. In response to a variety of perturbations, muscle activity during the initial burst of EMG scaled linearly with peak platform acceleration, while activity during the plateau region scaled linearly with peak platform velocity. The predictions of an optimal feedback model (DQR) of human postural control were consistent with these experimental observations, predicting that feedback parameters should be adjusted according to perturbation strength. However, muscle activity did not match the optimal solution in all conditions and a pendulum model using constant feedback gains predicted EMG across conditions with equal success. Further investigation using two data-matching models (TSyID and jigsaw) resulted in the successful reconstruction of recorded EMG across all conditions. Comparisons of feedback gains derived from these models across conditions suggested that the feedback parameters should remain constant with respect to perturbation characteristics. Together, these results suggest that the human postural control mechanism uses a feedback law with invariant feedback parameters to develop the entire time course of muscle activity following postural perturbation, though the selected feedback formulation may not be consistent with the optimal strategy.

Scaling of Muscle Activity with Perturbation Characteristics

In response to support surface translations in the sagittal plane, subjects activated muscles throughout the lower limbs and trunk to counteract perturbation-induced postural sway. Subjects exhibited postural sway in the opposite direction of platform motion, characterized by coordinated joint motions about the ankle, knee, and hip (Figure 3.2). Here, we will discuss results for the right-leg ankle dorsiflexor tibialis anterior (TA-R) during forward perturbations and for the right-leg ankle plantar flexor medial gastrocnemius (MG-R) during backward perturbations, though results were generally shared among all muscles evaluated. In response to forward perturbations of varying motion characteristics, the postural response of TA-R was characterized by an initial burst of EMG, after a latency of 119 ± 22 ms, followed by a sustained plateau region of tonic activity (Figure 3.2). Similarly, in response to backward perturbations, MG-R showed the characteristic initial burst and plateau regions at a latency of 136 ± 49 ms. The muscular response varied over the range of perturbation conditions, while maintaining this same temporal muscle activation profile (Figures 3.4A and C). Subjects typically returned to an upright position within one second, resulting in the offset of muscle activity.

The effects of acceleration and velocity on EMG activity were temporally separated within the time course of the postural response. Mean EMG during IB was correlated significantly with platform acceleration, but not with platform velocity (Figure 3.4B). Peak platform acceleration had a significant effect during IB (TA-R: $p = 1.11\times10^{-16}$; MG-R: $p = 7.94\times10^{-7}$), while the effect of peak platform velocity was insignificant

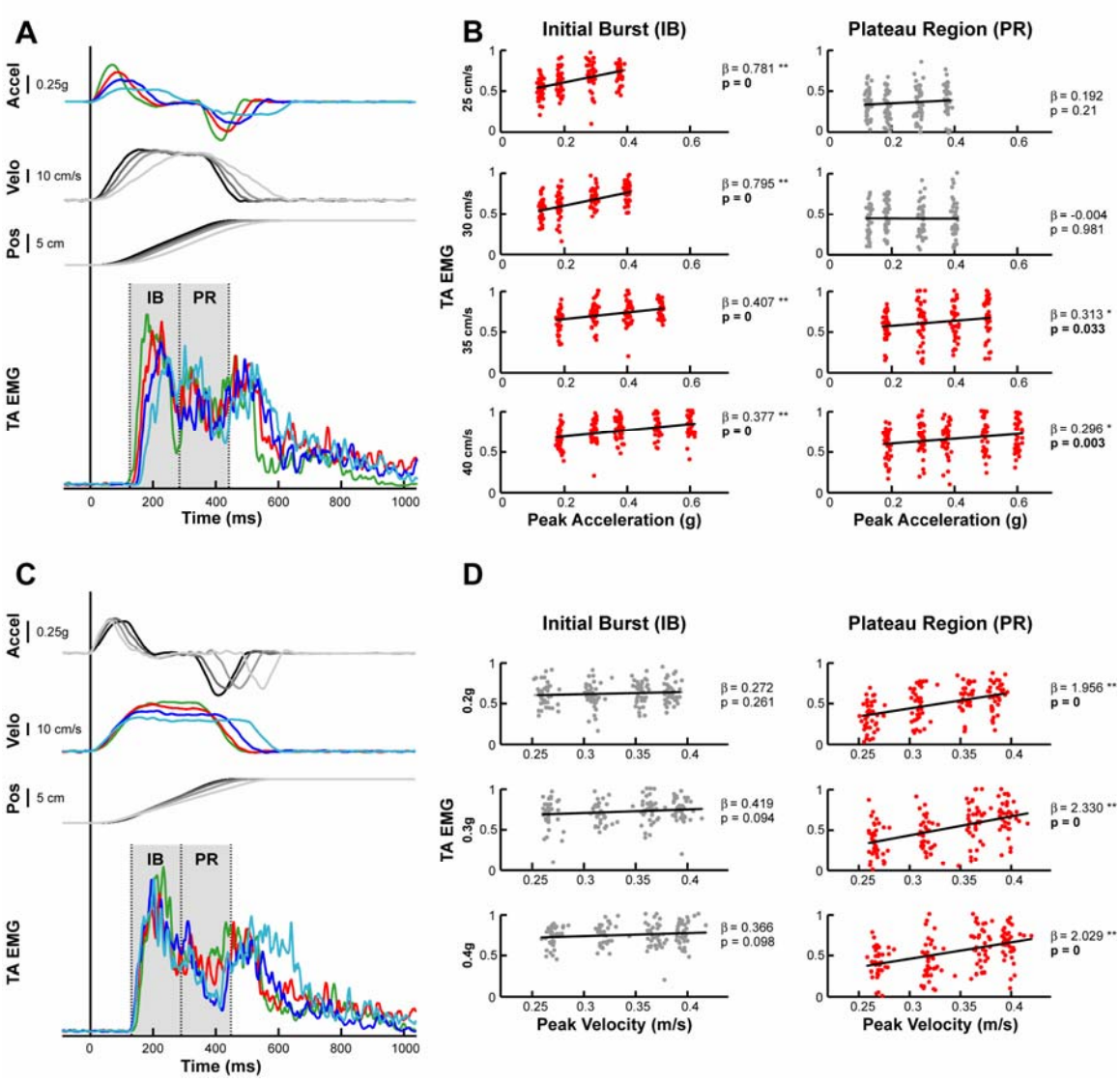

Figure 3.4 Scaling of human postural response with perturbation characteristics. Our custom perturbation platform allowed **A)** the variation of acceleration independent of peak velocity or **C)** the variation of velocity independent of peak acceleration. The muscle activity during the initial burst (IB) and plateau region (PR) of the automatic postural response scaled with platform acceleration and velocity, respectively. Depicted right-leg tibialis anterior (TA-R) EMG waveforms were collected during experimental sessions with Subject G for **(A)** a constant peak velocity of 30 cm/s with varying acceleration from 0.2 – 0.4g and **(C)** for a constant peak acceleration of 0.4g with varying velocity from 25 – 40 cm/s. **B)** At a constant peak velocity, muscle activity during the initial burst scaled linearly with platform acceleration, while no significant scaling is observed in the plateau region. **D)** Conversely, when peak acceleration was constant, muscle activity during the plateau region scaled linearly with platform velocity, while no significant scaling was observed in the initial burst. Results from the linear regression analysis are indicated by slope (β) and p-values. Significant regression results are indicated by * ($p < 0.01$) and ** ($p < 10^{-5}$), with regression data in red and p-values in **bold** font.

(TA-R: $p = 0.03$; MG-R: $p = 0.77$; see Tables 3.1 and 3.2). During IB, mean muscle activity scaled linearly with peak platform acceleration (TA-R: $p < 10^{-16}$; MG-R: $p < 0.016$) with an average TA-R slope between subjects of 0.56 ± 0.16 g^{-1} and average MG-R slope of 0.41 ± 0.27 g^{-1}. Conversely, during PR, mean EMG was correlated significantly with platform velocity (TA-R: $p < 10^{-16}$; MG-R: $p = 8.86 \times 10^{-10}$), but not with platform acceleration for TA-R ($p = 0.26$; Figure 3.4D); MG-R showed a significant correlation of PR activity with platform acceleration ($p = 2.65 \times 10^{-5}$). Mean muscle activity during PR scaled significantly with peak platform velocity (TA-R: $p < 10^{-16}$; MG-R: $p < 0.008$) with an average TA slope between subjects of 2.25 ± 0.72 s/m and average MG-R slope of 1.35 ± 0.80 s/m. For both IB and PR, regression slopes were similar between both sides of the body when muscles were collected bilaterally (data not shown).

Throughout the temporal pattern of activation, mean EMG gradually evolved from scaling with acceleration to velocity. Over the time course of each individual postural response, linear regression slopes decreased for acceleration scaling while gradually increasing for velocity scaling (Table 3.3). Mean TA-R EMG during APR1 scaled linearly with peak platform acceleration ($p < 10^{-16}$), but not with peak platform velocity ($p > 0.362$). Similarly, significant scaling with peak platform acceleration was found for APR2 ($p < 0.004$), with velocity scaling only observed at higher acceleration levels (0.3g and 0.4g; $p < 0.004$). Scaling with peak platform acceleration was not significant for APR3 ($p > 0.069$) and only at velocities of 40 cm/s ($p < 10^{-16}$) for APR4. Velocity scaling was significant at all acceleration levels for both APR3 and APR4 ($p < 10^{-16}$). Similar results were obtained for all other muscles (data not shown). These

observations suggest that EMG during postural control may be formed by feedback from channels relaying temporally-separated information regarding CoM kinematics.

Table 3.1 ANOVA p-values for EMG response to peak acceleration and velocity following forward perturbations

Muscle	Forward Perturbations			
	Initial Burst		*Plateau Region*	
	Peak Accel	**Peak Velo**	**Peak Accel**	**Peak Velo**
TA-L	**$< 10^{-16}$**	**0.0086**	0.089	**$< 10^{-16}$**
MG-L	**2.36×10^{-4}**	0.76	0.42	**7.26×10^{-4}**
TA-R	**1.11×10^{-16}**	0.03	0.26	**$< 10^{-16}$**
MG-R	**5.27×10^{-6}**	0.092	**0.0011**	**1.92×10^{-10}**
SOL	**5.91×10^{-6}**	**5.18×10^{-6}**	0.11	**0.0054**
VLAT	**6.75×10^{-7}**	0.64	**0.0091**	**2.82×10^{-10}**
RFEM	**$< 10^{-16}$**	0.40	**0.010**	**0.0019**
SEMB	**2.22×10^{-16}**	**7.03×10^{-4}**	0.092	**5.61×10^{-11}**
SEMT	**1.55×10^{-15}**	**0.0014**	0.040	**4.20×10^{-10}**
BFLH	**7.07×10^{-11}**	**0.0039**	0.26	**1.42×10^{-11}**
BFSH	**2.39×10^{-11}**	0.018	0.41	**1.47×10^{-10}**
ES-L	**1.83×10^{-8}**	**0.0055**	0.23	0.20
ES-R	**6.93×10^{-7}**	**0.0072**	0.058	**0.0039**
RA-L	**3.79×10^{-7}**	0.42	**0.0050**	**3.17×10^{-9}**
RA-R	**9.05×10^{-4}**	0.47	0.71	**2.26×10^{-6}**

p-values indicated in **bold** are significant at $p < 0.0125$ for $n = 4$ comparisons. For all muscles during all periods, the subject factor was significant ($p < 10^{-5}$) and the interaction between velocity and acceleration was not significant ($p > 0.045$).

Table 3.2 ANOVA p-values for EMG response to peak acceleration and velocity following backward perturbations

Muscle	Backward Perturbations			
	Initial Burst		*Plateau Region*	
	Peak Accel	**Peak Velo**	**Peak Accel**	**Peak Velo**
TA-L	**6.66×10^{-16}**	0.54	**6.14×10^{-7}**	**3.71×10^{-9}**
MG-L	**4.48×10^{-5}**	0.016	**4.55×10^{-5}**	**8.61×10^{-13}**
TA-R	**5.02×10^{-9}**	0.39	**0.0019**	**3.51×10^{-10}**
MG-R	**7.94×10^{-7}**	0.77	**2.65×10^{-5}**	**8.86×10^{-10}**
SOL	**1.39×10^{-9}**	**0.0020**	**0.0021**	**$< 10^{-16}$**
VLAT	**1.68×10^{-5}**	0.092	**9.66×10^{-5}**	**1.61×10^{-9}**
RFEM	**1.11×10^{-7}**	**0.0015**	**0.0011**	**2.62×10^{-9}**
SEMB	**1.11×10^{-16}**	0.039	**1.39×10^{-11}**	**$< 10^{-16}$**
SEMT	**$< 10^{-16}$**	0.22	**9.12×10^{-7}**	**$< 10^{-16}$**
BFLH	**1.70×10^{-7}**	0.54	0.031	**0.0031**
BFSH	**1.30×10^{-16}**	0.18	0.017	**1.62×10^{-4}**
ES-L	**0.0022**	0.10	**1.29×10^{-5}**	**$< 10^{-16}$**
ES-R	**3.74×10^{-5}**	0.89	**1.56×10^{-4}**	**5.92×10^{-11}**
RA-L	**4.70×10^{-8}**	0.10	0.13	**2.34×10^{-6}**
RA-R	**1.86×10^{-7}**	0.35	**0.0078**	**0.0024**

p-values indicated in **bold** are significant at $p < 0.0125$ for $n = 4$ comparisons. For all muscles during all periods, the subject factor was significant ($p < 10^{-5}$) and the interaction between velocity and acceleration was not significant ($p > 0.045$).

Feedback Law on CoM Kinematics for Postural Control

A feedback law transforming CoM kinematics to muscle output was capable of reconstructing EMG waveforms from several muscles throughout the lower limb and trunk in response to perturbations with a variety of velocity and acceleration characteristics. In general, model-derived muscle activation patterns contained an initial burst of muscle activity, followed by an extended plateau region of tonic muscle activity. Optimal feedback predictions derived from the DQR model resemble muscle activity in ankle muscles, but over-predicted low-level proximal muscle activity, resulting in low variability accounted for (VAF) in many muscles (Figure 3.5A), suggesting that the individual activity in these muscles is insufficient to stabilize the body using an optimal feedback control scheme. The goodness of fit between model and experimentally-observed EMG was improved with the use of data-matching optimizations. EMG reconstructions from the TSyID model showed significant improvements in VAF; however, model kinematics deviated greatly from the pattern of CoM kinematics exhibited by experimental subjects. By using recorded CoM motion to reconstruct EMG patterns and modeling the acceleration-dependent response of the muscle spindle, VAF was increased to >61% across all subjects, muscles, and conditions (VAF = 0.91 ± 0.05). A comparison of recorded EMG in the right-leg tibialis anterior (TA-R) and model-derived muscle activation patterns across all feedback models is illustrated in Figure 3.5B.

Table 3.3 Postural response scaling evolves temporally from acceleration to velocity scaling

	Postural Response Period			
	APR1	**APR2**	**APR3**	**APR4**
Velocity Level	*Acceleration Scaling Slope*			
25 cm/s	**0.739** *	**0.673** *	0.312	0.066
30 cm/s	**0.852** *	**0.606** *	0.042	–0.076
35 cm/s	**0.446** *	**0.305** †	0.257	0.275
40 cm/s	**0.388** *	**0.295** *	0.129	**0.408** *
Acceleration Level	*Velocity Scaling Slope*			
0.2g	0.067	0.403	**1.367** *	**2.214** *
0.3g	–0.074	**0.749** †	**1.835** *	**2.393** *
0.4g	–0.235	**0.810** †	**1.393** *	**2.314** *

Significant regression slopes are in **bold** with the significance level denoted * ($p < 10^{-5}$) and † ($p < 0.05$).

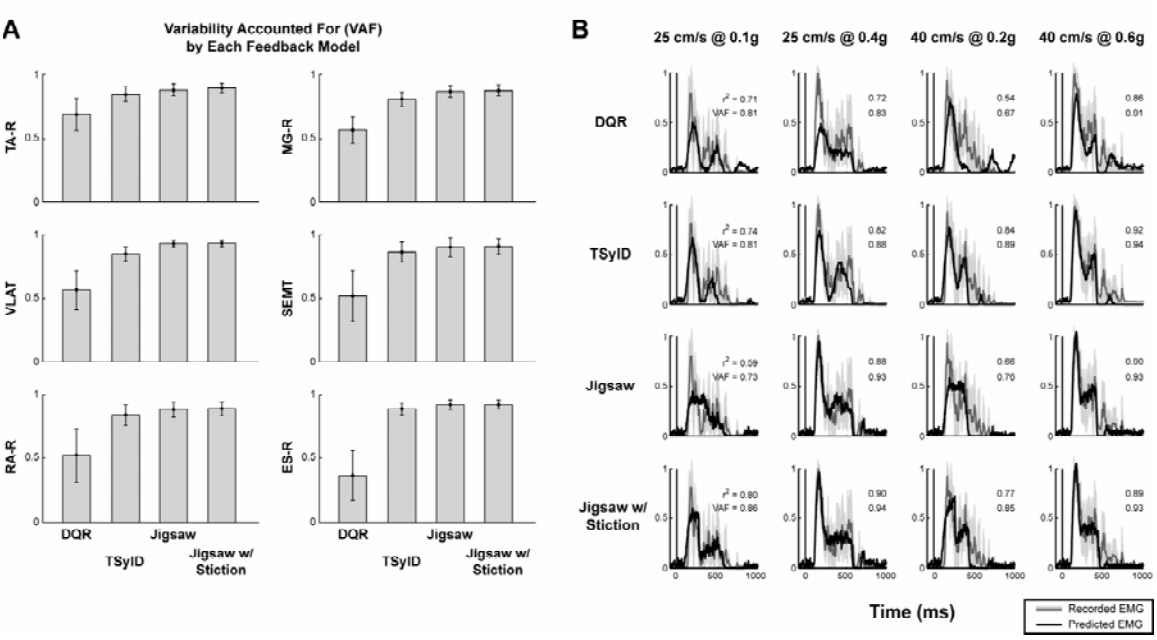

Figure 3.5 Summary of modeling results for all feedback models. A) Mean variability accounted for (VAF) across all subjects and conditions for each of the feedback models (DQR, TSyID, jigsaw, and jigsaw w/ stiction response) in antagonistic pairs of muscles on each segment of the lower limb and trunk. Large variability in the goodness of fit between optimal feedback (DQR) solutions and experimental EMG responses was observed across conditions and muscles, suggesting that the activity in individual proximal muscles is not sufficient to stabilize the body to postural perturbations under an optimal feedback control scheme. The use of data-matching models increased the VAF for all muscles, while reducing the variability of the VAF measure across subjects and conditions. Including the stiction response within the jigsaw model resulted in the best model fits, resulting in VAF = 0.91 ± 0.05 across all subjects, muscles, and conditions. **B)** The comparison of recorded EMG signals to model predictions/reconstructions for four conditions of extreme perturbation characteristics in right-leg tibialis anterior (TA-R) collected from Subject A. Optimal solutions derived from the DQR model resemble recorded EMG patterns, but are missing many features of the experimental data. The data-matching inverted-pendulum model (TSyID) significantly improved the matching of these features, but drastically altered the pendulum kinematics to arrive at these solutions. Using the recorded CoM kinematic data to make EMG reconstructions, the jigsaw model matched most features of the recorded EMG data, but was most successful in conditions with high accelerations (larger than 0.2g). By modeling the acceleration-dependent muscle spindle stiction response, jigsaw model matches were significantly improved across all subjects and conditions.

Prediction of Muscle Activity using DQR Model

An optimal feedback control law predicted the changes in optimal response patterns that occur with the experimental manipulation of perturbation characteristics. Optimal muscle activation patterns for human postural control were computed, using the DQR model, to minimize both kinematic deviation of an inverted pendulum and total

muscle activation. Similar to the EMG patterns observed experimentally, optimal control predictions typically consisted of an initial burst of activity, followed by a period of tonic muscle activity, described as the plateau region (Figure 3.6). These features of the EMG predictions arose from separate feedback channels – the initial burst was predicted to be formed by feedback of CoM acceleration, while the plateau region was formed by a combination of CoM velocity and displacement feedback. Due to the simplicity of the

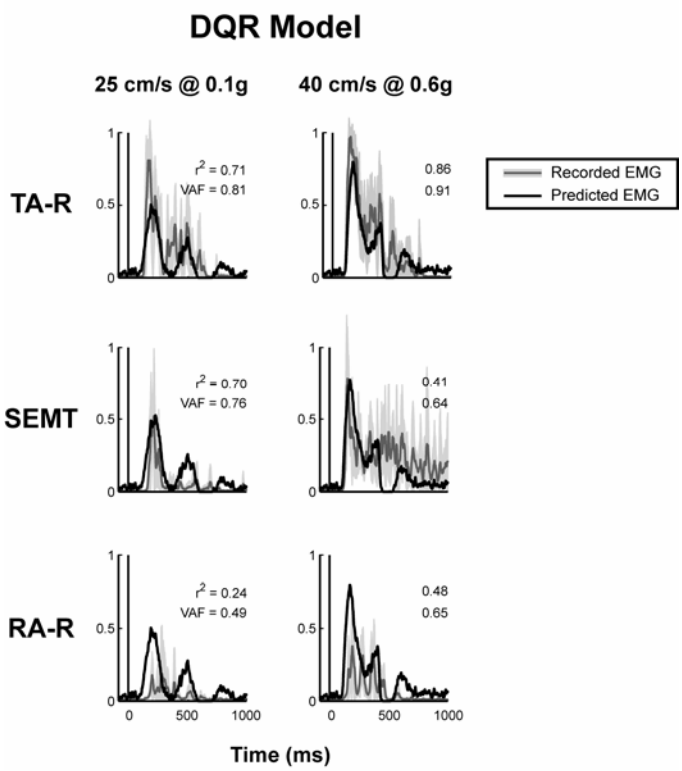

Figure 3.6 Optimal EMG patterns derived from DQR model. The time course of recorded (solid gray) and optimal (solid black) EMGs for low- and high-velocity/acceleration experimental conditions in muscles collected from Subject A. Gray shaded regions indicate one standard deviation of the mean recorded EMG. Recorded muscle activation patterns for the right-leg tibialis anterior (TA-R) in Subject A resemble the optimal control solution in all conditions with >64% VAF; however, the EMG patterns do not exactly match the optimal solution. EMG patterns from proximal leg and trunk muscles (*e.g.*, SEMT and RA-R) are typically over-predicted by the model, suggesting that the activity in these muscles alone is not sufficient for stabilization, requiring that they rely more heavily on the concerted activity of several muscles to stabilize the body.

inverted pendulum model, the use of identical optimal criteria between subjects and muscles, and the high repeatability of platform motion in each experimental condition, DQR optimal EMG predictions for each condition were identical between muscles and very similar among all subjects.

Experimentally-recorded EMG exhibited a large amount of inter-subject and inter-muscle variability, preventing an exact match of this optimal solution by any subject or muscle for all conditions. EMG of TA in both legs most closely resembled the optimal pattern in all subjects across conditions, with >41% VAF (VAF = 0.78 ± 0.07), with EMG from the triceps surae and proximal leg and trunk muscles exhibiting weaker matches to the optimal DQR solution, with only >25% and >3% VAF across conditions, respectively (triceps surae: VAF = 0.68 ± 0.09; proximal: VAF = 0.61 ± 0.12) (Figure 3.6). While many muscles, especially those located proximally at the hip joint, rely heavily on the concerted activity of several muscles to stabilize the body, the DQR model required that each muscle stabilize the inverted pendulum alone during simulations. Therefore, the low-level activation exhibited by proximal muscles was not sufficient to maintain the pendulum in the upright configuration, resulting in the over-prediction of optimal muscle patterns and weak matches to the optimal solution for these muscles. Feedback gains derived using the optimal DQR model were highly variable between conditions (for all gains, $p < 10^{-16}$ with respect to velocity and $p < 1\times10^{-3}$ with respect to acceleration) (Figure 3.7), suggesting that the optimal postural control solution may involve the adjustment of feedback gains with changes in perturbation characteristics.

To determine whether a feedback law with constant feedback gains could also predict muscle activity for postural control, we used subject-specific feedback gains from

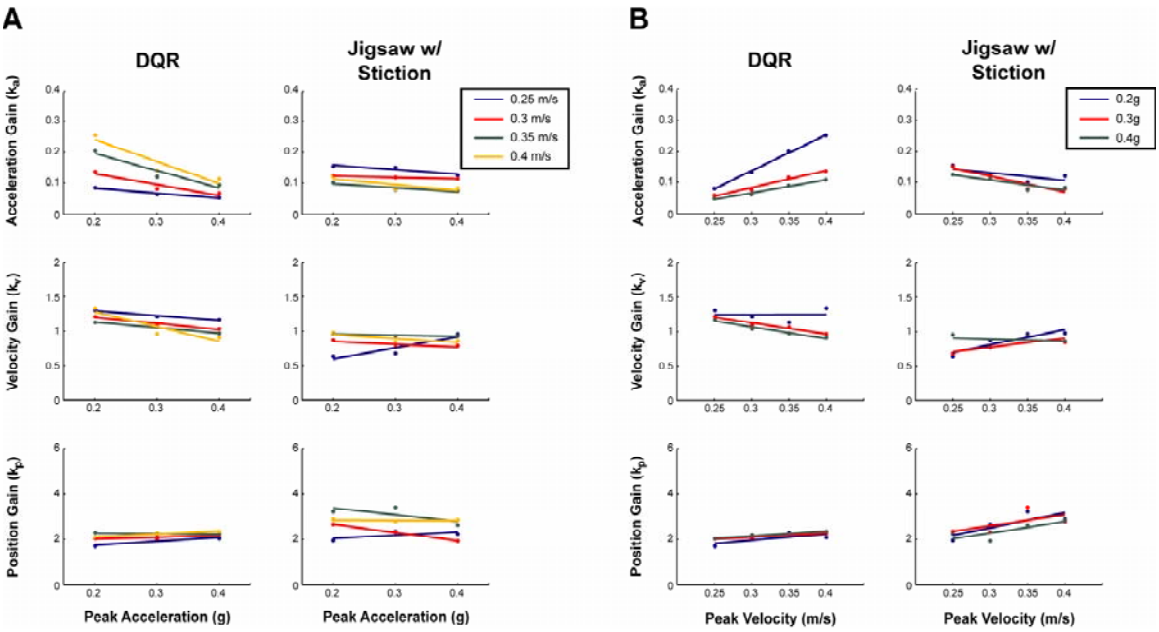

Figure 3.7 Variations in feedback gains between experimental conditions. The variability of acceleration, velocity, and displacement gains for right-leg tibialis anterior (TA-R) are illustrated across **(A)** peak acceleration and **(B)** velocity levels for the DQR model and the jigsaw model with stiction response. Data points represent the mean feedback gain across all subjects for the indicated acceleration and velocity level. The optimal DQR model predictions suggest that feedback gains should change significantly with respect to acceleration and velocity. The jigsaw model indicates similar feedback gains that vary less with respect to perturbation characteristics, suggesting that subjects may be approaching an optimal strategy for feedback-mediated postural control.

a perturbation of intermediate magnitude (Table 3.4) to predict the muscle activity in all perturbation conditions. With constant feedback gains, the feedback law implemented within the inverted pendulum model showed equivalent performance to the optimal DQR model across all experimental conditions. Predictions of muscle activity using constant gains were similar to those with gains chosen for each condition separately (Figure 3.8), consisting of an initial burst dominated by acceleration feedback and a plateau region comprised from velocity and displacement feedback. Constant-gain EMG predictions closely resembled bilateral TA EMG in all subjects across conditions with >46% VAF (VAF = 0.75 ± 0.10), while the predictions of triceps surae and proximal leg and trunk

muscles resulted in less successful matches to experimental data with >27% and >6% VAF, respectively (triceps surae: VAF = 0.67 ± 0.11; proximal: VAF = 0.58 ± 0.17). In general, constant-gain simulations better matched recorded EMG in conditions with peak accelerations greater than 0.2g.

Table 3.4 Subject-specific gains from model predictions of TA-R activity for an intermediate forward perturbation (35 cm/s at 0.4g)

Subject	Mass (kg)	CoM Height (m)	Optimal Feedback Gains			
			k_p	k_v	k_a	λ
A	73.08	1.04	3.8385	1.3879	0.1495	78.6209
B	57.65	1.06	6.4977	0.5681	0.1081	60.0833
C	76.40	1.15	2.2893	1.6221	0.1266	98.4857
D	70.22	1.08	5.3632	0.7808	0.0862	105.0212
E	65.18	1.05	12.8104	0.7027	0.1698	82.1591
F	73.31	1.17	7.5426	0.6675	0.1151	77.0736
G	81.45	1.23	6.9351	0.9289	0.1261	115.9319

Optimal feedback model simulations in both the standard and constant-gain formulations predicted a temporal scaling phenomenon of EMG magnitude with perturbation characteristics that was similar to the observed trend in experimentally-observed EMG. With constant velocity, changes in acceleration feedback were predicted to affect muscle onset slope and early muscle activity during the initial burst period (IB) ($p < 10^{-16}$; Figures 3.9A-B). In contrast, when acceleration was maintained at a constant level, variations of velocity feedback were predicted to affect later muscle activity during the plateau region (PR) ($p < 10^{-16}$; Figures 3.9C-D). Significant effects of velocity

feedback on IB activity were also noted for higher acceleration levels. These observations confirm that the scaling of muscle activity with perturbation acceleration during IB and with perturbation velocity during PR may arise from a postural mechanism that uses a feedback law on CoM kinematics.

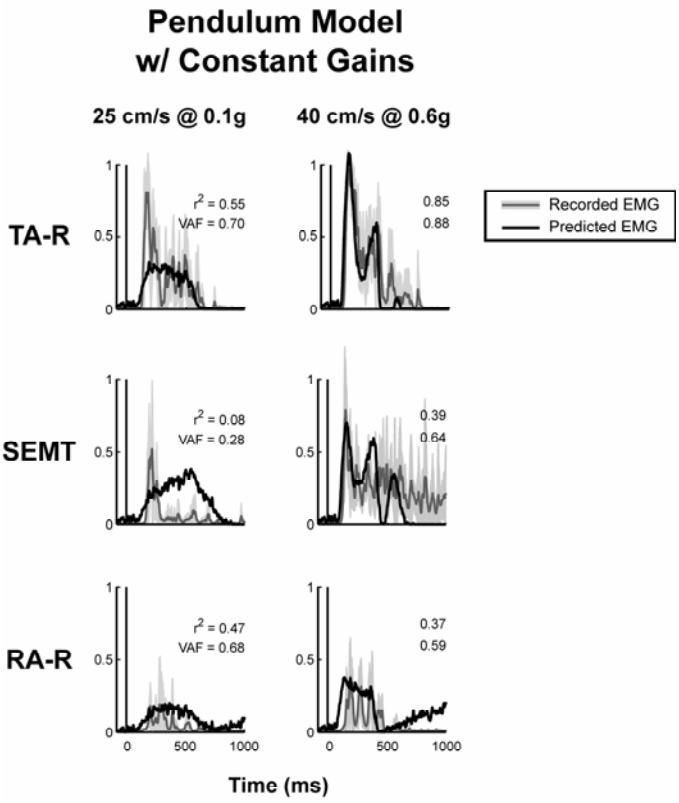

Figure 3.8 Constant-gain EMG predictions derived from pendulum model. The time course of recorded EMG (solid gray) and constant-gain EMG predictions (solid black) for low- and high-velocity/acceleration experimental conditions in muscles collected from Subject A. Gray shaded regions indicate one standard deviation of the mean recorded EMG. Predictions of EMG to all experimental conditions were made using feedback gains determined for an intermediate condition (35 cm/s at 0.4g). Similar to optimal feedback control solutions, model predictions obtained using constant feedback gains matched experimentally-recorded right-leg tibialis anterior (TA-R) EMG signals in Subject A across all conditions with >65% VAF. The constant-gain predictions of proximal leg and trunk EMG (*e.g.*, SEMT and RA-R) were less successful, resulting in over-prediction in many conditions. This suggests that the feedback gains used during postural control may be robust to changes in perturbation characteristics, despite the range of gains selected during optimal feedback model simulations.

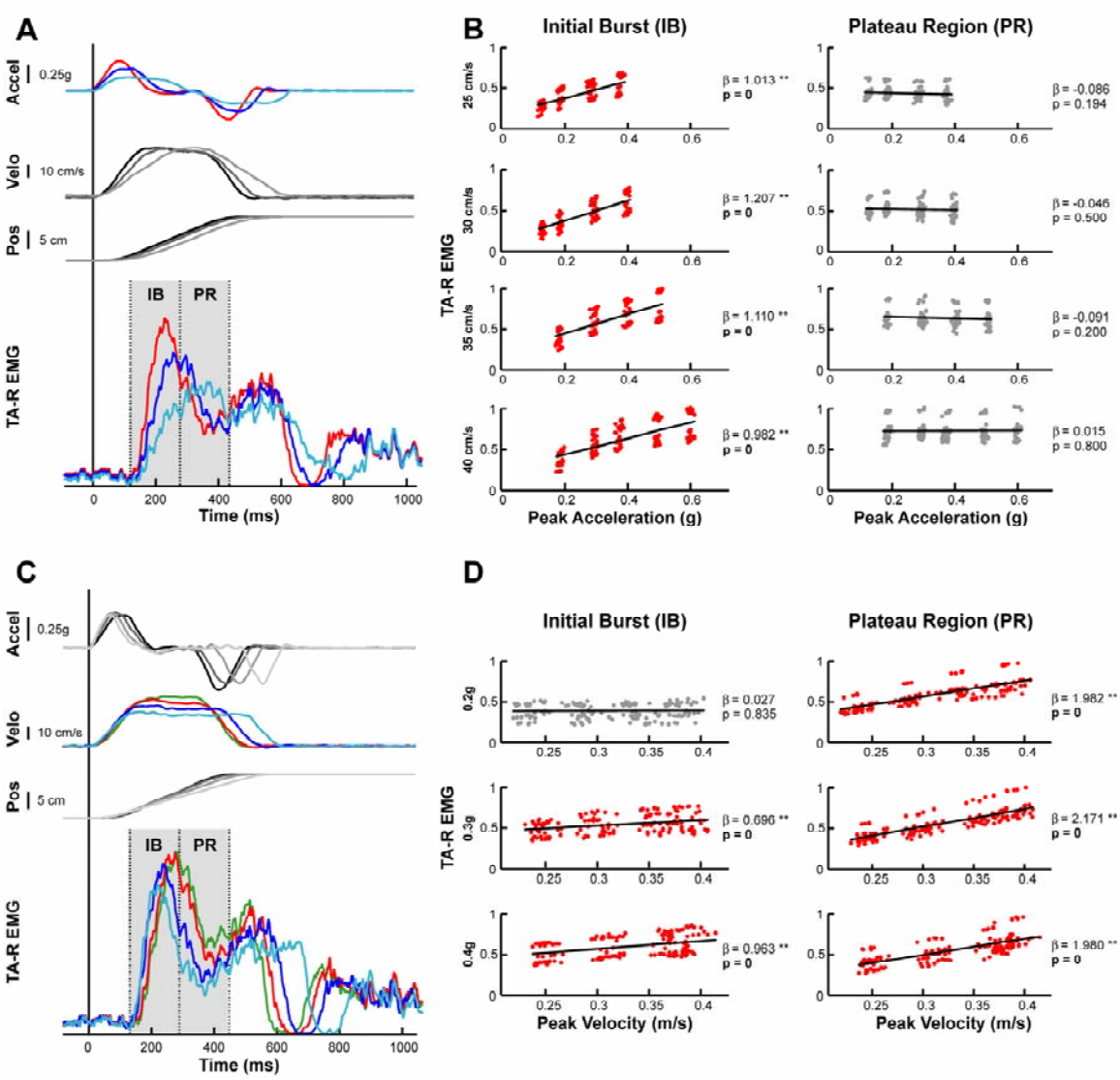

Figure 3.9 Inverted pendulum model predicts changes in muscle activity associated with perturbation characteristics. A) With constant feedback gains, changes in acceleration are predicted to affect the onset slope and magnitude of the initial burst of muscle activity. Depicted right-leg tibialis anterior (TA-R) EMG predictions are for a constant peak velocity of 30 cm/s with varying acceleration from 0.2 – 0.4g in Subject G. **B)** For constant feedback gains, the feedback model predicts a linear increase in muscle activity during the initial burst (IB) period, but no effects during the plateau region (PR) due to changes in peak perturbation acceleration. **C)** Changes in muscle activity due to velocity feedback are predicted to occur in the plateau region. Depicted TA-R EMG predictions are for a constant peak acceleration of 0.4g with varying velocity from 25 – 40 cm/s in Subject G. **D)** The model predicts an increase in muscle activity during the IB period for high acceleration levels and a similar increase in activity during the PR due to changes in peak perturbation velocity. Results from the linear regression analysis are indicated by slope (β) and p-values. Significant regression results are indicated by * ($p < 0.01$) and ** ($p < 10^{-5}$), with regression data in red and p-values in **bold** font.

Reconstruction of Muscle Activity using TSyID Model

Because subjects did not match optimal control model predictions in all conditions, a data-matching version of the inverted pendulum model (TSyID) was used to determine the sub-optimal feedback parameters used to create muscle activity during postural control. Reconstructed muscle activity derived from the TSyID model matched experimentally-recorded EMG for several muscles throughout the lower limb in all conditions (Figure 3.10). The waveforms of EMG reconstructions typically consisted of an initial burst of activity followed by an extended plateau region of muscle activation, which was similar to the time course of recorded EMG waveforms. We previously demonstrated that the feedback decomposition of reconstructed EMG indicates that the initial burst regions of muscle activity was predominated by CoM acceleration feedback, while CoM velocity and displacement feedback contributed to muscle activity during the plateau region (Welch and Ting 2008). Here, we demonstrate that, by modulating 4 feedback parameters, this feedback law is capable of predicting the large variety of temporal muscle activation patterns evoked when perturbation characteristics are altered. TSyID optimizations resulted in a variable set of feedback gains between conditions and subjects (Table 3.3); however, the resulting predictions of muscle activity accounted for >61% of the variability in ankle muscle activity (right-leg SOL and bilateral TA and MG) across all subjects and conditions (VAF = 0.86 ± 0.05). Activity in proximal leg and trunk muscles was also well-reconstructed by the TSyID model, accounting for >27% of variability (VAF = 0.82 ± 0.11).

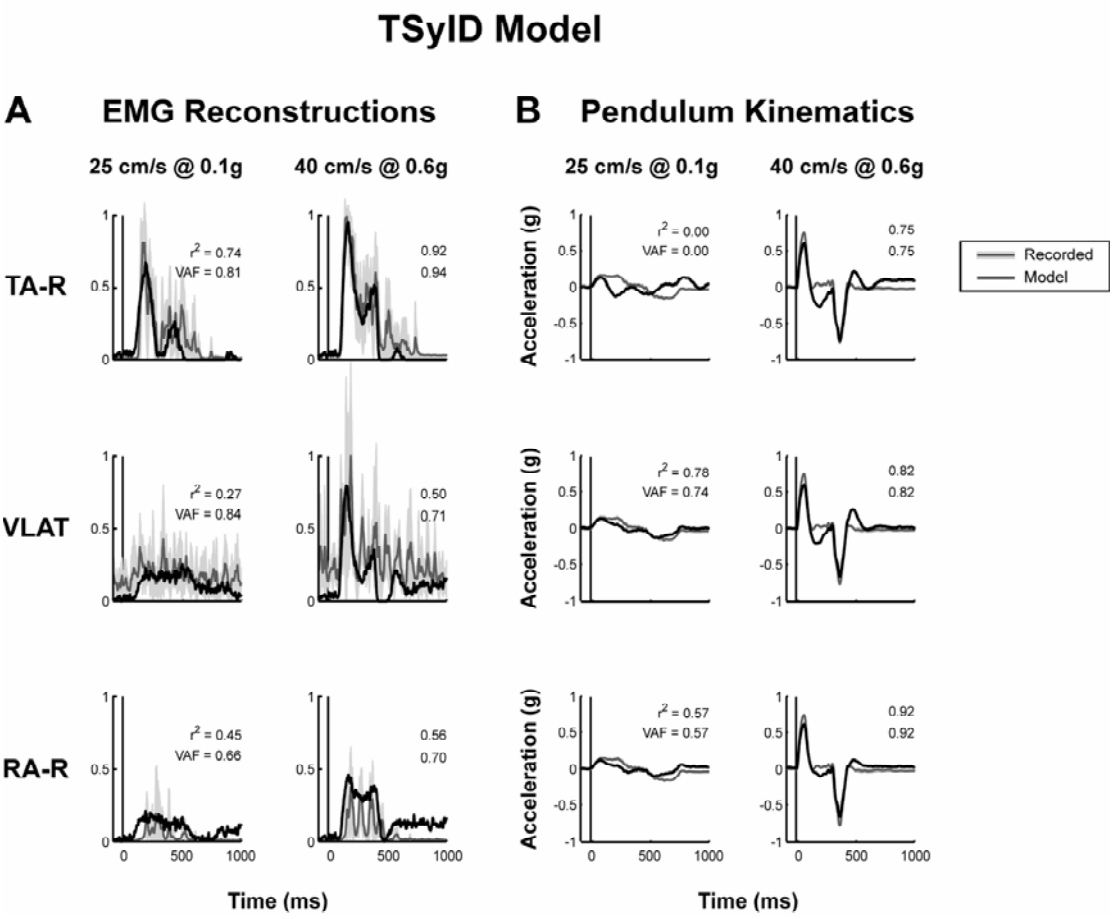

Figure 3.10 TSyID model reconstructions of experimental EMG. The time course of recorded (solid gray) and model-derived (solid black) EMGs and kinematics for low- and high-velocity/acceleration experimental conditions from TSyID simulations of muscles collected from Subject A. Gray shaded regions indicate one standard deviation of the mean recorded signal. **A)** The feedback law on pendulum motion reconstructed experimentally-recorded right-leg tibialis anterior (TA-R) EMG patterns in all conditions with >78% VAF. Proximal muscle activity was reconstructed with varying degrees of success, as indicated by reconstructions of VLAT and RA-R. **B)** Each muscle activation pattern resulted in a unique pattern of pendulum motion because of the interaction between muscle and perturbation torques. Though EMG reconstructions were successful in many conditions, the pendulum kinematics used to make EMG reconstructions for conditions with low peak acceleration and velocity did not match recorded CoM kinematic motion.

Simulations for proximal muscles often resulted in the over-prediction of muscle activity, especially during the plateau region of the response, yielding low VAF in several muscles/conditions. This may have resulted because the low level of activity in these muscles was insufficient to maintain the pendulum in the upright configuration, requiring additional muscle activity to satisfy this terminal constraint. In general, better matches of model reconstructions to experimental data were obtained for accelerations larger than 0.2g, where pendulum kinematics were well-matched to recorded CoM kinematics (kinematic VAF > 66%; kinematic VAF = 0.87 ± 0.08), despite the fact that kinematic matching was not specified in the cost function. Still, the reconstruction of muscle activity from those conditions with accelerations at or below 0.2g resulted in good matches to recorded EMG, however the kinematics of the pendulum often differed substantially from the recorded CoM kinematics (kinematic VAF > 38%; kinematic VAF = 0.68 ± 0.15). This dependence upon kinematic matching for model success, paired with the emergent matching of kinematics without specification within the model, provides strong support for the idea that task-level feedback is encoded within the muscle activity patterns for postural control.

Reconstruction of Muscle Activity using Jigsaw Model

To further investigate the role of kinematic feedback within the formation of muscle activity for postural control, we reconstructed temporal muscle activation patterns using the jigsaw model, which directly transformed recorded CoM kinematics into an EMG reconstruction. Like the reconstructions derived from the pendulum model, jigsaw model EMG reconstructions consisted of an initial burst of activity followed by a plateau region, with a similar time course to recorded EMG data. The jigsaw EMG

reconstructions reproduced recorded EMG with >55% VAF in all muscles and subjects for all conditions (VAF = 0.90 ± 0.06) (Figure 3.11). The model predicted that feedback gains were constant with respect to peak acceleration, but found variable gains with respect to peak velocity. Similar to TSyID model results, jigsaw reconstructions of muscle activity were best in conditions with peak accelerations larger than 0.2g, where >66% of variability was accounted for (VAF = 0.90 ± 0.05); the reconstruction of EMG from conditions with accelerations at or below 0.2g resulted in short, wide initial burst regions in comparison to experimentally-recorded data, accounting for >55% of variability (VAF = 0.90 ± 0.07). This discrepancy was more pronounced in subjects and muscles with EMG patterns that contain strong, well-defined initial burst regions (*e.g.*, all muscles for Subjects A and G; ankle muscles for all subjects).

The reconstruction of muscle activity during low-acceleration conditions was improved by including the transient initial response of the muscle spindle within the jigsaw model formulation. The muscle spindle exhibits an acceleration-dependent burst in firing frequency near the beginning of stretch (Schafer 1967) that is ended abruptly as force and strain accumulate within the fiber, causing cross-bridges to either break or rapidly detach (Henatsch 1971). These cross-bridges then reattach to allow the continued accumulation of fiber force with length changes (Getz et al. 1998). We empirically modeled this 'stiction' response by eliminating acceleration feedback within the jigsaw model from 175 – 300 ms following platform motion onset. This jigsaw model formulation, denoted 'jigsaw model w/ stiction', resulted in the selection of feedback gains that approached constancy for MG, but increased the variability of feedback gains

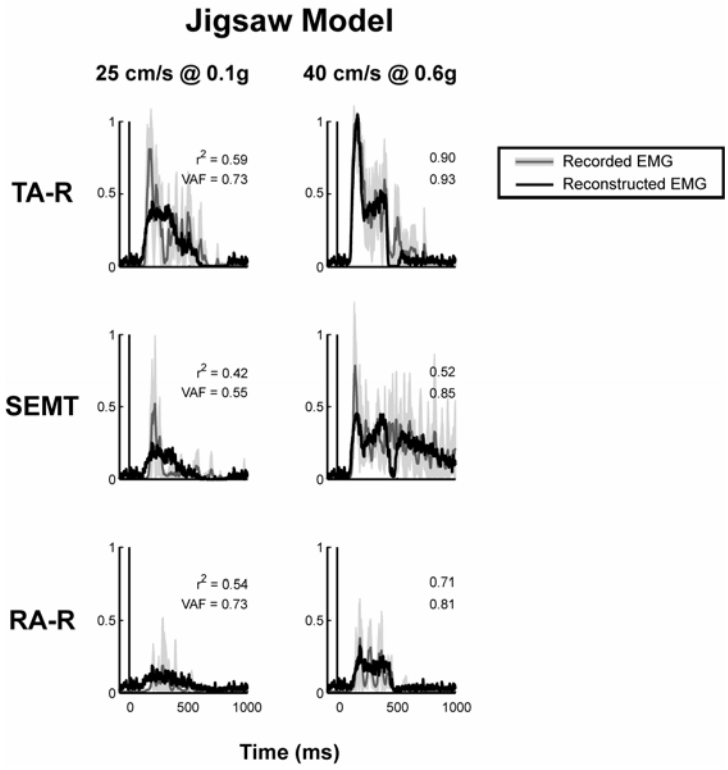

Figure 3.11 Jigsaw model reconstructions of experimental EMG. The time course of recorded (solid gray) and reconstructed (solid black) EMGs for low-velocity/acceleration and high-velocity/acceleration experimental conditions in muscles collected from Subject A. Gray shaded regions indicate one standard deviation of the mean recorded EMG. The feedback law on CoM motion reconstructed experimentally-recorded right-leg tibialis anterior (TA-R) EMG patterns in all conditions with >84% VAF. The reconstruction of EMG in conditions with low acceleration and velocity was less successful, especially during the initial burst region of EMG patterns. Nevertheless, the jigsaw model was capable of reconstructing EMG from all muscles and conditions with >55% VAF across all subjects, suggesting that information related to the control of the CoM is encoded within the EMG used for postural control.

for TA with respect to perturbation condition, though remaining relatively constant (Figure 3.7). Reconstructions of EMG patterns using the jigsaw model w/ stiction were significantly improved for all muscles in conditions with accelerations at or below 0.2g (ΔVAF = -0.05 – 0.22; $p = 1.73 \times 10^{-17}$) and those with accelerations greater than 0.2g (ΔVAF = -0.09 – 0.18; $p = 6.83 \times 10^{-30}$). The observed improvements to model reconstructions were most pronounced in subjects and muscles with strong, well-defined initial burst regions, resulting in well-matched model reconstructions accounting for >61% variability in all subjects, muscles, and conditions (VAF = 0.91 ± 0.05) (Figure 3.12). By showing the direct relationship between CoM kinematics and EMG patterns observed during postural control, these results demonstrate that a feedback law transforming task-related variables to muscle activation patterns may be used to maintain balance during postural disturbances across a range of perturbation characteristics.

Discussion

Our results suggest that the neural mechanisms responsible for postural control reflect feedback control, even at the level of muscle activity. By perturbing a feedback model of postural control with experimentally-recorded acceleration waveforms, we directly assessed the effects of perturbation characteristics on the resulting muscle activation pattern. Through the manipulation of four feedback parameters related to CoM kinematics, three feedback models successfully accounted for the experimentally-observed changes in muscle activity that occur with changes to task conditions, reinforcing the robustness of this feedback law for postural control. While the scaling of muscle activity during specific time periods was accomplished through the independent modulation of four feedback parameters, each subject used a unique and constant set of

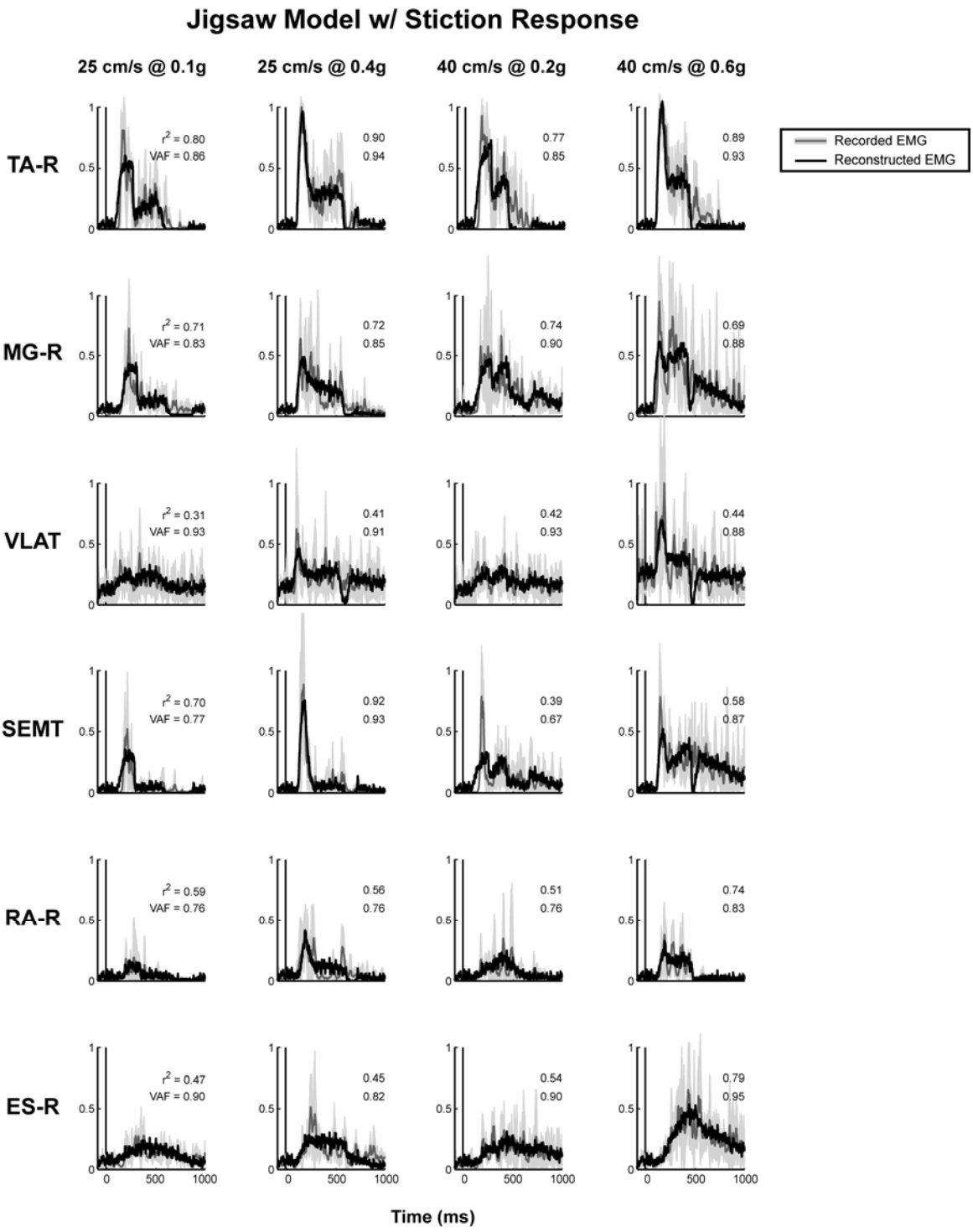

Figure 3.12 EMG reconstructions from modified jigsaw model including spindle stiction response. The time course of recorded (solid gray) and reconstructed (solid black) EMGs for four experimental conditions in several muscles collected from Subject A. Gray shaded regions indicate one standard deviation of the mean recorded EMG. By including the acceleration-dependent stiction response in muscle spindles, the reconstruction of EMG during low acceleration and velocity conditions in all subjects and muscles was improved ($p < 10^{-16}$), without adversely affecting reconstructions at higher acceleration and velocity levels (VAF = 0.91 ± 0.05).

feedback gains, accounting for a wide range of inter-subject and inter-trial variability.

The identification of the scaling relationship between the muscle activity for postural control and peak acceleration and velocity was only possible due to precise control over perturbation dynamics. In previous studies, the attribution of observed scaling phenomena to particular perturbation characteristics was often precluded by the covariation of acceleration and velocity that is typical with many perturbation paradigms (Maki and Ostrovski 1993b; Szturm and Fallang 1998), possibly resulting from the use of controllers in which only the displacement waveform is specified (Brown et al. 2001). In addition, perturbation platforms may have exhibited positional overshoot and an underdamped 'ringing' in the acceleration characteristics of platform motion, similar to our findings with a standard industrial controller (Figure 3.1A). If the postural mechanism shapes its response using feedback of the encountered perturbation, then it can be expected that any intertrial differences in platform motion will alter the resulting response. Therefore, in order to test specific hypotheses regarding the effects of perturbation dynamics on the postural response, strict but flexible control over those dynamics is of critical importance.

The Importance of Feedback in Postural Control

Because of the high redundancy in the muscular patterns that can be used to produce a given kinematic output, previous models that focused on kinematics alone were unable to suggest the consequences of altered feedback on muscle activation patterns for postural control. In order to gain such insight from a feedback model of human posture, a muscle model must be included to translate functional feedback signals into muscle torques. With the addition of a muscle model, the use of higher-order

acceleration feedback signals is required to mitigate time-delayed, low-pass effects in the muscles. Such phase-leading acceleration feedback is also beneficial to offset neural processing and transmission delays, along with delays associated with muscle activation dynamics, leading to more stable system dynamics. By using acceleration information in addition to lower-order feedback, the current model not only successfully reconstructed experimentally-recorded EMG patterns, but also predicted the scaling with perturbation characteristics derived from EMG data collected over a variety of experimental conditions. Without the use of acceleration feedback, realistic EMG patterns do not emerge from model simulations (Welch and Ting 2008).

This feedback structure provides a mechanism to explain the experimentally-observed temporal scaling of muscle activity with perturbation characteristics. The influences of perturbation characteristics highlighted by Diener and colleagues (1988) are demonstrated by the feedback components of our model reconstructions. Consistent with their findings, reconstructed EMG exhibited velocity dependence during the late portions of the initial burst of muscle activity, as well as throughout the plateau region, with the effects of displacement predominant only in the plateau region. Our experimental data may also serve to better clarify the scaling phenomenon reported in their important study. While the current study identified scaling of muscle activity during the initial burst with peak acceleration, which seems to contradict their suggestion that muscle activity during this time period scales with perturbation velocity, when data are evaluated over all conditions rather than at each individual velocity or acceleration level, the results of the two studies are in agreement (Figure 3.13). Velocity scaling is present in the initial burst only if all data are pooled across all conditions; if segregated by acceleration level, when

the peak acceleration is increased, the muscle activation increases to a larger but constant level with respect to velocity (Figure 3.4D). A similar scaling result can be observed with acceleration during plateau region if data are pooled together, but not when separated by velocity level. These results suggest that the velocity scaling previously observed during the initial burst of muscle activity may have resulted from the interaction between acceleration and velocity feedback due to their temporal overlap.

The scaling of postural responses to perturbation acceleration suggests that acceleration information is available to the CNS, although the specific sensory modalities are not known. Cutaneous receptors, such as plantar mechanoreceptors in the foot, may transmit shear force information when stimulated by the onset of platform motion that is proportional to horizontal accelerations (Maki and Ostrovski 1993b; Morasso et al. 1999). Acceleration information may also be derived from Golgi tendon organs, which are very sensitive to muscle tension (Gregory et al. 2002; Houk and Simon 1967). Golgi tendon organs also play a role in the formation of muscle activity for weight support (Dietz 1998; Dietz et al. 1992) further suggesting their role in providing feedback for postural control.

The muscle spindle stretch response exhibits a burst in firing frequency at the onset of stretch, which has been shown to scale with stretch acceleration (Schafer 1967), and may represent the local acceleration of the part of the muscle in which the spindle is embedded (Schafer and Kijewski 1974). This acceleration response likely results from stiction within the intrafusal fiber (Jansen and Matthews 1962; Lennerstrand and Thoden 1968). As the fiber is stretched, force accumulates due to the resistance to stretch of

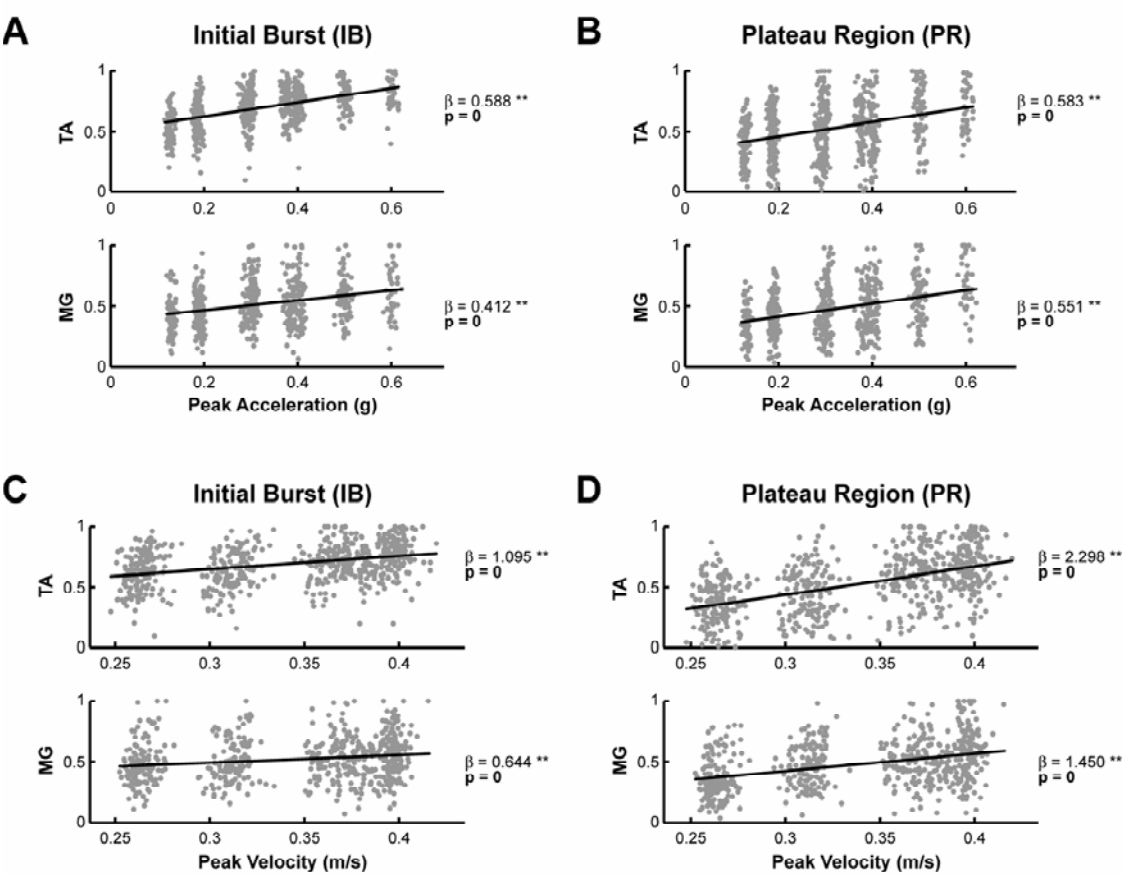

Figure 3.13 The interaction between acceleration and velocity masks results when data from all conditions are pooled. A) When pooled together, data suggest significant scaling of the initial burst (IB) with both peak acceleration and velocity ($p < 10^{-16}$). **B)** A similar trend of both acceleration and velocity scaling appears in the plateau region ($p < 10^{-16}$). These universal scaling trends may occur due to the interactions between acceleration and velocity feedback during postural control. Significant regression results are indicated by ** ($p < 10^{-5}$), with p-values in **bold** font.

temporarily-attached actin-myosin complexes. The end of this acceleration response was initially thought to result from the breaking of these actin-myosin complexes as force within the fiber increases (Henatsch 1971), however modeling efforts demonstrated that the forces within the muscle spindle are consistent with the detaching of cross-bridges in prepowerstroke phase at a critical strain level (Getz et al. 1998). We hypothesize that this process may end the encoding of acceleration feedback by the spindle. After detaching, these cross-bridges rapidly reattach, allowing for further increases in force with length changes (Getz et al. 1998), and thereby allowing for the renewed encoding of acceleration feedback.

The duration of the initial burst in spindle firing frequency also varies with respect to the acceleration and velocity characteristics of the stretch. In fast stretches to the muscle spindle at ~12% resting length per second, the initial burst was characterized by a sharp elevation in firing frequency of a few spikes, lasting only tens of milliseconds (Haftel et al. 2004). However, in slow 2°/s wrist movements, eliciting slower stretches to the muscle spindle of ~0.2% resting length per second, the initial burst was broader, lasting up to 500 ms (Cordo et al. 2002). In our modified jigsaw model, we empirically selected the time period during which acceleration feedback was removed to begin 175 ms following perturbation. Using published human muscle morphometric data for TA (Maganaris et al. 1999) and the measured angular movement of the ankle during our postural perturbations, we estimate that the stretches experienced by muscles spindles in the present study to be ~1–2% resting length per second, which lies within the range established by these previous studies. Together, this may serve to explain the observed

short-duration initial burst periods for recorded EMG during low-acceleration conditions, where the broad initial CoM acceleration lasts in excess of 175 ms.

Feedback of Task-Level Variables for Postural Control

Are local variables, such as joint angles, sufficient to provide feedback for postural control? An examination of joint angular kinematics reveals that these local signals reflect neither the motion of the CoM nor that of the platform itself (Figure 3.14). In fact, the initial direction of changes in joint kinematics upon perturbation were not consistent between conditions, even within the same subject. These changes also occurred in close timing with the onset of EMG, especially in slower perturbations, lending them inappropriate as feedback signals for muscle activity formation (Figure 3.14, right panel). Further, joint kinematic changes did not scale with platform motion characteristics, suggesting that the local joint changes may be an inappropriate signal for feedback control for balance. Instead, our experimental data corroborated by modeling simulations demonstrate that feedback related to CoM kinematics, a global task-related variable, is likely used to create appropriately-scaled responses in the face of postural perturbations.

The nervous system may derive a global estimate of the destabilizing effects of a postural perturbation through the integration of multiple sensory channels. Spatial patterns of muscle activation in the legs, trunk, and neck during the automatic postural response cannot be attributed to any single somatosensory or vestibular signal, but require multisensory integration, whether subjects are standing (Carpenter et al. 1999; Inglis and Macpherson 1995; Keshner et al. 1988; Ting and Macpherson 2004) or seated

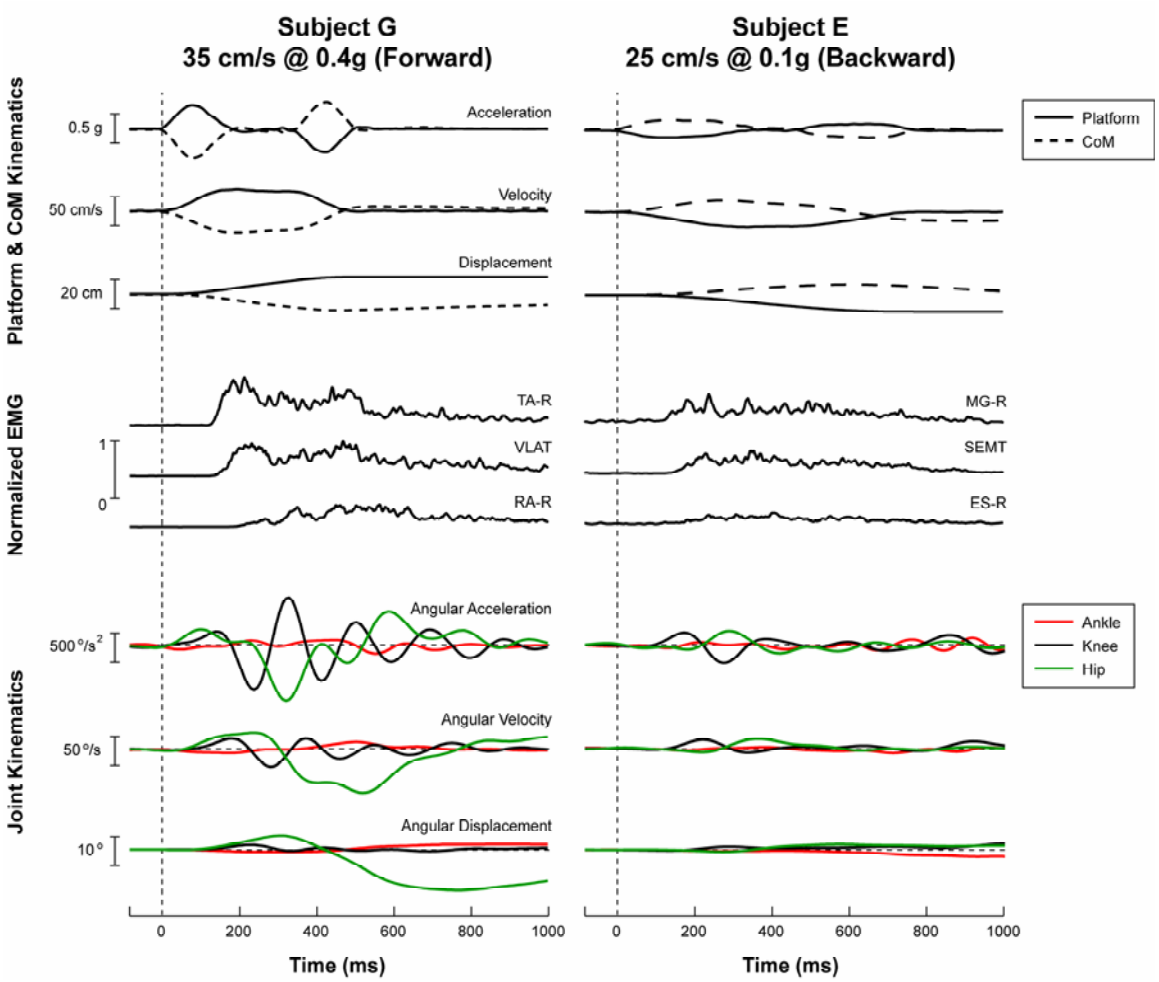

Figure 3.14 A comparison of platform, CoM, and joint angular kinematics. The acceleration, velocity, and displacement signals, each as related to platform, CoM, and joint motion, are illustrated for Subject G in response to a forward perturbation of 35 cm/s at 0.4g (left panel) and for Subject E in response to a backward perturbation of 25 cm/s at 0.1g (right panel). Positive joint angular kinematics indicate ankle plantar flexion, knee extension, and hip extension. While platform and CoM motion seem to have similar kinematic characteristics which are reflected in the magnitude of EMG patterns elicited following the perturbations, joint angular kinematics show significant deviation from these patterns of motion, characterized by high frequency variations of angular acceleration and velocity. In slower perturbations, the timing of joint angle changes occurs in close proximity to the onset of EMG – too late to be used as a feedback signal for the formation of muscle activation patterns. In addition, the timing of joint angular deflections does not correspond to the timing of muscle activity at the respective joints. Further, the initial direction of joint motion varied between conditions and peak joint excursion did not scale with respect to perturbation characteristics. Together, these observations suggest that local variables, such as joint motion, are not an appropriate signal for feedback-mediated postural control.

(Forssberg and Hirschfeld 1994; Keshner 2003). Moreover, when similar postural response patterns are observed across a variety of conditions, the only variable that correlates with the spatial pattern of the response is total body CoM excursion (Gollhofer et al. 1989; Nashner 1977), which cannot be estimated from any single sensory channel. For example, rotations and translations of the support surface that elicit similar patterns of muscle activation induce *opposite* changes in joint angles, but *similar* changes in CoM displacement in both humans and cats (Carpenter et al. 1999; Diener et al. 1983; Nardone et al. 1990; Ting and Macpherson 2004).

An estimate of CoM motion may be used for postural control, as similar task-level global variables are represented at many levels in the nervous system. CoM kinematics are more tightly regulated in postural control than are individual joint angles (Allum and Carpenter 2005; Brown et al. 2001; Gollhofer et al. 1989; Krishnamoorthy et al. 2003; Szturm and Fallang 1998). Similarly, it has been shown that the hand trajectory is well-controlled in reaching tasks (Adamovich et al. 2001; Tseng et al. 2002), and global variables such as hand direction, velocity, and end-point force are encoded in the primate motor cortex (Georgopoulos et al. 1992; Georgopoulos et al. 1986; Scott and Kalaska 1997). Even at the level of the spinal cord, global variables such as leg length, orientation, velocity, and end-point force are computed from the ensemble of sensory receptor information (Bosco and Poppele 2001; 1997; Bosco et al. 1996; Lemay and Grill 2004; Poppele et al. 2002).

A feedback rule based on CoM kinematics might be used by the nervous system to control muscle activity for postural control. Theoretical studies suggest that the nervous system controls movements using a low-dimensional, hierarchal feedback

control law (Todorov 2004). Under such a control scheme, a small set of descending neural commands is distributed among the multiple muscles. Here, our results suggest that a consistent feedback relationship based on CoM kinematics exists across a number of muscles throughout the body (also in cats by Lockhart and Ting 2007) and that the number of descending signals to modulate these muscles is limited. Muscle synergies have been suggested as a neural strategy to simplify the coordination of multiple muscles during postural tasks using only a few neural commands. Previously, muscle synergy activation has been correlated to anteroposterior CoM motion during anticipatory postural adjustments (Krishnamoorthy et al. 2003). Further, postural perturbation studies indicate that muscle synergy activation level is modulated by the direction of the postural disturbance (Torres-Oviedo et al. 2006; Torres-Oviedo and Ting 2007), suggesting the involvement of task-related feedback in the simultaneous coordination of multiple muscles. While a feedback relationship describing responses to mediolateral perturbations has yet to be established, it is possible that the limited set of muscles synergies previously identified in multi-directional postural perturbations in cats (Ting and Macpherson 2005; Torres-Oviedo et al. 2006) and humans (Torres-Oviedo and Ting 2007) is modulated by temporal command signals arising from neural feedback mechanisms related to global variables such as CoM kinematics.

Optimal Feedback Patterns for Postural Control

Our modeling efforts were intended to demonstrate principles underlying the development of muscle activation patterns following perturbation, not to make predictions of the exact postural responses that should be evoked. In order to make such predictions, a more complex model containing additional pendulum links might be

necessary to better match subject kinematics during postural responses, which often contain a mixture of ankle and hip motions (Alexandrov et al. 2001a; Horak and Nashner 1986; Runge et al. 1999). The addition of pendulum links would require the simultaneous prediction or reconstruction of multiple muscles, each controlling a separate pendulum joint, which is computationally expensive. Also, because a wide range of muscle activation patterns result in similar CoM kinematics, including those muscle responses without acceleration feedback (Lockhart and Ting 2007; Welch and Ting 2008), the quadratic cost function used for the selection of feedback gains may not be sensitive enough to represent small changes in perturbation dynamics. This idea is supported by our observations that both simulations with constant feedback gains and those in which the controller selects gains for each perturbation condition result in similar matches to recorded EMG patterns. A feedback scheme that schedules response-strategy-specific gains may improve the optimization of feedback gains for postural control (Jo and Massaquoi 2004), resulting in different sets of feedback gains for ankle and hip strategies. In addition, the use of time-varying gains near the beginning and end of trajectories may improve the accuracy of model predictions during those periods in time when initial conditions and terminal objectives may take precedence (Kuo 1995). This may be the source of mismatched predictions for muscles with moderate level activity, where objectives to maintain an upright configuration may cause an over-prediction of muscle activity near the end of simulation. However, by using all three feedback signals simultaneously to develop a prediction of muscle activity, the model is successful at demonstrating the interactions between acceleration, velocity, and displacement feedback. The model suggests that the CNS takes advantage of the naturally-occurring

physical relationships between acceleration, velocity, and displacement to provide feedback control of the CoM during perturbations to quiet stance.

Our human subjects responded to postural perturbations with muscle activity that merely resembled but did not reflect optimal feedback control. Optimal feedback predictions suggested that feedback gains for postural control should be adjusted with respect to perturbation characteristics, while the data-matching jigsaw model suggested that the feedback parameters used by the subjects were, in actuality, invariant. The scaling relationships of optimal velocity and position gains with perturbation characteristics were relatively constant and closely matched the relationships identified by the jigsaw model. However, of particular interest are the optimal predictions of acceleration gain – a parameter that produces the initial muscle response to perturbation. Optimal acceleration gains were predicted to dramatically decrease with peak acceleration and increase with respect to peak velocity; this change was five-fold at the highest velocity and lowest acceleration levels, respectively. This optimal control strategy reflects the optimality criteria specified for the DQR model. Acceleration gains increase with respect to velocity, allowing for a strong initial reaction to help prevent significant deviation from an upright configuration. Similarly, acceleration gain is highest during low acceleration perturbations, promoting a robust initial response to prevent large destabilization. Concurrently, to minimize total muscle activation, acceleration gain is decreased at high acceleration levels, where large gains would result in very strong muscle activation.

Human subjects may achieve an optimal strategy for postural control with additional training. Our previous studies suggest that postural responses in cats reflect

optimal feedback control (Lockhart and Ting 2007). These cats underwent an extensive training regimen over the course of several months before they were included within the postural studies. On the other hand, human subjects that participated in the current study were naïve to postural control experiments and were only exposed to the platform paradigm for one hour total during the experimental session. With additional exposure to postural perturbations, human subjects may eventually learn to adjust their feedback gains with respect to perturbation strength to allow for a reduction in neural effort and kinematic deviation. Alternatively, as suggested by the results of the current study, humans may simplify postural control by using an invariant feedback scheme for the formation of reactive muscle activity.

CHAPTER 4

A FEEDBACK MODEL EXPLAINS ADAPTATION OF MUSCLE ACTIVITY FOR HUMAN POSTURAL CONTROL

This chapter is in preparation for submission to *Nature*:

Welch TDJ and Ting LH. Searching for optimal motor patterns in balance. (in prep)

Abstract

Our goal is to understand the mechanisms used during the adaptation of balance control to repetitive or changing task conditions. We hypothesized that, similar to the adaptation of voluntary movements, the nervous system uses both feedback and feedforward mechanisms to adapt the automatic postural response to repetitive and unexpected perturbations. We perturbed the balance of naïve human subjects with repetitive unidirectional and reversing support-surface translations and characterized the time course of changes in CoM motion, as well as tibialis anterior (TA) and medial gastrocnemius (MG) activity. We then compared the experimental EMG patterns to the pattern predicted by an optimal feedback control model. We predicted that the feedback model could account for the adaptive changes to EMG through the adjustment of four feedback parameters. Further, if feedforward mechanisms were involved, we predicted that inappropriate TA responses to reversing perturbations would be gradually eliminated, while the MG response would advance in time, anticipating the change of perturbation direction. We found that, in response to reversing perturbations, subjects did

not use the predicted feedforward mechanisms to anticipate platform reversal. However, several other anticipatory strategies were observed, suggesting the use of more subtle, biomechanically-related feedforward changes to the response strategy. By modifying four feedback parameters, the feedback model accounted for 80% of the variability in all observed EMG patterns as subjects adapted their responses. An optimal feedback model demonstrated that subjects were navigating toward the optimal solution for postural control based on the minimizing motion of the CoM and total muscle activation.

Introduction

From infancy to adulthood, humans show the capacity for motor learning in a variety of contexts. During early development, the task of motor learning as related to postural control, such as learning to sit upright, stand, and walk, is quite difficult and takes several years to master. For example, human infants can produce direction-specific postural adjustments from the age of one month (Hedberg et al. 2004). However, until aged three months, these postural responses show large variability and are not well-adapted to environmental constraints (Hedberg et al. 2005). Over the next six months, infants begin to develop more expert control over postural muscle activity and adapt their responses to be appropriate for specific situational balance challenges (Hadders-Algra et al. 1996; van der Fits et al. 1999). Still, the adult patterns of postural adaptation are not well-developed until adolescence (van der Heide et al. 2003). With age and experience, humans become skilled learners that can adapt quickly to new postural situations, such as standing on a boat or walking across unknown terrains, within minutes of first exposure. In addition, humans can adapt their balance mechanisms when the postural system is compromised, whether by neuromuscular deficit (Alessandrini et al. 2003; Horak and

Hlavacka 2001; Visser and Bloem 2005), musculoskeletal injury (Demeritt et al. 2002; Myer et al. 2006), or amputation (Geurts et al. 1991; Mouchnino et al. 1998). What are the signals and mechanisms used to train the postural system during motor adaptation?

Much of what is known regarding motor adaptation has been learned from studies of voluntary arm reaching movements (e.g., Shadmehr and Mussa-Ivaldi 1994; Takahashi et al. 2001). Typically, subjects perform several center-out arm movements with a robotic manipulandum that can apply a viscous force field to alter the arm trajectory. The subjects first perform movements in a null force field to become acclimated to the use of the robotic manipulandum. Next, reaches are made in a velocity-dependent force field that immediately changes reach paths from straight to curved trajectories; as subjects adjust their reaching strategy, these errors in trajectory are eventually eliminated. Finally, the subjects repeat reaches in the null field; this changed reaching environment causes large errors, in the opposite direction of those observed in the viscous force field, which are gradually eliminated as the reaching strategy readapts.

Results from these arm reaching studies suggest that both feedback and feedforward mechanisms are used to adapt volitional movements. Online feedback is used to correct the trajectory of arm movements, yet feedback alone will only reduce errors – not eliminate them – for ongoing movements (Hwang and Shadmehr 2005). Further, the learning of the novel reaching task is not accomplished simply by memorizing the performance of previous trials, as learning generalizes to other types of movements, including movements to other directions (Sainburg et al. 1999), using different arm configurations (Morton et al. 2001; Shadmehr and Moussavi 2000), with different trajectories (Conditt et al. 1997; Goodbody and Wolpert 1998), and those of the

other arm (Criscimagna-Hemminger et al. 2003; Morton et al. 2001). To eliminate movement error, the initial trajectory of the next trial is modified in a feedforward manner using the error-driven motor response of previous erroneous trials (Thoroughman and Shadmehr 1999). These feedforward adaptations are incorporated into the internal model for planning the movement, changing both the motor command executed and the expected sensory feedback resulting from that movement (Flanagan and Wing 1997; Gandolfo et al. 1996; Lackner and Dizio 1994; Miall et al. 1993; Shadmehr and Mussa-Ivaldi 1994; Takahashi et al. 2001). Many studies have characterized the adaptation of reaching movements by observing task-related variables, such as end-point trajectory. However, by examining the corresponding changes in electromyographic activity (which is the output of the nervous system that represents the internal model prediction), Thoroughman and Shadmehr (1999) revealed the feedback-mediated modification of the internal model with training. Their results indicated that force-field-appropriate EMG began as a delayed feedback response to the perturbing force and was progressively initiated earlier within the movement, until appropriate muscles were activated in a feedforward manner, before sensory information regarding the perturbation was available. Do these same principles apply to the adaptation of postural tasks?

The adaptation of involuntary motor tasks, such as the automatic postural response, has not been explored extensively. Unlike volitional arm movements, the automatic postural response is a reactionary task, typically observed in response to a postural perturbation such as support surface translation or rotation, and its related muscle activity is formed using feedback of ongoing center-of-mass (CoM) motion (Lockhart and Ting 2007; Welch and Ting in prep), presumably derived through the

integration of information from a variety of sensory receptors. Adaptation of leg and trunk muscle activity during the postural response is considered to be formed by *central set*, defined as the changes that occur over many trials with the same sensory conditions due to CNS plasticity (Horak 1996; Keshner et al. 1987). However, postural adaptation is difficult to study because adaptation of the APR occurs over much fewer trials than that for other motor responses (Lisberger 1988) and is often masked by differences associated with subtle changes in biomechanical configuration and sensory signals (Horak 1996). In addition, monotonous or repetitive sensory input is known to cause habituation, which is characterized by a decrease in attention to repetitive sensory signals resulting in the waning of response amplitude. Changes in muscle activity due to habituation can therefore be easily mistaken with adaptive changes. The automatic postural response is thought to exhibit habituation, as muscle activation level decreases when the same perturbation is given in succession (Chong et al. 1999; Hansen et al. 1988; Horak et al. 1989; Timmann and Horak 1997). A few studies have investigated the differences that arise when perturbations are presented at random as opposed to serial blocks. Specifically, these authors highlight bracing strategies to reduce muscle stress (Blouin et al. 2003), anticipatory changes in muscle activity in response to previous experience with velocity and displacement (Horak et al. 1989), and the anticipation of the timing of platform deceleration (Carpenter et al. 2005). However, none have performed quantitative analysis on individual muscle activation patterns, in conjunction with task kinematics, to illustrate the trial-by-trial adaptation of the automatic responses that are evoked following postural perturbation and their effects on task performance (*i.e.*, maintaining upright stance).

In the current study, our goal was to characterize the trial-by-trial adaptive changes in muscle activity and CoM motion during human postural responses to repetitive perturbations. We hypothesized that, similar to the adaptation of voluntary motor tasks, the human postural mechanism uses both feedback and feedforward strategies to adapt to both repetitive and changing task conditions. We assessed CoM motion and EMG patterns during responses to both unidirectional and reversing support surface translations. Our experimental design is inspired by that of previous arm reaching studies; however, repetitive movements in a force field were replaced with a countermanding task, similar to those used in the study of saccadic eye movements (e.g., Hanes and Carpenter 1999; Lappin and Eriksen 1966). Here, we tested the mutability of the automatic postural response by reversing the direction of platform motion at or before the expected timing of the initial EMG response, yielding this response inappropriate and destabilizing. To determine whether feedforward mechanisms can be exploited during the adaptation of postural responses, we examined the trial-by-trial changes in EMG activity to answer two questions: 1) can the inappropriate initial EMG response be eliminated from the response strategy; and 2) can the EMG response to the reversed platform motion be advanced in time to anticipate and minimize the disturbance caused by the secondary perturbation. Next, we investigated the changes to the postural mechanism in the context of a feedback model of postural control (Welch and Ting in prep), by examining the adjustment of four feedback parameters during repetitive perturbations.

Our results demonstrate that feedforward mechanisms may not be used to completely mute or advance the timing of feedback-mediated postural responses in anticipation of postural perturbations. However, initial lean and up-regulation of leg

stiffness through co-contraction can be used to mitigate the effects of expected perturbations in a feedforward manner. These changes in muscle activity were represented as smooth, unidirectional changes to feedback gains in the context of a model of postural control. As subjects adapted their postural response strategy, they moved toward an optimal solution for postural control based on the minimization of kinematic deviation and total muscle activation, suggesting that motor learning processes involve the directed optimization of both task performance and energy expenditure.

Methods

Data Collection

Fifteen healthy subjects (7 male, 8 female), ages 22.5 ± 3.2 years (mean ± SD), were recruited from the Georgia Institute of Technology student population to participate in an experimental protocol that was approved by both the Georgia Institute of Technology and Emory University Internal Review Boards. All subjects signed an informed consent form before participating and indicated that they were naïve to postural control studies and had never experienced a perturbation on a moveable platform. Subjects stood with weight evenly distributed upon two force plates installed on a moveable platform that could translate in the horizontal plane. Subjects focused vision to a scenic view 4.6 meters away and were instructed to cross their arms at chest-level and react naturally to the support surface perturbations.

During postural perturbations, platform acceleration and position, and surface EMG from fifteen muscles in the legs and trunk were collected at 1080 Hz, synchronized with body segment kinematics collected at 120 Hz. Data collection for each trial lasted for 3 seconds, including a 500-ms quiet period before platform motion onset. Platform

signals were low-pass filtered at 30 Hz (3rd order zero-lag Butterworth filter). Platform velocity was calculated by numerical differentiation of the filtered platform position. The current study focused on EMGs collected from right-leg tibialis anterior (TA) and medial gastrocnemius (MG). Raw EMG signals were high-pass filtered at 35 Hz (3rd order zero-lag Butterworth filter), demeaned, half-wave rectified, and low-pass filtered at 40 Hz (1st order zero-lag Butterworth filter). Center of mass motion was calculated from kinematic data as a weighted sum of segmental masses. Body segment kinematics were recorded with a 6-camera motion analysis system (Vicon; Centennial, CO) using a custom bilateral Helen Hayes 25-marker set that included head-arms-trunk (HAT), thigh, and shank-foot segments.

Experimental Protocol

Without acclimatization to platform motion, subjects participated in a paradigm consisting of 150 anterior-posterior support surface translations designed to examine the changes in feedback and feedforward elements associated with the adaptation of the automatic postural response (Figure 4.1). As their first experience of a postural perturbation, subjects were subjected to a series of 30 unidirectional forward perturbations (peak acceleration = 0.4g; peak velocity = 35 cm/s; total excursion = 12 cm), herein denoted as the Training session. Without notice, the perturbation was changed to a series of 60 reversing perturbations (Reversal). These perturbations began in the forward direction, with the same motion characteristics as the Training session, but reversed directions after 100 ms, traveling 12 cm in the backward direction. The timing of platform reversal was selected to coincide with the approximate timing of the TA response to the initial platform motion. After the Reversal session, the perturbation was

unexpectedly changed to another series of 30 unidirectional forward perturbations (Washout), matching the motion characteristics of the Training session. A minimum of five minutes mandatory seated rest was enforced after every 60 perturbations to reduce the effects of muscular fatigue. This requirement split the Reversal session into two sets of 30 perturbations.

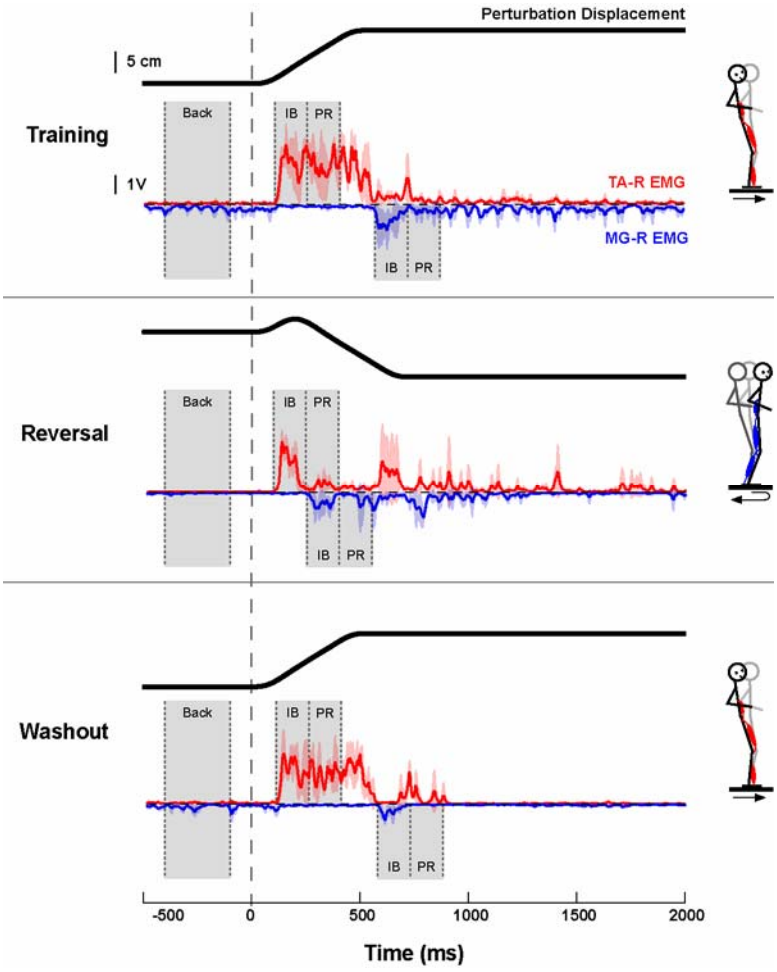

Figure 4.1 Experimental protocol and example EMG data. Representative data from Subject M describing the platform displacement and the resulting EMG for the administered experimental protocol. Completely naïve subjects encountered 30 unidirectional forward perturbations (Training), which elicited TA muscle activity. Then, the platform motion was unexpectedly changed to forward perturbations that reversed directions after 100 ms (Reversal), chosen to approximately coincide with the timing of TA onset. After 60 reversing perturbations, the platform motion was again unexpectedly changed to a set of 30 unidirectional forward perturbations (Washout), allowing the observation of any feedforward adaptations to the response strategy. Mean EMG was evaluated during a 300-ms background period before platform motion (Back) and two consecutive 150-ms time periods following muscle onset – the initial burst (IB) and the plateau region (PR).

Data Analysis

The trial-by-trial adaptive changes in postural performance and control were quantified by examining the motion characteristics of the CoM and the magnitude and onset latency of the EMG response. Peak CoM excursion and velocity in the forward and backward directions were calculated during each trial and averaged across subjects. Those trials that elicited a stepping response were not included in these data averages, but were preserved for the examination of the transition from stepping to non-stepping postural responses. Recorded EMG was examined during a 300-ms background time period (Back) before platform motion and two consecutive 150-ms time periods following muscle onset — the initial burst (IB) and plateau region (PR) (Figure 4.1). Mean EMG during each time period, as well as muscle onset latency, was calculated for each trial, normalized to the average value across the first three trials of the Training session, and averaged across subjects. Exponential fit analysis with respect to trial number was used to quantify the time course of the adaptation of all measured parameters, as indicated by the time constant, τ. The goodness-of-fit of each exponential fit was evaluated using Pearson's correlation coefficient, r^2. Additionally, paired t-test analysis ($\alpha = 0.05$) was used to determine statistically significant changes between the first and last trials of each session for each measured parameter.

Feedback Models

We used three previously-described models to investigate whether the adaptive changes to the postural response strategy during repetitive perturbations could be explained by adjusting gains in a feedback law for postural control (Welch and Ting in prep). Briefly, the models derived muscle activation patterns (EMG_p) through the linear

combination of delayed feedback regarding CoM kinematics (acceleration, velocity, and displacement), either recorded during experimental manipulation or predicted by an inverted pendulum model of standing balance:

$$EMG_p = k_p p(t-\lambda) + k_v v(t-\lambda) + k_a a(t-\lambda). \quad (1)$$

In the 'jigsaw' model, recorded CoM kinematics were used to directly reconstruct experimentally-observed EMG patterns (Figure 4.2A). A single feedback delay (λ) and feedback gains on each kinematic channel (k_p, k_v, k_a) were chosen to develop model reconstructions that match recorded EMG data. The temporal systems identification (TSyID) model also chose feedback parameters to match model reconstructions to recorded EMG data, but derived CoM kinematics from an inverted pendulum model that was perturbed by experimentally-recorded acceleration waveforms (Figure 4.2B). In addition, this model penalized solutions that did not result in an upright pendulum configuration. The inverted pendulum model was scaled to each subject by adjusting the mass (m) and height (h) of the pendulum. The final model, termed the delayed quadratic regulator (DQR) model, used the model formulation of the TSyID model to create an optimal prediction of muscle activation patterns. The DQR model does not use recorded data, but rather develops an optimal solution by minimizing both the total muscle activation level and the kinematic deviation of the pendulum from the upright configuration. While the feedback parameters derived from the jigsaw and TSyID models may change with each recorded EMG waveform, those derived from the DQR model represent the optimal feedback parameters for responding to a given perturbation and therefore do not change with respect to the muscle activation pattern or with repetition of the perturbation.

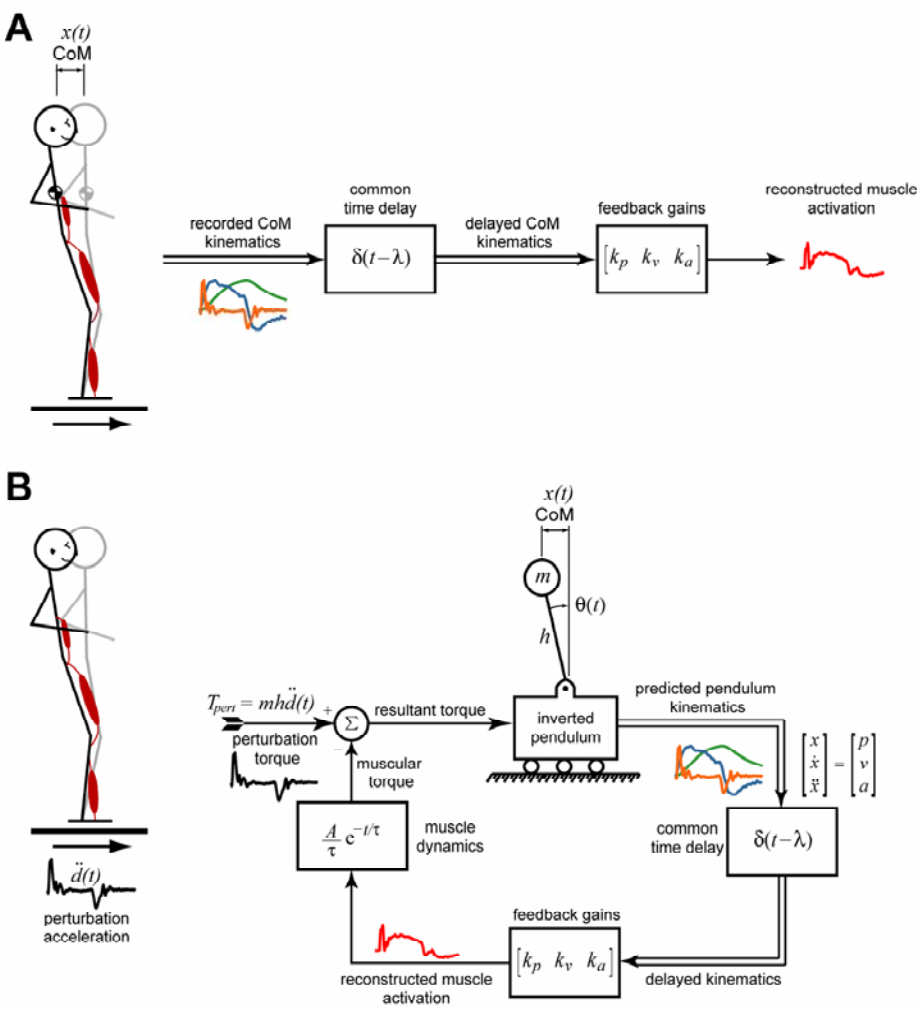

Figure 4.2 Feedback models for responding to unidirectional perturbations. A) To examine the changes in the feedback parameters responsible for the formation of muscular responses during repetitive unidirectional perturbations, the jigsaw model was used to reconstruct muscle activity directly from CoM kinematic motions. Recorded CoM kinematic signals (acceleration, velocity, and displacement) were delayed, weighted by feedback gains on each channel, and summed to provide a reconstruction of recorded EMG responses. The feedback delay and gains were chosen to minimize the error between the model reconstruction and recorded EMG signals. **B)** An inverted pendulum model of human balance was used to further examine the extent to which feedback parameters were adapted to respond to repetitive unidirectional perturbations. The height (h) and mass (m) of the inverted pendulum model was adjusted to fit the measurements of each individual subject. The inverted pendulum model was perturbed using torques calculated from experimentally recorded platform motion. The horizontal kinematics (acceleration, velocity, and displacement) of the pendulum model were delayed, weighted by feedback gains on each channel, and summed to provide a reconstruction (in the case of the TSyID model) or prediction (in the case of the DQR model) of EMG responses. A first-order muscle model was then used to convert this model-derived muscle activity into a muscular torque to counteract the perturbation. For the TSyID model, feedback parameters were chosen to provide the best match between reconstructed muscle activity and recorded EMG data. For the DQR model, the optimal feedback solution was determined by optimizing feedback parameters that resulted in minimal deviation from the upright configuration and minimal muscle activation levels.

The recorded platform and CoM (or pendulum) motion for each subject and trial were used to develop model reconstructions of recorded EMG waveforms or optimal feedback solutions. However, because the antagonistic action of two muscles was required to respond to reversing perturbations, a two-muscle variation of each model was created that simultaneously reconstructed muscle activity from antagonistic pairs during the Reversal session (Figure 4.3); muscle activity from the Training and Washout sessions was reconstructed using the one-muscle models illustrated in Figure 4.2. DQR predictions for all sessions were also made using the two-muscle model to better estimate the optimal roles of antagonistic muscles. This model optimized a separate set of feedback parameters for each muscle by using a direct copy of CoM kinematics for the prediction of the EMG from one muscle (e.g., TA) and the additive inverse of CoM kinematics for the prediction of the antagonist EMG (e.g., MG). In the pendulum-based models, the torques generated by each muscle were then summed to determine the total reactive torque for counteracting the perturbation.

For all modeling results, the goodness-of-fit between model-derived muscle activation patterns and recorded EMG were determined by calculating the coefficient of determination (r^2) and the uncentered coefficient of determination (variability accounted for; VAF). Next, we performed exponential fit analysis of mean feedback parameters with respect to trial number to reveal the time course of changes in the feedback mechanism for postural control. We also performed a paired t-test on each feedback parameter ($\alpha = 0.05$) to determine whether these feedback parameters changed significantly due to repetitive perturbation conditions. Finally, to track the optimization of human responses, the error between recorded EMG and the optimal feedback solution

was calculated for each trial as the sample-by-sample difference between EMG patterns and the optimal solution normalized by the number of data samples.

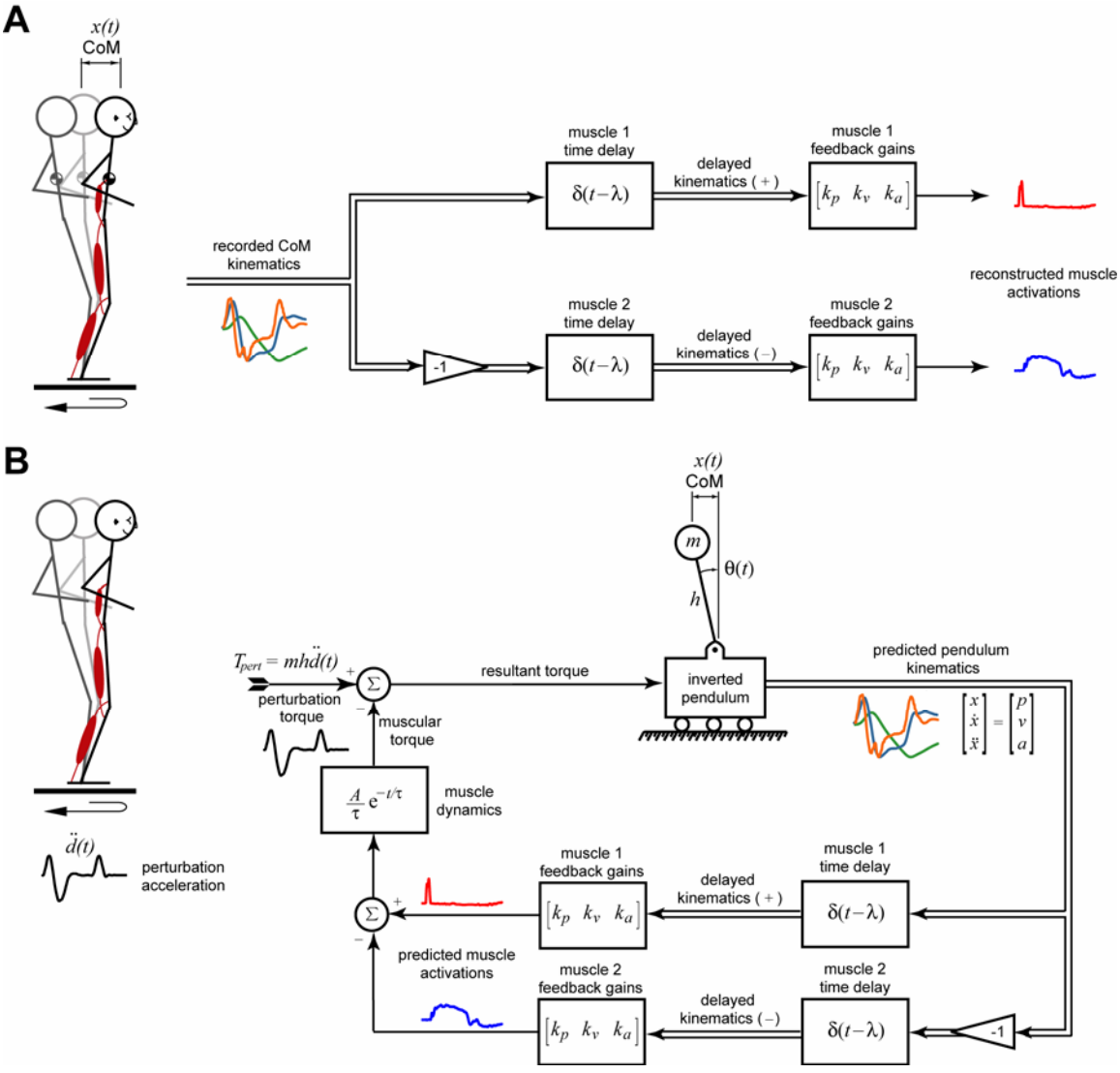

Figure 4.3 Feedback models for responding to reversing perturbations. Feedback models that simultaneously reconstructed or predicted muscle activity in antagonistic muscles were used to evaluate changes in feedback parameters during repetitive reversing perturbations. The general model configuration was similar between the one-muscle models (see Figure 4.2) and the two-muscle models. However, the two-muscle models allowed an agonist muscle to respond to forward-directed kinematic signals and an antagonist muscle to respond to the opposite kinematic signals, corresponding to backward-directed kinematic feedback (calculated as the additive inverse of the CoM or pendulum kinematics). **A)** The jigsaw model simulations chose separate feedback delays and gains for each antagonistic pair to match recorded EMG data. **B)** Similarly, the pendulum models chose separate feedback delays and gains for each antagonistic pair, either to match recorded EMG data (TSyID model) or to determine the optimal solution that minimized both muscle activation and pendulum deviation from the upright configuration.

Results

Here, we characterized the trial-by-trial changes to CoM motion (task performance) and muscle activity (motor control) during adaptation to repetitive and changing postural perturbations. We observed gradual changes to CoM motion with repetitive trials of each perturbation type, identifying a continuum between stepping and non-stepping postural responses. Associated with these kinematic changes, changes in muscle activity were represented as gradual changes in magnitude of EMG during distinct periods of the postural response, without changes in the general shape of the activation pattern. Through the smooth, directed adjustment of four feedback parameters, a feedback model reconstructed the adaptive changes to muscle activity, accounting for 80% of the variability in EMG responses to both unidirectional and reversing perturbation across subjects. Contrary to our predictions, subjects were unable to mute inappropriate TA responses or to advance the onset of MG responses in anticipation of reversing perturbations. Nevertheless, feedforward biomechanical changes, including changes to initial lean and increased leg stiffness through co-contraction, were using to mitigate the effects of expected perturbations. Together, these adaptive changes in response strategy moved subjects closer to the optimal solution for postural control, as predicted by an optimal feedback control model.

Adaptive Changes to Repetitive Perturbations

The adaptation of the postural control mechanism to repetitive perturbations was observed as changes in CoM motion (Figure 4.4 and 4.5) and the timing and magnitude of antagonistic muscle activity during the automatic postural response (Figures 4.6 and 4.7). During the Training session, in response to unidirectional perturbations in the

forward direction, large backward CoM sway was observed in all subjects, often resulting in stepping postural responses for several trials before non-stepping responses were adopted. Peak CoM excursion in the backward direction decreased over the course of the Training session ($p = 0.004$) equilibrating to a peak CoM excursion near 10 cm, with an insignificant decrease in peak CoM velocity ($p = 0.13$) (Figure 4.8). Initial lean of CoM moved from backward to forward lean within the first 3 trials (Figure 4.5). Throughout the Training session, TA background activity remained constant ($p = 0.99$) (Figure 4.9), while background MG activity increased; these changes in MG muscle tone did not reach significance ($p = 0.15$) (Figure 4.10). The magnitude of TA activity decreased insignificantly during both IB and PR periods (IB: $p = 0.056$; PR: $p = 0.22$) and no changes in TA onset latency were observed ($p = 0.83$). While co-contraction responses were common during the first few exposures to these perturbations, the inappropriate MG activity to the forward platform motion was quickly eliminated within four trials ($p = 0.0005$).

Adaptive Changes to Reversing Perturbations

In response to repetitive reversing perturbations, we observed adaptive changes in both postural task performance and control. When subjects encountered the abrupt switch to the reversing perturbations, an immediate response with appropriate timing was observed in both muscles, however all subjects required a forward stepping response on the first trial. With each successive repetition, the steps became shorter until a non-stepping response was sufficient. Within five trials, all subjects were able to withstand reversing perturbations without stepping, but continued to reduce the overall motion of the CoM (Figure 4.4). While changes in peak CoM excursion in the backward direction

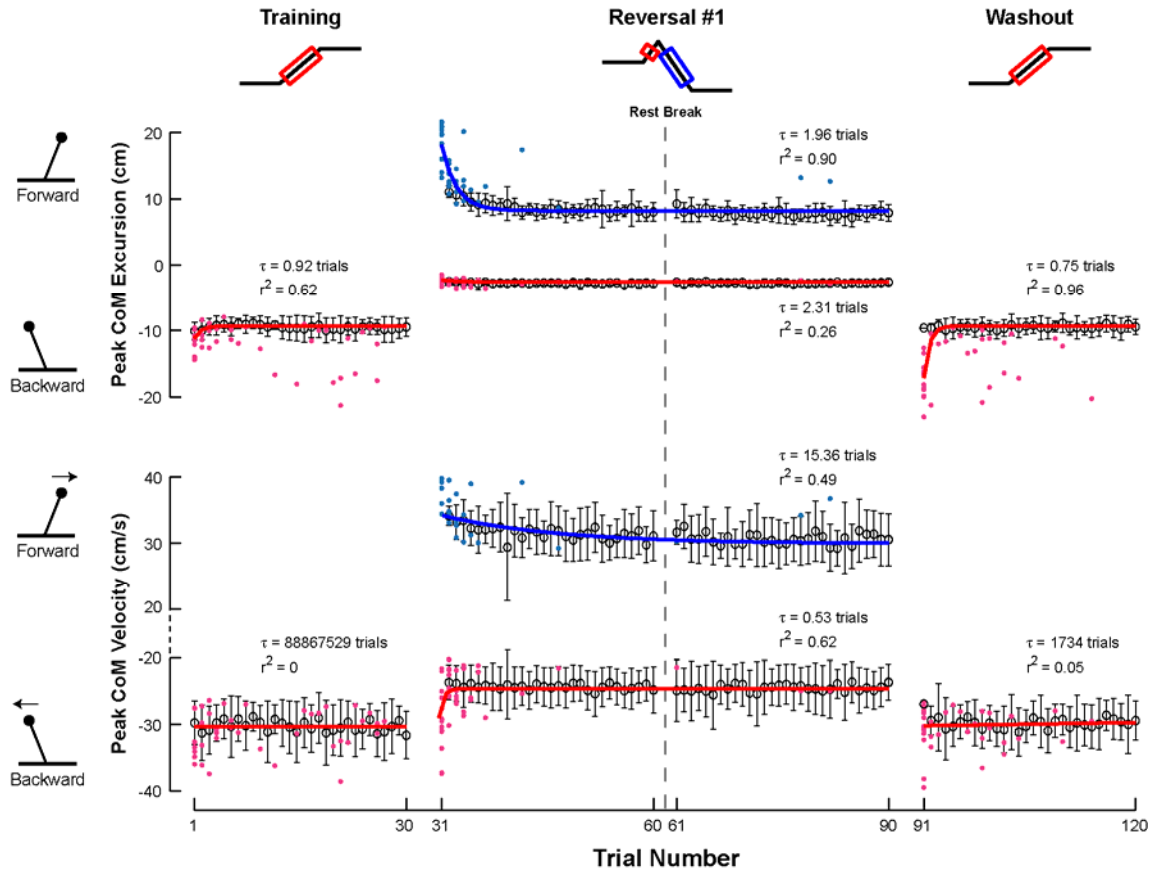

Figure 4.4 Time course of changes in CoM motion with repetitive perturbations. The changes in mean peak CoM excursion and velocity during each experimental session are illustrated with respect to trial number. Open circles and error bars represent the intersubject mean and standard deviation of CoM motion during each trial. On trials in which a subject took a step to recover their balance, the peak CoM excursion and velocity during the step is indicated with a filled circle. An exponential fit of peak CoM excursion and velocity with respect to trial number was calculated for each session, represented by the time constant τ, and the goodness-of-fit is indicated by Pearson's correlation coefficient, r^2. Peak CoM motion in response to both directions of perturbation is color-coded, where red represents CoM motion in response to forward platform motion and blue represents CoM motion in response to backward platform motion. Positive excursions and velocities correspond to forward motion of the CoM. Over the course of each session, subjects show adaptive changes in the control of CoM motion, as exhibited by a progressive decrease in peak CoM excursion and velocity in both directions across trials. Interestingly, stepping responses also follow this trend, with steps progressively shortening in length and slowing in velocity until the subject is able to respond to the perturbation without stepping.

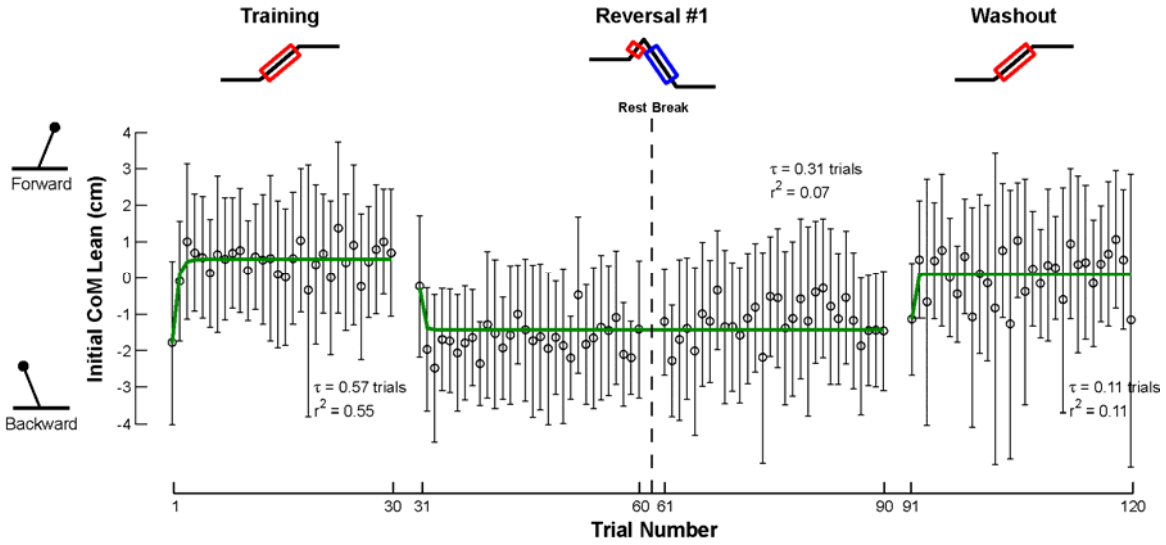

Figure 4.5 Time course of changes to initial lean of CoM with repetitive perturbations. The changes in mean initial CoM lean during each experimental session are illustrated with respect to trial number. Open circles and error bars represent the intersubject mean and standard deviation of initial lean during each trial. An exponential fit of initial CoM lean with respect to trial number was calculated for each session, represented by the time constant τ, and the goodness-of-fit is indicated by Pearson's correlation coefficient, r^2. Positive values correspond to forward lean of the CoM. Over the course of each session, the direction of initial lean changes within the first few trials, with forward lean during unidirectional perturbations and backward lean for reversing perturbations.

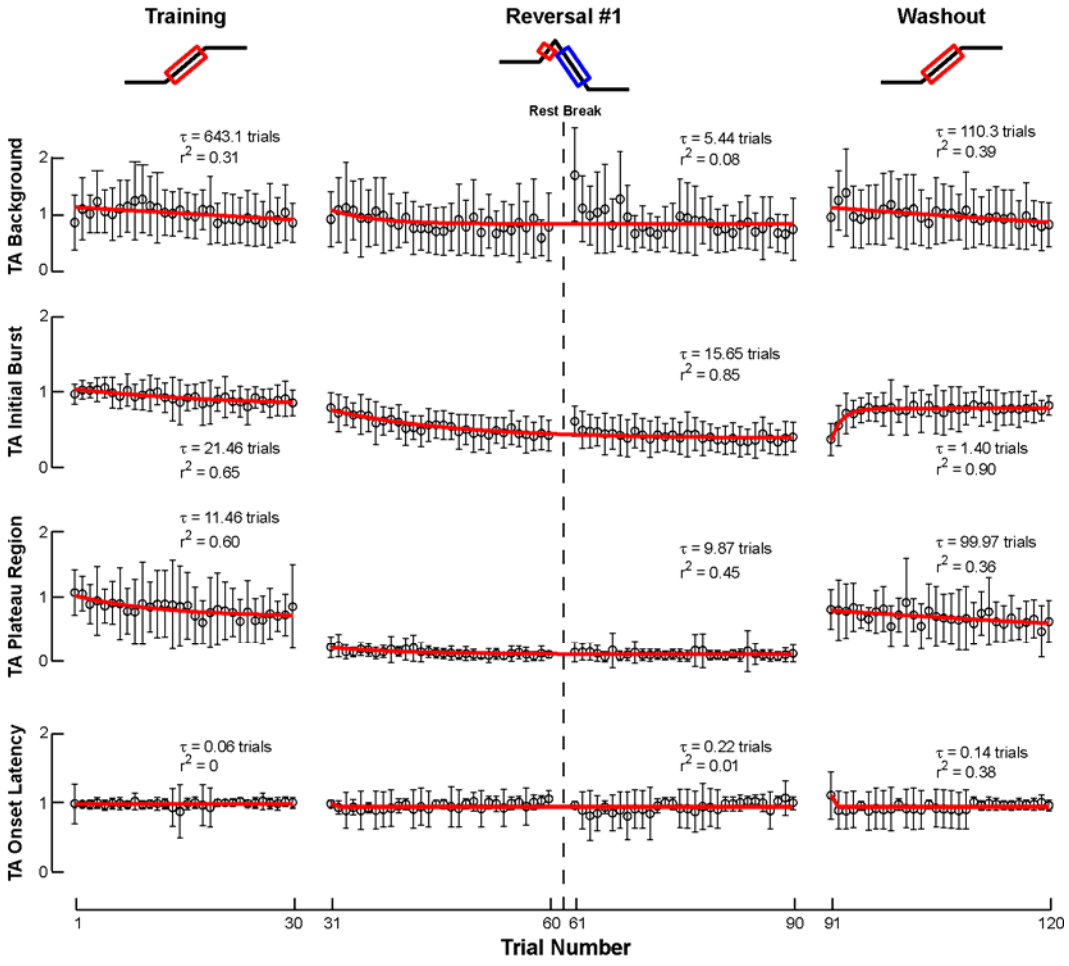

Figure 4.6 Time course of adaptive changes to TA activity with repetitive perturbations. The changes in mean TA-R EMG magnitude and onset latency during each experimental session are illustrated with respect to trial number. Mean EMG data represent all subject responses, both stepping and non-stepping, and are normalized to the mean activity across the first three trials of the Training session. An exponential fit of muscle activity was calculated for each session, represented by the time constant τ, and the goodness-of-fit is indicated by Pearson's correlation coefficient, r^2. EMG in response to both directions of perturbation is color-coded, where red represents muscle activity appropriate for responses to forward platform motion. Large increases in background TA activity were observed after each rest break and this background tone progressively decreased to its level at the beginning of the experimental protocol. The magnitude of TA responses to reversing perturbations significantly decreased throughout the Reversal session; however, this inappropriate activity was not eliminated from the response. TA activity was slowly increased during the Washout session, when the activity was again appropriate and stabilizing.

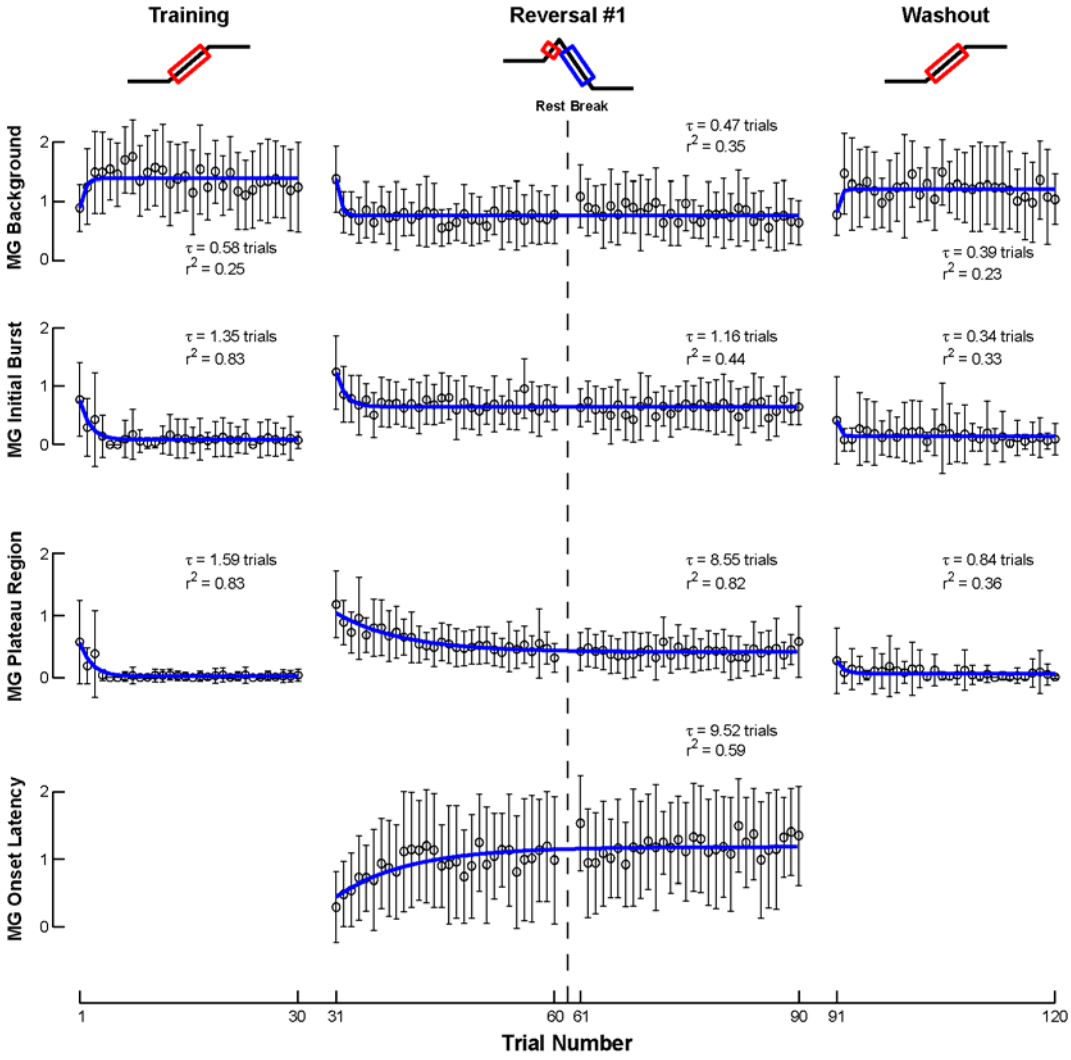

Figure 4.7 Time course of adaptive changes to MG activity with repetitive perturbations. The changes in mean MG-R EMG magnitude and onset latency during each experimental session are illustrated with respect to trial number. Mean EMG data represent all subject responses, both stepping and non-stepping, and are normalized to the mean activity across the first three trials of the Training session. An exponential fit of muscle activity was calculated for each session, represented by the time constant τ, and the goodness-of-fit is indicated by Pearson's correlation coefficient, r^2. EMG in response to both directions of perturbation is color-coded, where blue represents muscle activity appropriate for responses to backward platform motion. In response to unidirectional perturbations, background MG activity increased throughout the Training and Washout sessions. Then, over the course of the Reversal session, this activity progressively decreased to its level at the beginning of the experimental protocol. An increase in background MG activity was also observed after the rest break during the Reversal session. The magnitude of inappropriate MG activity following unidirectional perturbations was quickly eliminated from the response strategy within five trials. MG responses to reversing perturbations appeared immediately and progressively decreased throughout the Reversal session. Surprisingly, MG onset latency increased throughout this session. During the Washout session, MG activity showed an immediate decrease in magnitude and was eventually eliminated from the postural response.

did not change significantly ($p = 0.29$), we observed decreases in CoM excursion in the forward direction ($p < 10^{-16}$), as well as peak CoM velocity in both directions ($p < 10^{-16}$) (Figure 4.8). Additionally, initial lean of CoM moved from forward to backward lean by the second trial (Figure 4.5). No change in background muscle tone was observed for TA ($p = 0.12$), however MG showed a significant reduction in background tone ($p = 0.0035$) over the course of the session. The magnitude of the initial EMG response in TA continued from its level at the end of the Training session and decreased over the course of the Reversal session ($p < 10^{-16}$), though this inappropriate activity was never fully eliminated from the response and the response latency remained unchanged ($p = 0.54$) (Figure 4.10). Late activity in TA was eliminated from the response immediately upon experiencing reversing perturbations. Initial burst activity in MG, which appeared immediately upon exposure to reversing perturbations, quickly decreased to an equilibrium over the course of the Reversal session ($\tau = 1.13$ trials; $p = 0.0013$), while PR activity more slowly decreased throughout the session ($\tau = 8.55$ trials; $p = 0.037$). Rather than anticipating the timing of platform reversal with earlier MG activation, the onset latency of MG responses was significantly increased over the course of the Reversal session ($p = 0.0066$) (Figure 4.9). Peak CoM excursion in the forward direction was slightly increased by the rest break administered during the Reversal session and quickly equilibrated to a peak CoM excursion near 8 cm within one trial. This rest break also caused an increase in TA and MG background activity, as well as TA activity during the IB period; this elevated activity was removed within six trials.

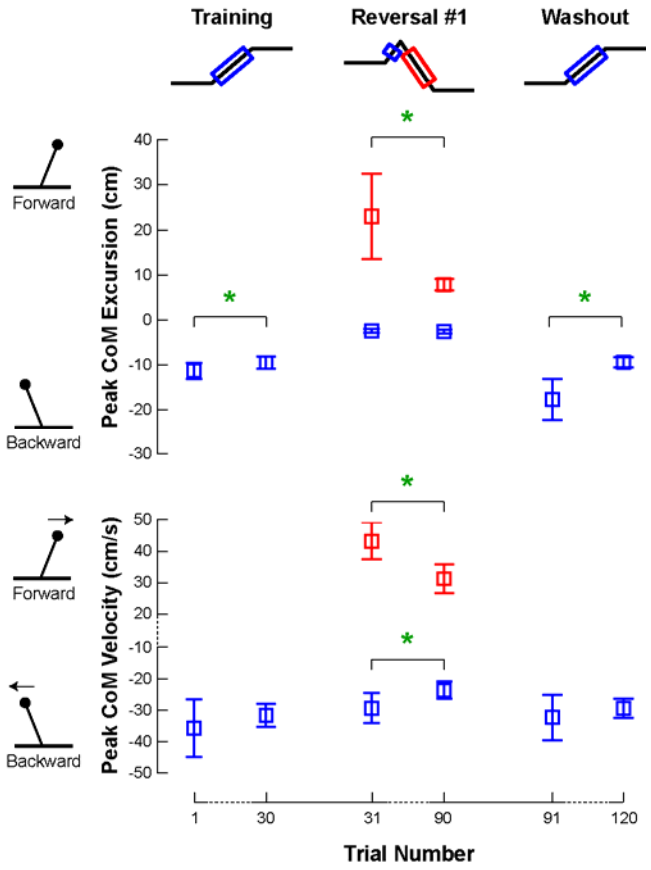

Figure 4.8 Absolute changes in CoM motion with repetitive perturbations. The intersubject mean and standard deviation of peak CoM excursion and velocity are shown for the first and last trial of each session. Paired t-tests were performed to determine during which sessions significant changes in CoM motion were observed. In general, peak CoM excursion in the backward direction was reduced during unidirectional perturbations. During Reversal perturbations, peak CoM excursion in the forward direction was significantly reduced. Peak CoM velocity in both directions was significantly reduced.

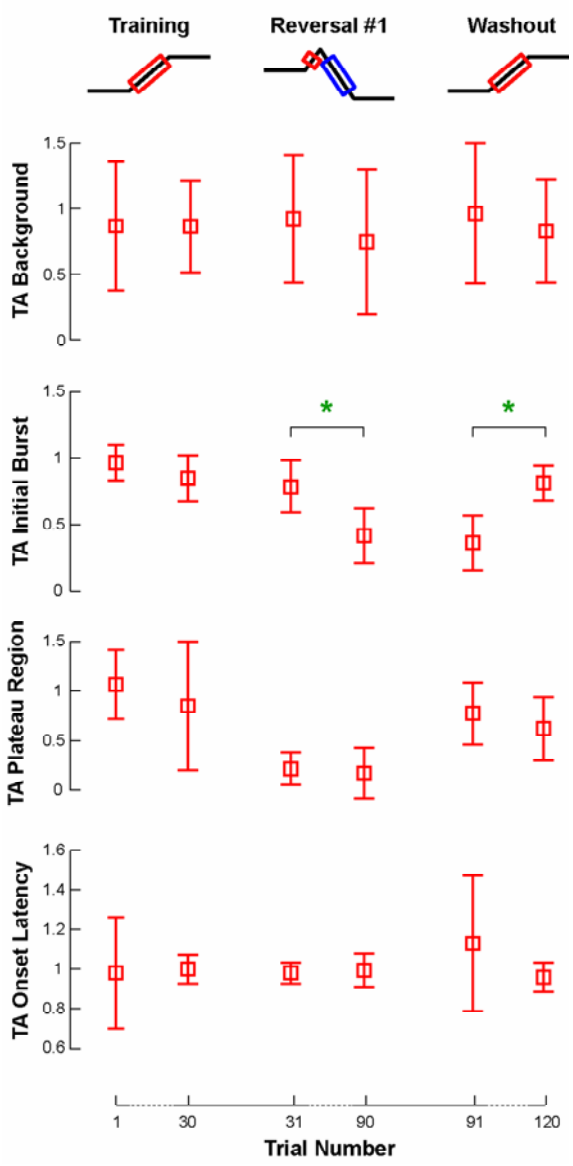

Figure 4.9 Absolute changes to TA activity with repetitive perturbations. The intersubject mean and standard deviation of TA muscle activity are shown for the first and last trial of each session. Paired t-tests were performed to determine during which sessions significant changes in muscle onset and activity during the background, initial burst, and plateau region were observed. Changes in TA initial burst activity were observed during Reversal and Washout sessions. These changes are consistent with the adaptation of response strategy, as reduced TA activity from the Reversal session was maintained during the first trials of the Washout session before de-adapting.

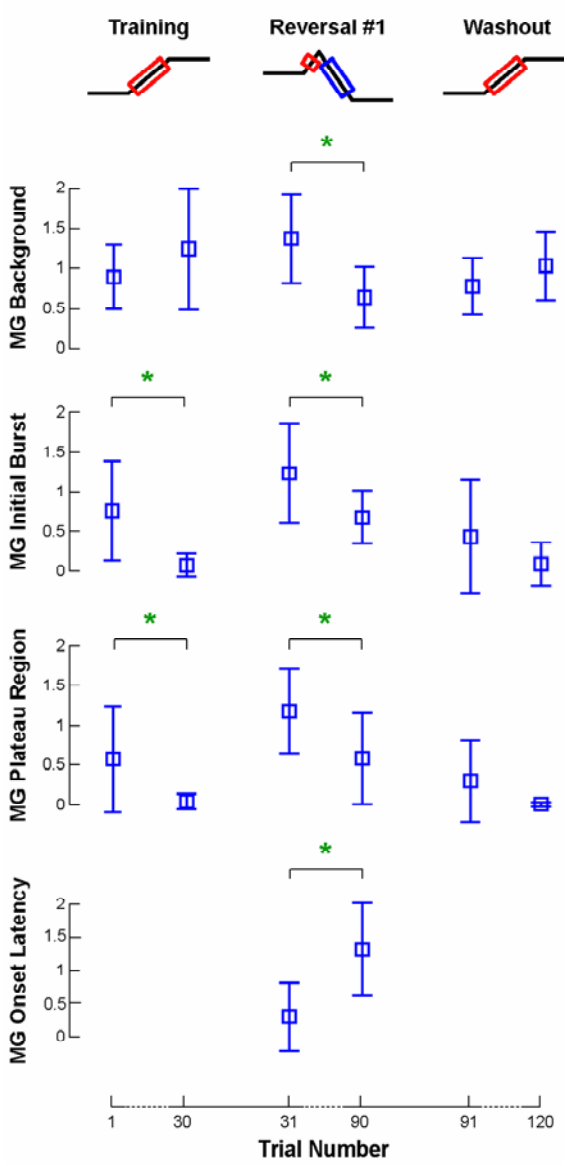

Figure 4.10 Absolute changes to MG activity with repetitive perturbations. The intersubject mean and standard deviation of MG muscle activity are shown for the first and last trial of each session. Paired t-tests were performed to determine during which sessions significant changes in muscle onset and activity during the background, initial burst, and plateau region were observed. Inappropriate MG activity during unidirectional perturbations was eliminated over the course of the Training and Washout sessions. Significant changes in all parameters were observed during the Reversal session – MG activity was reduced in all periods and its onset latency was extended.

After-Effects and the Washout of Adaptive Changes

During the Washout session, after-effects in the form of large steps in the backward direction were evoked in many subjects. In general, a stepping strategy was more prevalent during unidirectional perturbations, as these forward perturbations were quite challenging and the subjects could not benefit from the assistive torques generated by the reversal of the platform motion. These steps became smaller with each successive repetition and eventually non-stepping responses were sufficient to maintain balance, often within four trials. Peak CoM excursion continued to decrease ($p < 10^{-16}$) until equilibrating near 10 cm (Figure 4.4). An insignificant decrease in peak CoM velocity was observed during the Washout session ($p = 0.21$). Initial lean of CoM returned to a forward lean within one trial (Figure 4.5), though the direction of this lean was less consistent than during the Training and Reversal sessions. Background muscle tone in MG increased throughout the Washout session, while TA tone decreased; neither change reached significance (MG: $p = 0.15$; TA: $p = 0.52$). In response to the unidirectional perturbations, TA activity during the IB period increased gradually from the level at the end of the Reversal session to the level at the end of the Training session ($p < 10^{-16}$) (Figure 4.10). TA activity during the PR period increased immediately to the level at the end of the Training session and decreased insignificantly over the course of the Washout session ($p = 0.25$). An insignificant reduction in TA onset latency was also observed ($p = 0.061$). A marked reduction in MG activity was immediately observed during the IB and PR periods and the remaining inappropriate MG activity was eliminated from the response within four trials (Figure 4.9). Due to large intersubject variability in the extent of the immediate reduction of this destabilizing EMG response, the overall reduction in

MG activity over the course of the Washout session was near but not significant (IB: $p = 0.098$; PR: $p = 0.055$).

Adaptive Changes to Feedback Parameters toward an Optimal Feedback Solution

Using feedback of recorded CoM kinematics during experimental perturbations, the jigsaw model accurately reconstructed the changes to muscle activation patterns during adaptation to both unidirectional and reversing perturbations. Jigsaw model reconstructions accounted for >57% of the variability in TA and MG patterns recorded across all subjects and sessions (VAF = 0.80 ± 0.06). During the Training session, jigsaw model reconstructions matched >88% variability in experimental EMG (VAF = 0.89 ± 0.01) in TA and >76% VAF for MG response patterns (VAF = 0.77 ± 0.01) (Figure 4.11). During the Reversal session, jigsaw model reconstructions matched >57% VAF of experimental TA EMG (VAF = 0.76 ± 0.05) and >74% VAF for MG responses (VAF = 0.79 ± 0.02) (Figure 4.12). During the Washout session, jigsaw model reconstructions matched experimental TA EMG with >86% VAF (VAF = 0.88 ± 0.02) and MG EMG with >67% VAF (VAF = 0.73 ± 0.03) (Figure 4.13).

The adaptive changes in muscle activity pattern were matched by smooth changes in feedback gains with experience. Feedback parameters chosen by jigsaw optimizations displayed gradual, unidirectional changes over the course of each session for both TA (Figure 4.14) and MG (Figure 4.15). Surprisingly, k_a remained constant across all sessions and muscles ($p > 0.36$), with the exception of an increase in TA k_a during the Washout session ($p = 0.0022$). The value of λ chosen by the jigsaw optimization also remained constant for TA across all sessions ($p > 0.75$), save an increase during the Washout session ($p = 0.0011$). The value of λ for MG was constant over all sessions ($p >$

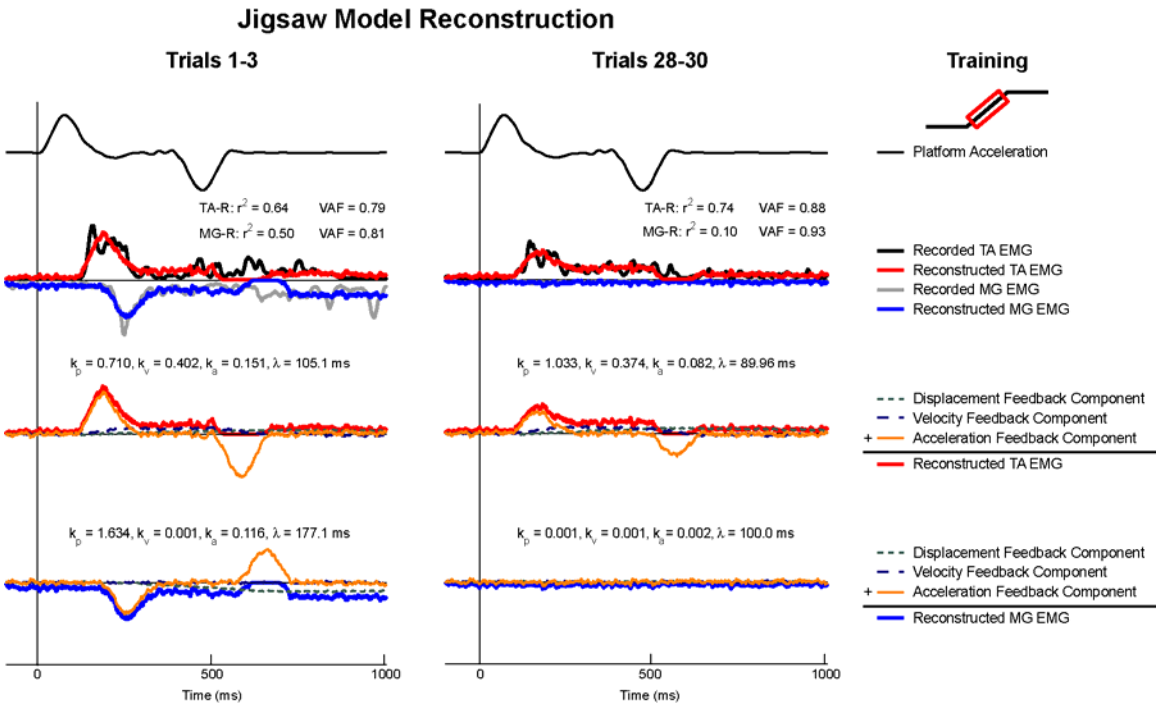

Figure 4.11 Feedback decomposition of EMG from early and late Training session. A) Recorded (black/gray) and reconstructed (red/blue) TA and MG EMG signals for Subject P. **B)** Decomposition of the reconstructed EMG signal (red/blue) into individual feedback components from acceleration feedback (orange line), velocity feedback (blue dashed line), and displacement feedback (green dotted line). In early adaptation, acceleration feedback contributes to the rapid initial rise in EMG activity; velocity and displacement feedback contribute to later activity during the plateau region. Later in the session, inappropriate MG EMG is eliminated and the acceleration-dependent initial burst of TA EMG has been reduced.

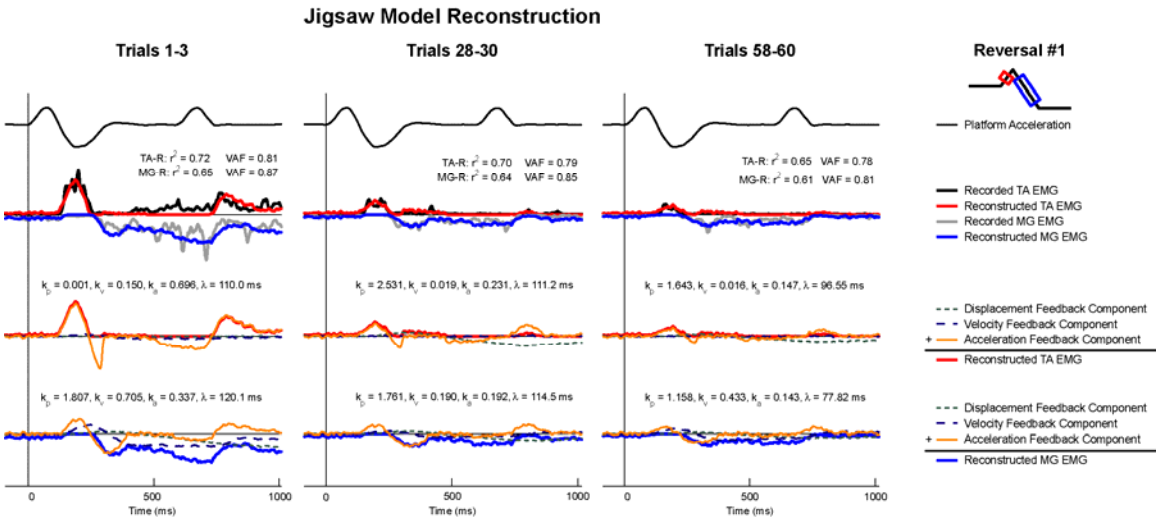

Figure 4.12 Feedback decomposition of EMG from early, middle, and late Reversal session. A) Recorded (black/gray) and reconstructed (red/blue) TA and MG EMG signals for Subject K. **B)** Decomposition of the reconstructed EMG signal (red/blue) into individual feedback components from acceleration feedback (orange line), velocity feedback (blue dashed line), and displacement feedback (green dotted line). Throughout adaptation, contributions from acceleration feedback predominate TA EMG; MG EMG is comprised of feedback from all three kinematic channels. As adaptation continues, EMG in both muscles is reduced throughout the time course, while maintaining the same pattern of activation.

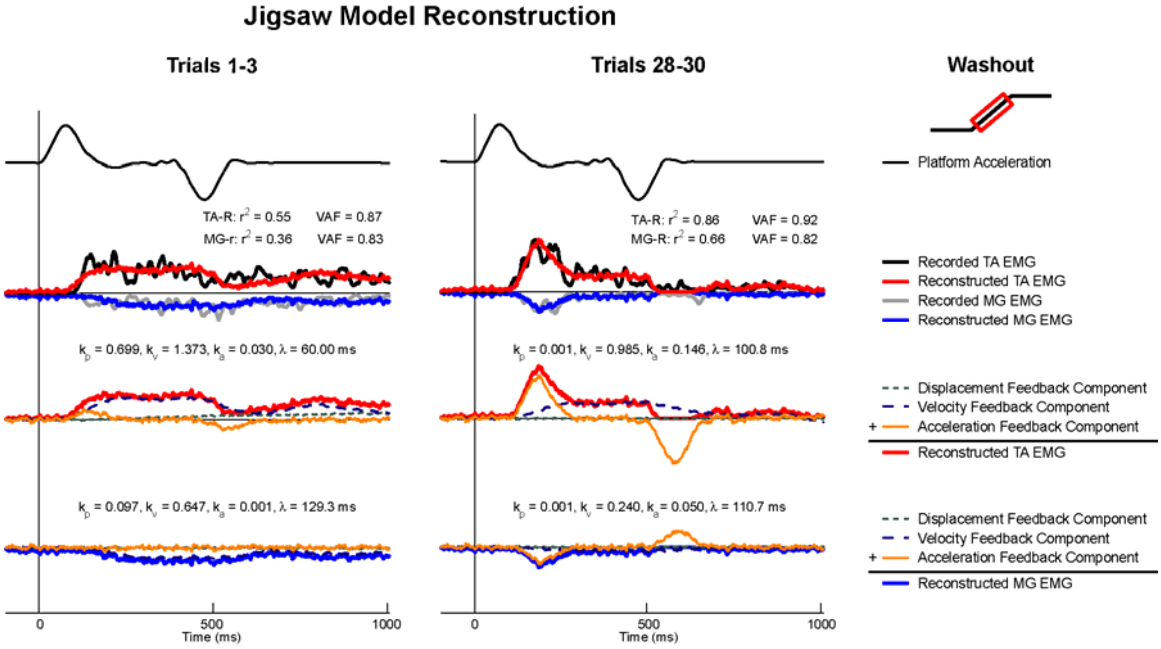

Figure 4.13 Feedback decomposition of EMG from early and late Washout session. A) Recorded (black/gray) and reconstructed (red/blue) TA and MG EMG signals for Subject W. **B)** Decomposition of the reconstructed EMG signal (red/blue) into individual feedback components from acceleration feedback (orange line), velocity feedback (blue dashed line), and displacement feedback (green dotted line). In early adaptation, acceleration feedback is nearly absent from both EMG patterns; velocity feedback predominates. As adaptation continues, acceleration feedback returns to the feedback response.

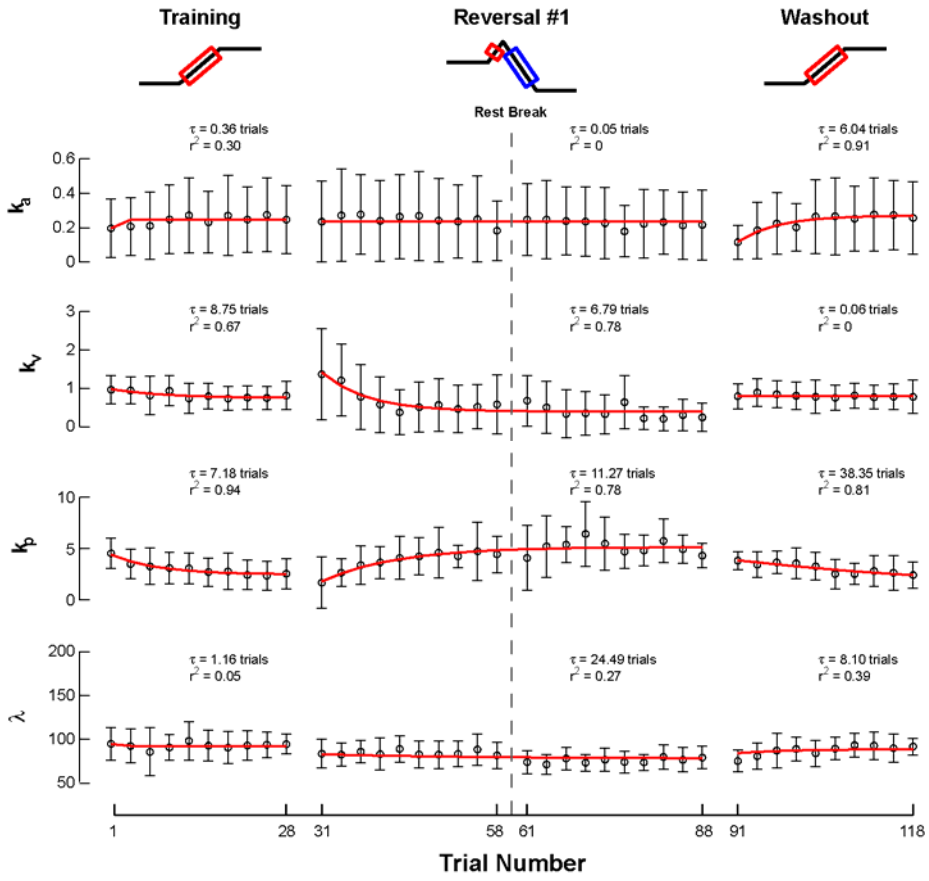

Figure 4.14 The adaptation of TA feedback gains across each session. The average acceleration (k_a), velocity (k_v), and displacement (k_d) gains, along with the time delay (λ) across all subjects. The adaptation of the response was confined to changes in velocity and displacement gain, while acceleration gain and time delay remained constant across all sessions.

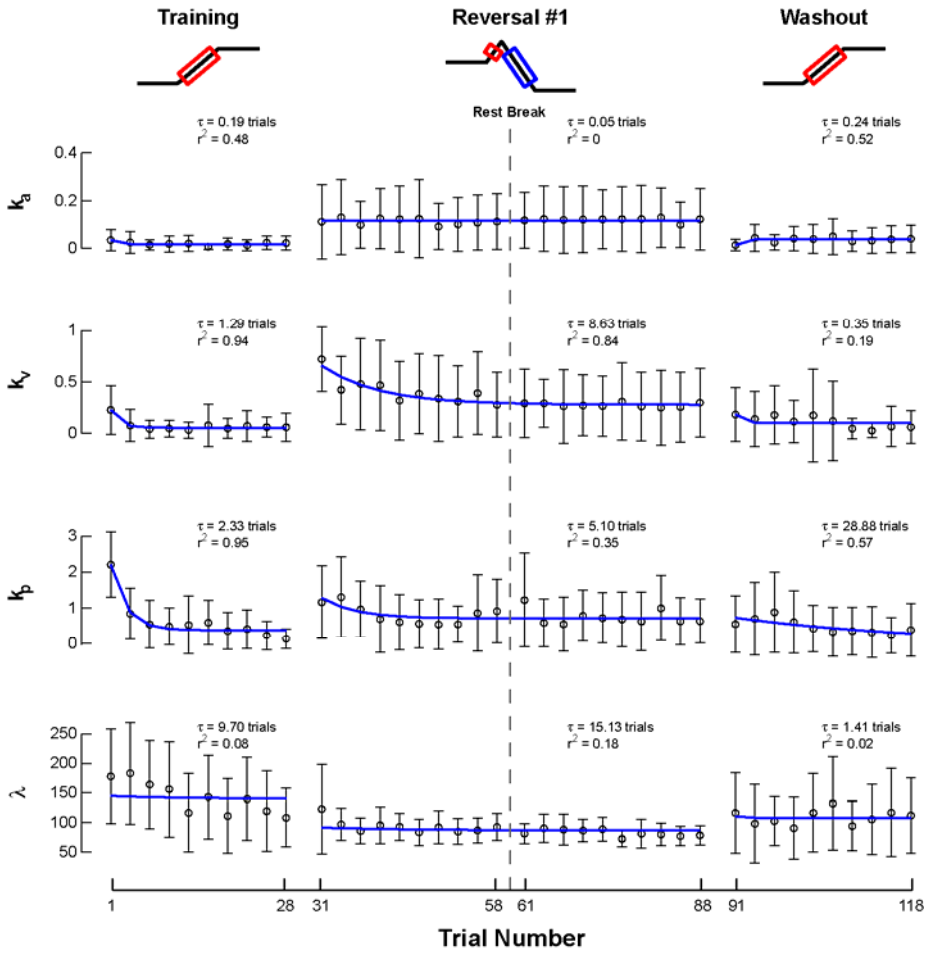

Figure 4.15 The adaptation of MG feedback gains across each session. The average acceleration (k_a), velocity (k_v), and displacement (k_d) gains, along with the time delay (λ) across all subjects. Similar to TA, the adaptation of the response was confined to changes in velocity and displacement gain, while acceleration gain and time delay remained relatively constant across all sessions.

0.067), except a decrease during the Training session ($p = 0.012$). Reductions in TA activity during the Training session were reconstructed as modest reductions in k_v ($p = 0.15$) and significant reductions in k_p ($p = 2.35 \times 10^{-4}$). The elimination of inappropriate MG activity during the Training session was represented by a reduction of all feedback gains to zero. During the Reversal session, a reduction in TA k_v ($p = 0.0022$) was matched by an increase in k_p ($p = 0.013$). Changes to MG activation during the Reversal session were realized by a decrease in both k_v ($p = 0.0042$) and k_p ($p = 0.059$). During the Washout session, inappropriate MG activity was eliminated by the reduction of all feedback gains. A reduction similar to that observed during the Training session was identified for TA k_v and k_p during the Washout session.

DQR optimal feedback simulations suggested that, as subjects adapted their postural responses to repetitive exposure to both unidirectional and reversing perturbations, they moved closer to the optimal solution for postural control. While the time course of EMG exhibited by subjects during all trials, subjects, and sessions were well-constructed by the feedback law (Figures 4.11 – 4.13), with experience these EMG patterns migrated toward the optimal solution (Figures 4.16 – 4.18). Because the time delay for optimal solutions was set *a priori* to be 100 ms, often subjects matched the shape but not the timing of optimal solutions during Reversing perturbations (Figure 4.17). In general, the level of muscle activation observed in response to Washout perturbations was more elevated than the responses to the same perturbation in the Training session (compare Figures 4.16 and 4.18), but still migrated toward the optimal solution. Normalized error between experimentally-recorded EMG and the DQR optimal solution reduced from 19.3 to 10.5% during the Training session ($p = 1.70 \times 10^{-6}$);

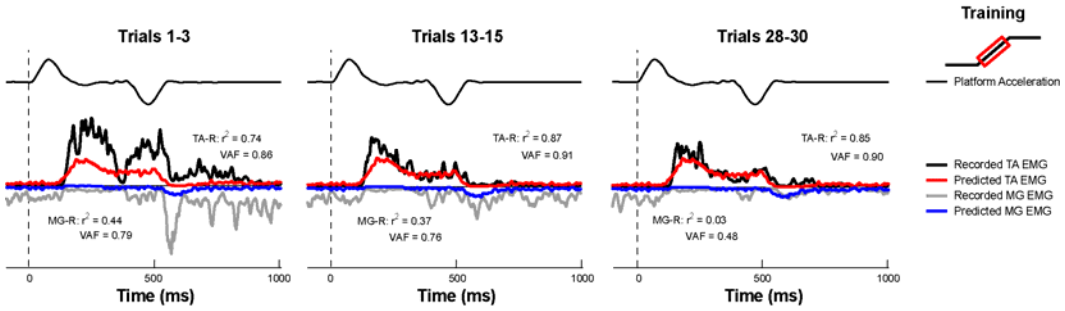

Figure 4.16 Adaptation toward optimal solution: Training session. Recorded (black/gray) and optimal (red/blue) TA and MG EMG signals for Subject K. With repeated exposure to unidirectional Training perturbations, subject responses navigated toward the optimal solution for both muscles.

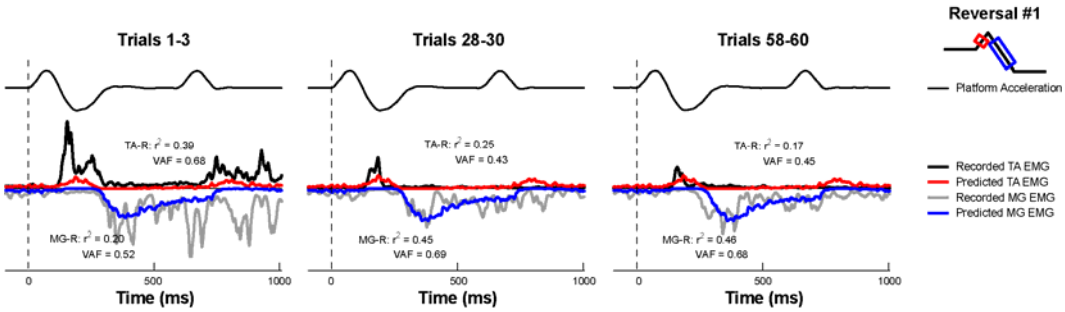

Figure 4.17 Adaptation toward optimal solution: Reversal session. Recorded (black/gray) and optimal (red/blue) TA and MG EMG signals for Subject J. With repeated exposure to bidirectional Reversal perturbations, subject responses navigated toward the optimal solution for both muscles. Because the optimal DQR model chooses a solution based on a time delay of 100 ms, specified *a priori*, the illustrated subject gradually begins to respond earlier than the onset timing of the optimal solution.

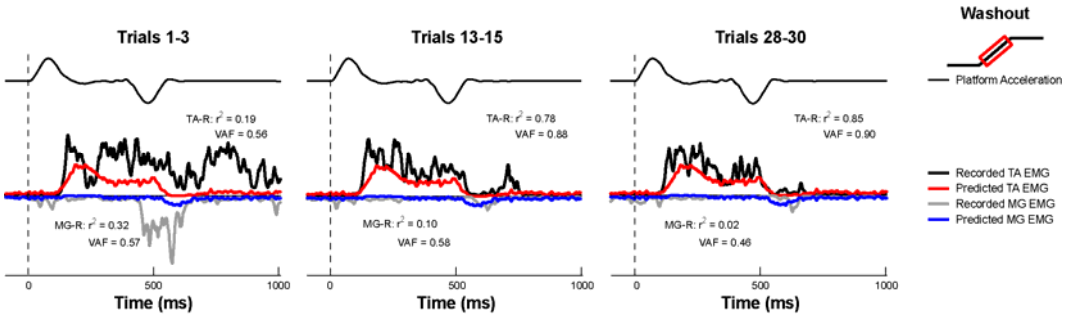

Figure 4.18 Adaptation toward optimal solution: Washout session. Recorded (black/gray) and optimal (red/blue) TA and MG EMG signals for Subject M. With repeated exposure to unidirectional Washout perturbations, subject responses navigated toward the optimal solution for both muscles. In general, EMGs in response to Washout perturbations were more elevated than for the same perturbations during the Training session.

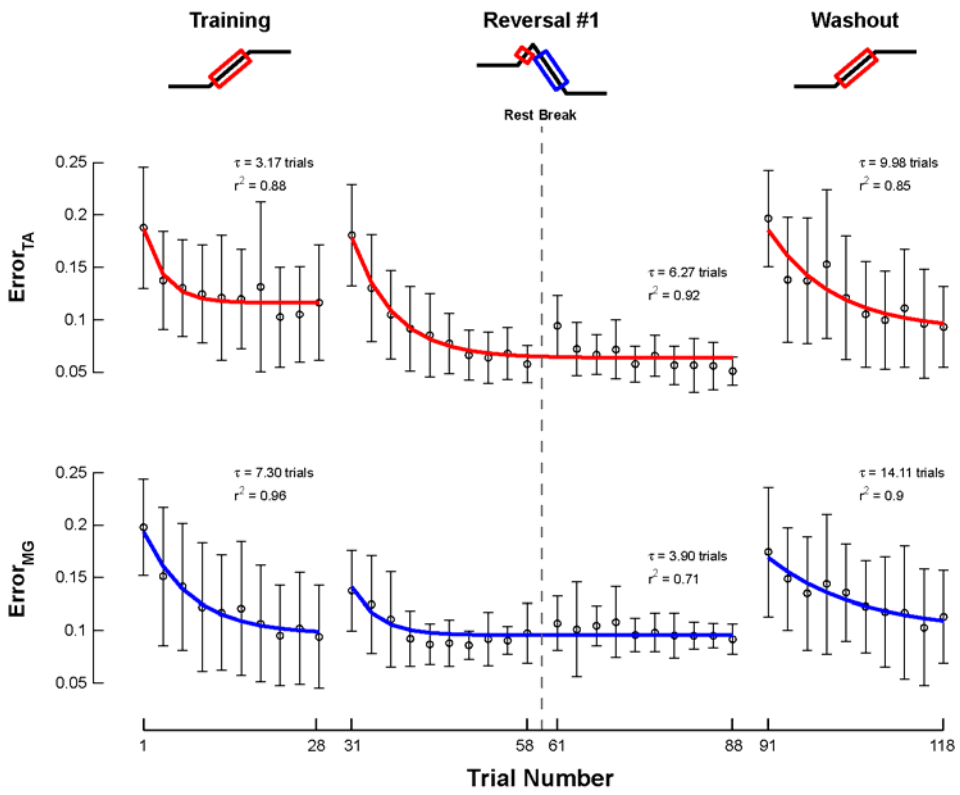

Figure 4.19 Reduction of error between recorded and optimal EMG patterns. The average total error between recorded TA and MG EMG patterns and the optimal feedback solution from the DQR model is illustrated with respect to trial number. As subjects adapt their postural response to repetitive exposure to both unidirectional and reversing perturbations, they navigate toward the optimal solution. This is indicated by a reduction in total error over the course of each session. Sharp increases in total error between sessions indicate the initial effects of the reversing perturbations and the after-effects when returning to unidirectional perturbations.

similar reductions in total error were observed during the Reversal (15.9 to 7.1%; $p = 2.74 \times 10^{-9}$) and Washout (18.6 to 10.3%; $p = 4.48 \times 10^{-7}$) sessions (Figure 4.19).

Discussion

Our results suggest that both feedback and feedforward mechanisms are used to adapt the postural responses to repetitive support-surface translations. Feedback strategies were used to adjust the magnitude of muscle activity throughout the time course of the

postural response through the adjustment of feedback gains related to CoM motion. While feedforward strategies were not able to completely mute or advance the evoked postural responses to reversing perturbations, biomechanical changes before the onset of disturbance were used to mitigate both unidirectional and reversing perturbations. This interplay between feedback and feedforward strategies served to improve control of the CoM, reducing the sway magnitude and velocity of the kinematic response to perturbations. These adaptive changes to the postural response strategy are consistent with the feedforward adjustment of feedback control through central set toward an optimal solution of postural control.

The current study represents the first effort to quantitatively characterize the time course of changes to both performance and muscle activation during a balance task. Previous reports have quantified the absolute changes in the magnitude of muscle activity evoked during postural responses. Here, we extended this previous analysis by assessing both the time course to the final postural control solution, in terms of muscle activity, and the resulting changes in task performance, as evidenced by CoM excursion and velocity. By determining the time constant of adaptation for postural responses, we corroborated previous observations that the time course of adaptation during postural tasks occurs on a much faster timescale than voluntary movements (Lisberger 1988). We also observed, for the first time, a smooth transition in the control of the CoM from stepping to non-stepping postural responses. This suggests that the continuum between ankle and hip strategies within the postural control mechanism extends to include stepping responses, where hip strategies mix with increasingly longer steps as disturbances become more challenging.

Each of the observed changes in task performance, as measured by CoM peak excursion and velocity, were matched by changes in muscle activity. We observed a smooth, unimodal progression from stepping to non-stepping postural responses in both excursion and velocity characteristics of CoM motion, rather than a bifurcated behavior. This was matched by smooth, unidirectional changes to muscle activity and feedback controller gains throughout each session. As peak CoM motion continued to diminish after the change in response strategy, muscle activity and related gains also continued to reduce in magnitude throughout the time course of activity. In addition, feedforward changes in kinematics, such as initial lean, were matched by co-contraction strategies, marked by increases in background EMG levels. This connection between kinematic and muscular changes reinforces the feedback relationship between task-related variables and muscle activity for postural control.

While the expected manifestations of feedforward strategies were not observed, adaptation of postural control may involve more subtle feedforward mechanisms. While the expected elimination of the TA response was not observed throughout the reversing perturbations in the current study, a complete suppression of feedback-mediated responses may be difficult to achieve, regardless of feedforward adaptive effort. Further, the lengthening of onset latency to the reversed motion of the platform may indicate a feedforward incorporation of platform-generated torques into the response strategy. This idea is further supported by the reduction in EMG magnitude in both TA and MG over the course of reversing perturbations. By clamping the error signal that drives these adaptive changes, it may be possible to observe directly the feedforward adaptations to the response strategy (Ethier et al. 2008; Scheidt et al. 2000). In the context of standing

balance, this may be accomplished using sway referencing, where the support surface rotates with the sway angle of the body, altering the proprioceptive cues that result from the motion (Nashner and Berthoz 1978; Peterka 2002). Nevertheless, the observed changes in muscle activation may result from the feedforward adjustment of feedback gains for postural control.

As humans adjust their muscle activity to improve CoM control, they may be searching for an optimal solution for performing the balance task at hand. In the traditional postural control experiments performed with cats (Macpherson et al. 1987), animals were trained over the course of several months to stand with forces distributed between four force plates and to respond to postural perturbations much like the ones described in the current work. Using an inverted pendulum model under optimal feedback control, the patterns of muscle activity elicited in cats was shown to match the optimal control solution, aimed to reduce kinematic deviation and total muscle activity (Lockhart and Ting 2007). However, naïve human subjects did not match this optimal pattern, only resembling the shape of the muscle activity predicted by the inverted pendulum model (see **Chapters 2 and 3**; Welch and Ting in prep; Welch and Ting 2008).

Here, by parameterizing EMG signals into feedback gains for postural control, we demonstrated that the changes in muscle activity during adaptation may be caused by a directed optimization of the response strategy. The smooth trajectory of the adaptation of muscle activity with experience suggests a directed optimization of muscle activity to control the CoM in the face of postural perturbations rather than a random search for effective solutions. This observation was supported by the smooth, unidirectional changes in the feedback parameters used to reconstruct muscle activity throughout the adaptation

process. When compared to the optimal solution for balance control, experimentally-recorded EMG moved closer to the optimal pattern for all perturbation types, reducing the error between these two response patterns while improving task performance. These observations suggest that humans may optimize balance performance to maximize control of the CoM while minimizing energy expenditure. The optimization of motor control for minimum-energy task performance may be broadly applicable to other motor learning tasks, including both voluntary movements and involuntary reactions.

CHAPTER 5

CONCLUSIONS

Despite recent advances in rehabilitation and postural research, falls remain the leading cause of injury-related death in seniors over age 75 (Anderson et al. 2004). While healthy adults fall primarily when pushing the limits of their postural control system or when there is a mismatch between expected and actual support surface properties (*e.g.*, unknowingly stepping onto a wet or slippery surface), seniors often fall during activities of daily living, costing nearly $19 billion in direct medical costs each year (Stevens et al. 2006). Therefore, improving postural control and balance is a clinically important goal for our aging population and is a prerequisite for the rehabilitation of voluntary movement in individuals with neurological dysfunction. The specific motor improvements resulting from targeted training are also of great interest to the fields of rehabilitation science and sports medicine alike.

Here, I described the adaptive neuromuscular transformations from sensory information to reactive muscle activity that may be responsible for postural control in healthy adults — a necessary first step in the investigation of postural control in neuromuscular disease or deficit. I identified a scaling relationship between muscle activity for postural control and the characteristics of the experienced perturbation, which led to a feedback law for the formation of muscle activity during postural control. By modulating four feedback parameters related to CoM kinematics, humans can produce the wide range of temporal muscle activation patterns necessary to maintain balance in the face of perturbations of varying perturbation dynamics. This feedback law may be the

basis of the intricate changes to muscle activity during postural adaptation to both repetitive and changing postural demands. During adaptation, humans may continually update these four feedback parameters until they reach an optimal postural control solution, presumably seeking to minimize both the total postural disturbance and the energy expenditure in response to that disturbance. Also, by using mechanically-related feedforward mechanisms, such as postural lean and the up-regulation of leg stiffness through co-contraction, humans may seek to mitigate the initial effects of expected perturbations.

My approach provided an integrated investigation of the neuromuscular and biomechanical behaviors associated with postural control, an essential step towards understanding how muscles are coordinated to achieve the wide variety of postural tasks demanded by everyday life. This work may provide a quantitative framework for evaluating the temporal changes in muscle activity during postural control that occur with age, under neuromuscular impairments, and following musculoskeletal injury and interventional therapy. In addition, this approach allowed for the quantification of the time course and feedback-driven changes that occur during adaptation to new postural demands, which represents a large advance to the analytical methods offered by previous, more observational studies of postural adaptation. My work thereby provides an avenue for further investigating the mechanisms of adaptation through central set, which has previously been associated with anticipation, fear, or divided attention (Horak et al. 1989; Shumway-Cook et al. 1997; Shumway-Cook and Woollacott 2000; Woollacott and Shumway-Cook 2002). By identifying the feedback mechanisms responsible for the maintenance of balance under changing conditions, the road is also paved for the

investigation of more complex tasks, such as locomotion. We also gain knowledge useful for the effective design of athletic training and rehabilitation programs, neural prostheses, bipedal robots, and other interventional therapies.

Central Neural Control of Posture and Adaptation

While conclusive information regarding the central structures responsible for forming the automatic postural response is sparse, current evidence suggests that spinal circuits alone are not capable of producing the coordinated muscle activity following postural perturbations (Pratt et al. 1994). The circuitry responsible for automatic postural control is likely located in the higher centers of the nervous system. Integration of vestibular, somatosensory, and visual information has been shown to take place in the vestibular nuclear complex of the medulla and pons (Wilson and Melvill Jones 1979). Studies of patients with Parkinson's disease have implicated the basal ganglia in the control of tonic postural tone, centrally initiated postural adjustments, and externally triggered reactions (Horak and Macpherson 1996), though these patients retain the ability to habituate the APR to repeated perturbations (Bloem et al. 1998). Lesion studies show that the cerebellum plays several different roles in postural control. The most profound postural effects are observed following lesions to the anterior lobe of the cerebellum (Dichgans and Diener 1985), resulting in severe ataxia with high-frequency trunk tremor, likely due to difficulty controlling the magnitude rather than the timing of postural coordination (Horak and Macpherson 1996).

The neuroanatomical substrates responsible for motor adaptation are also as of yet unclear. Changes in the patterns of cortical motor activation have been regarded as the underlying mechanism of motor learning (Hund-Georgiadis and von Cramon 1999). The

cerebellum has been suggested as a possible location for internal model formation and storage, acting as a Smith Predictor updating both feedforward and feedback models to adapt to new environmental constraints (Miall et al. 1993). More recent evidence suggests that cerebellar patients are unable to scale postural responses appropriately based on prior experience (Horak and Diener 1994; Horak and Macpherson 1996), but show no impairment in the ability to habituate their automatic postural response to repeated perturbations (Nashner 1976; Schwabe et al. 2004).

Future Studies

Several interesting experimental observations not reported within this thesis deserve further attention due to the interesting perspectives on postural control they may provide. One such observation is that muscle onset timing changes with the peak jerk of the administered perturbation. During the study described in **Chapter 3**, perturbation jerk was not individually controlled, and therefore varied with perturbation acceleration. Nevertheless, the hastening of muscle onset with increased perturbation jerk can be observed in Figure 3.4A, where at each acceleration (and therefore jerk) level, muscle onset occurs at different timing. In Figure 3.4C, where acceleration and jerk levels are held constant, muscle onset occurs with similar timing in each condition. A more comprehensive study that includes the individual control and variation of peak perturbation jerk is necessary to fully understand the role of jerk feedback in shaping muscle activity for postural control.

While examining the bilateral ankle muscle EMG patterns in response to a variety of perturbation characteristics, I observed substantial interlimb differences in the evoked postural response. Previous observations suggest that, like with the hands (Sainburg and

Kalakanis 2000), the use of human legs is typically lateralized, where one leg is used for actions of mobilization and the other for postural stabilization (Hart and Gabbard 1997). To further investigate the roles of each leg during postural control, we asked right-legged subjects to stand quietly in both bipedal stance and one-legged stance on each leg. Our preliminary data indicate that right-legged subjects have smaller lateral center of pressure displacement and higher velocities during left-legged quiet stance, suggesting a lateralization of postural stability to the left leg (Surendran et al. 2007). While only preliminary, these results may have strong implications in the field of prosthetic design. To assure the correct control strategies are being used for the lateralized role appropriate for the amputated limb, the stability mechanisms for prosthetic limbs may require individualized modification. Future work can also examine the postural control of leg amputees and how it adapts as amputees gain experience with the prosthetic limb.

The experimental and analytical techniques discussed within this thesis can also be used to explore postural responses to perturbations containing mediolateral directional components and those incurred during locomotion. Here, I established that anterior-posterior postural control scales with perturbation characteristics and is consistent with a feedback law on CoM kinematics. While it is not clear whether these feedback mechanisms extend to perturbations with significant mediolateral components, similar temporal patterns of muscle activity have been observed for multidirectional perturbations (Macpherson 1988). Studies of spatial patterns of muscle activity in response to multidirectional perturbations in cats and humans have demonstrated that a small number of muscle synergies can describe the coordinated activity of muscle throughout the body that make up the postural response (Torres-Oviedo et al. 2006;

Torres-Oviedo and Ting 2007). We hypothesize that these muscle synergies are activated by neural commands related to CoM kinematic feedback. We further hypothesize that postural responses to perturbations incurred during locomotion will use the same muscle synergies and CoM feedback law as are used to respond to perturbations of quiet stance.

In addition to empirical investigation, the inverted pendulum models presented here may also be expanded to study mediolateral perturbations and stepping postural responses. By adding an additional limb (pendulum) to the model with the CoM suspended on a bar linkage between the two, the feedback law described here may be able to characterize postural responses to mediolateral perturbations. This new mediolateral model can also be used to study the effect of biomechanical configuration on postural response, allowing further investigation of the interplay between feedforward and feedback mechanisms in postural control (cf. Scrivens et al. 2008). By the inclusion of gain and/or response scheduling, our inverted pendulum model of postural control may also be extended to the inclusion of stepping postural responses. This inclusion may require a pre-programmed threshold response that allows one pendulum limb to be raised and moved in the appropriate direction to mimic a stepping response when the CoM moves beyond the base of support. The validity of the muscle spindle stiction response that was added to the jigsaw model should be verified by performing controlled muscle spindle stretches at a variety of accelerations and velocities to determine the modularity of the duration of its acceleration-dependent response.

A few additions and modifications to the feedback model for postural control are warranted to improve the insights that can be gained from this useful tool. First, additional links should be added to the current inverted pendulum model to allow better

matching between model and subject kinematics during postural control. As suggested in **Chapter 3**, by mimicking ankle and hip responses (and the continuum of mixed strategies in between), the individual roles of muscles in coordinating body segments during postural control can be elucidated, improving the results from out modeling efforts. This will require the simultaneous prediction of activity from multiple muscles, including antagonistic pairs of muscles at each joint. At the cost of additional computational expense, the addition of links and muscles to the current model may result in a more accurate reconstruction of low-level muscle activity in proximal muscles, providing better agreement between data-matching results from the jigsaw and TSyID models. This effort may also result in a set of optimal response patterns from the DQR model – rather than one solution for each perturbation – better representing the biomechanical roles of muscles at each joint.

This work has established a quantitative framework for the interpretation of complex muscle activation patterns for balance control. When combined with ongoing studies on muscle synergies and the spatial organization of muscle activation patterns, this work may provide a tool for the spatiotemporal prediction of muscle activation patterns in a number of experimental conditions and biomechanical constraints. Future studies can use this spatiotemporal framework to gain insight into the pathological changes that result from central and peripheral neural deficits, as well as the normal changes in postural responses due to sensory perturbations, cognition, emotional state, and anticipation.

APPENDIX A

USING WAVELET FANOVA AS A TOOL FOR EXAMINING THE TEMPORAL PATTERNS OF MUSCLE ACTIVITY

Previous investigators have noted several difficulties in showing significant changes in muscle activity with perturbation dynamics using conventional statistical analyses. We previously described a feedback law for transforming CoM kinematics into an EMG pattern in response to support-surface translations (see **Chapter 3**; Welch and Ting in prep). We demonstrated that CoM acceleration and velocity affect the postural response in different, but sometimes overlapping time windows. This confounds a traditional statistical analysis in which *a priori* time bins or features, such as the magnitude and timing of peak muscle activation, must be quantified. Such descriptive parameters do not fully encompass the differences between two EMG profiles. In addition, further complications arise due to the high inter-trial variability of muscle activation patterns, resulting from the difficulty in controlling subject kinematics at the time of perturbation (Horak and Moore 1993; Park et al. 2005; Siegmund et al. 2002; Szturm and Fallang 1998; Tokuno et al. 2006). Because we are interested in comparing the shapes of curves that are functions of time or space, there are few traditional statistical methods that can be used to effectively test our hypotheses without losing power due to multiple comparisons.

The wavelet transform is a versatile tool for the analysis of biomedical signals that contain high variability because it reveals not only the different frequency components of a signal, as with the Fourier transform, but also the temporal structure of

those components. Because of its power to handle signals containing events throughout the range of time-frequency localization, the wavelet transform has been used in many biomedical applications, from electroencephalogram (EEG) and electrocardiogram (ECG) analysis to positron emission tomography (PET) and magnetic resonance imaging (MRI) (see Unser and Aldroubi 1996 for a review). More recently, wavelet transforms have been used to evaluate electromyographic signals in several applications, including the extraction and classification of motor unit action potentials from EMG records (Fang et al. 1999; Ostlund et al. 2006; Ren et al. 2006), as well as to assess muscle fatigue (Kumar et al. 2003; Sparto et al. 2000) and the tuning of leg muscle activity in response to impact forces (Wakeling et al. 2001).

The analysis in the current study represents a novel extension of wavelet EMG analysis by using the wavelet transform to examine the spatiotemporal features of the EMG signal and compare multiple EMG waveforms. Previous studies often use wavelet decomposition as a means of filtering their signals and comparing the performance of several mother wavelets at feature detection within the signal, without evaluating the temporal characteristics of the EMG waveform itself. The discriminating attribute of our wavelet analysis is the reconstruction of the wavelets into the time domain after performing functional analyses, to reveal the temporal manifestation of the effects of experimental variables. This type of analysis also removes any biases due to the predetermined time windows specified in the traditional regression of means analysis.

Functional ANOVA (FANOVA) was performed in wavelet space to identify the temporal regions of the EMG waveforms that were significantly affected by changes in perturbation characteristics. The entire 3-second duration of the collected EMG signals

for each muscle (experimental protocol and data collection procedures explained in **Chapter 3**) were resampled to 360 Hz and pooled over all subjects. Only EMG data from perturbations with accelerations between 0.2 – 0.4g were included in the analysis to achieve a balanced statistical design, since only at these acceleration levels were all velocity levels achieved. Using the MATLAB wavelet toolbox, these data were padded using periodization and transformed to wavelet space using the third-order coiflets (coif3; see Cohen and Kovacevic 1996 for mathematical background). Three-way FANOVA (velocity × acceleration × subject) was performed on each wavelet coefficient with a significance level of $\alpha = 0.05$. The wavelet coefficients that varied significantly with perturbation characteristics were compared using a Scheffe pairwise comparison subject to a Bonferroni correction. Contrasts of significant wavelet coefficients were calculated with respect to the lowest velocity and acceleration conditions (25 cm/s and 0.2g, respectively). The statistically-significant wavelets were then transformed back into the time domain to reveal the temporal regions of the EMG waveform that are sensitive to perturbation velocity and acceleration. As an additional testbed for this novel technique, as well as to provide additional validation of the modeling results from **Chapter 3**, the wavelet FANOVA analysis was repeated on DQR optimal predictions of muscle activity in response to the experimental perturbations and the results from the experimental and modeling results were qualitatively compared.

Wavelet analysis provided an unbiased description of the temporal regions of the muscle response that were significantly affected by acceleration and velocity. Post hoc Scheffe contrasts for the effects of acceleration and velocity on TA activity are illustrated in Figures A.1A-B. The effects of acceleration predominate in the early periods of EMG

that correspond to the initial burst (IB) region defined during regression analysis ($p < 0.001$; $n = 47$ significant wavelets). Velocity effects dominate in the later periods of EMG that correspond to the plateau region (PR) ($p < 7\times10^{-4}$; $n = 72$ significant wavelets). Temporal scaling patterns were robust across all muscles examined, particularly in the triceps surae, quadriceps, and hamstrings (Figure A.2). While these scaling trends are in agreement with those identified using the traditional linear regression analysis (Figure 3.4), wavelet FANOVA results indicate that the scaling with both perturbation acceleration and velocity extends well beyond the predetermined time windows of the linear regression analysis.

While model EMG predictions during the variation of velocity better matched experimentally-recorded EMG traces at higher acceleration levels (Figure 3.8), wavelet FANOVA contrasts from pooled model predictions matched the results obtained from the same analysis on experimental data for both acceleration and velocity (Figures A.1C-D). Specifically, the main effects of perturbation peak acceleration on model predictions occurred during the initial burst period defined for linear regression analysis ($p < 2\times10^{-4}$; $n = 288$ significant wavelets), while the effects of peak velocity predominated during the plateau region ($p < 2\times10^{-4}$; $n = 290$ significant wavelets).

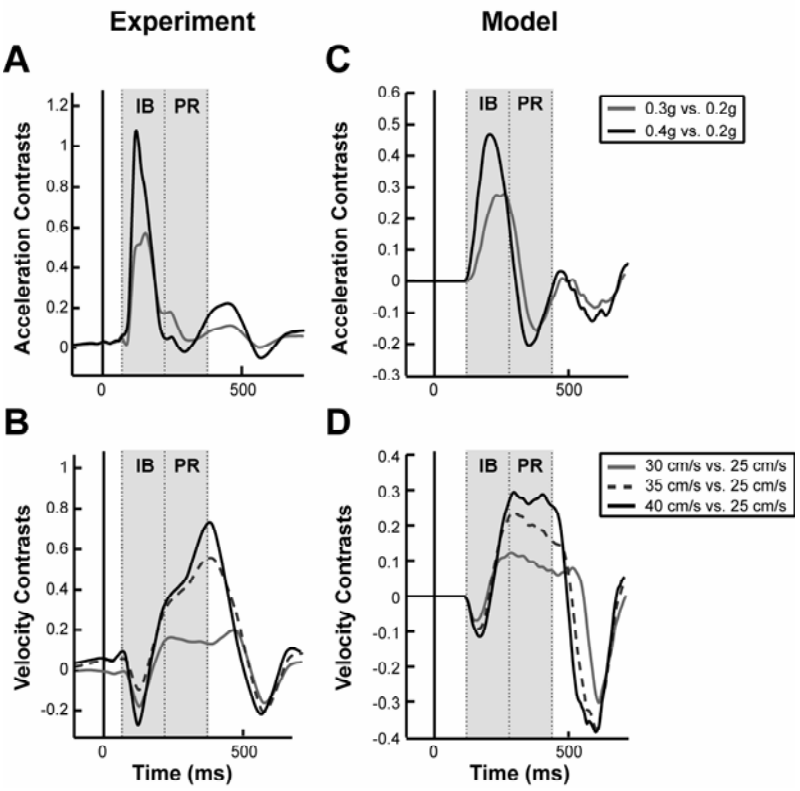

Figure A.1 Wavelet analysis reveals effects of perturbation characteristics. A and C) Contrasts between each acceleration level and the 0.2g condition indicated that the significant temporal effects of acceleration on experimental EMG ($p < 0.0011$; $n = 47$) and model predictions ($p < 2\times10^{-4}$; $n = 288$) lie within the initial burst period from regression analyses. **B and D)** Contrasts between each velocity level and the 25 cm/s condition indicated that the significant temporal effects of velocity on experimental EMG ($p < 7\times10^{-4}$; $n = 72$) and model predictions ($p < 2\times10^{-4}$; $n = 290$) lie within the plateau region. Significance levels for contrasts were adjusted from $p < 0.05$ using a Bonferroni correction based on the number of significant wavelet coefficients after wavelet FANOVA.

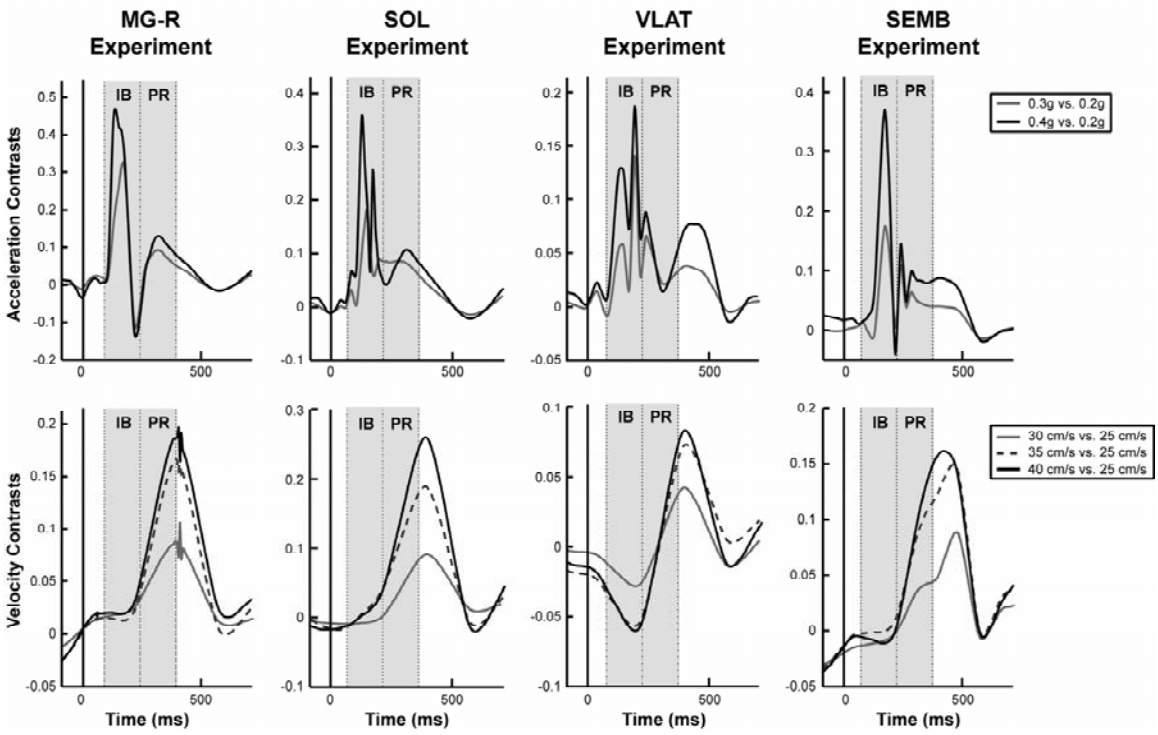

Figure A.2 Robustness of temporal scaling patterns across muscles. The scaling of muscle activity with perturbation characteristics is robust across muscles spanning the entire leg. Shown here are muscles from the triceps surae, quadriceps, and hamstrings. Contrasts between each acceleration level and the 0.2g condition indicate that activity during the initial burst period from regression analyses is sensitive to peak acceleration. Velocity contrasts to the 25 cm/s condition indicate that activity during the plateau region is sensitive to peak velocity. This velocity dependence often extends temporally beyond the window used for regression analysis.

Here, we performed functional ANOVA in the wavelet domain to identify the scaling relationship between muscle activity during the automatic postural response and the acceleration and velocity of the perturbation. By removing the biases of pre-determined time windows, the temporally-overlapping effects of perturbation dynamics were revealed in both experimental data and model predictions. The results of the wavelet FANOVA analysis were consistent with conclusions drawn for traditional statistical tests. More importantly, this analysis demonstrated that the effects of acceleration and velocity often extend well beyond the *a priori* time bins that have been traditionally chosen for

evaluating the scaling of muscle activity with perturbation characteristics. Wavelet FANOVA thereby represents a valuable statistical tool for evaluating temporal patterns of muscle activity, providing a quantitative means to assess the differences between two EMG signals despite large intertrial and intersubject variability.

REFERENCES

Adamovich SV, Archambault PS, Ghafouri M, Levin MF, Poizner H, and Feldman AG. Hand trajectory invariance in reaching movements involving the trunk. *Exp Brain Res* 138: 288-303, 2001.

Alessandrini M, D'Erme G, Bruno E, Napolitano B, and Magrini A. Vestibular compensation: analysis of postural re-arrangement as a control index for unilateral vestibular deficit. *Neuroreport* 14: 1075-1079, 2003.

Alexandrov AV, Frolov AA, and Massion J. Biomechanical analysis of movement strategies in human forward trunk bending. I. Modeling. *Biol Cybern* 84: 425-434, 2001a.

Alexandrov AV, Frolov AA, and Massion J. Biomechanical analysis of movement strategies in human forward trunk bending. II. Experimental study. *Biol Cybern* 84: 435-443, 2001b.

Allum JH, and Carpenter MG. A speedy solution for balance and gait analysis: angular velocity measured at the centre of body mass. *Curr Opin Neurol* 18: 15-21, 2005.

Anderson RN, Minino AM, Fingerhut LA, Warner M, and Heinen MA. Deaths: Injuries, 2001. *Natl Vital Stat Rep* 52: 1-86, 2004.

Bloem BR, van Vugt JP, Beckley DJ, Remler MP, and Roos RA. Habituation of lower leg stretch responses in Parkinson's disease. *Electroencephalogr Clin Neurophysiol* 109: 73-77, 1998.

Blouin JS, Descarreaux M, Belanger-Gravel A, Simoneau M, and Teasdale N. Attenuation of human neck muscle activity following repeated imposed trunk-forward linear acceleration. *Exp Brain Res* 150: 458-464, 2003.

Bortolami SB, DiZio P, Rabin E, and Lackner JR. Analysis of human postural responses to recoverable falls. *Exp Brain Res* 151: 387-404, 2003.

Bosco G, and Poppele RE. Proprioception from a spinocerebellar perspective. *Physiol Rev* 81: 539-568, 2001.

Bosco G, and Poppele RE. Representation of multiple kinematic parameters of the cat hindlimb in spinocerebellar activity. *J Neurophysiol* 78: 1421-1432, 1997.

Bosco G, Rankin AM, and Poppele RE. Representation of passive hindlimb postures in cat spinocerebellar activity. *J Neurophysiol* 76: 715-726, 1996.

Bothner KE, and Jensen JL. How do non-muscular torques contribute to the kinetics of postural recovery following a support surface translation? *J Biomech* 34: 245-250, 2001.

Brown LA, Jensen JL, Korff T, and Woollacott MH. The translating platform paradigm: perturbation displacement waveform alters the postural response. *Gait Posture* 14: 256-263, 2001.

Carpenter MG, Allum JH, and Honegger F. Directional sensitivity of stretch reflexes and balance corrections for normal subjects in the roll and pitch planes. *Exp Brain Res* 129: 93-113, 1999.

Carpenter MG, Thorstensson A, and Cresswell AG. Deceleration affects anticipatory and reactive components of triggered postural responses. *Exp Brain Res* 167: 433-445, 2005.

Chong RK, Horak FB, and Woollacott MH. Time-dependent influence of sensorimotor set on automatic responses in perturbed stance. *Exp Brain Res* 124: 513-519, 1999.

Cohen A, and Kovacevic J. Wavelets: the mathematical background. *Proc IEEE* 84: 514-522, 1996.

Conditt MA, Gandolfo F, and Mussa-Ivaldi FA. The motor system does not learn the dynamics of the arm by rote memorization of past experience. *J Neurophysiol* 78: 554-560, 1997.

Cordo PJ, Flores-Vieira C, Verschueren SM, Inglis JT, and Gurfinkel V. Position sensitivity of human muscle spindles: single afferent and population representations. *J Neurophysiol* 87: 1186-1195, 2002.

Criscimagna-Hemminger SE, Donchin O, Gazzaniga MS, and Shadmehr R. Learned dynamics of reaching movements generalize from dominant to nondominant arm. *J Neurophysiol* 89: 168-176, 2003.

Cunningham HA, and Welch RB. Multiple concurrent visual-motor mappings: implications for models of adaptation. *J Exp Psychol Hum Percept Perform* 20: 987-999, 1994.

Demeritt KM, Shultz SJ, Docherty CL, Gansneder BM, and Perrin DH. Chronic Ankle Instability Does Not Affect Lower Extremity Functional Performance. *J Athl Train* 37: 507-511, 2002.

Dichgans J, and Diener HC. Postural ataxia in late atrophy of the cerebellar anterior lobe and its differential diagnosis. In: *Vestibular and Visual Control of Posture and Locomotor Equilibrium*, edited by Black FO, and Igarashi M. Houston: Karger, 1985, p. 282-289.

Diener HC, Bootz F, Dichgans J, and Bruzek W. Variability of postural "reflexes" in humans. *Exp Brain Res* 52: 423-428, 1983.

Diener HC, Dichgans J, Bootz F, and Bacher M. Early stabilization of human posture after a sudden disturbance: influence of rate and amplitude of displacement. *Exp Brain Res* 56: 126-134, 1984.

Diener HC, Horak FB, and Nashner LM. Influence of stimulus parameters on human postural responses. *J Neurophysiol* 59: 1888-1905, 1988.

Dietz V. Evidence for a load receptor contribution to the control of posture and locomotion. *Neurosci Biobehav Rev* 22: 495-499, 1998.

Dietz V, Gollhofer A, Kleiber M, and Trippel M. Regulation of bipedal stance: dependency on "load" receptors. *Exp Brain Res* 89: 229-231, 1992.

Dietz V, Quintern J, and Sillem M. Stumbling reactions in man: significance of proprioceptive and pre-programmed mechanisms. *J Physiol* 386: 149-163, 1987.

Ethier V, Zee DS, and Shadmehr R. Spontaneous recovery of motor memory during saccade adaptation. *J Neurophysiol* 2008.

Fang J, Agarwal GC, and Shahani BT. Decomposition of multiunit electromyographic signals. *IEEE Trans Biomed Eng* 46: 685-697, 1999.

Fitzpatrick R, Burke D, and Gandevia SC. Loop gain of reflexes controlling human standing measured with the use of postural and vestibular disturbances. *J Neurophysiol* 76: 3994-4008, 1996.

Fitzpatrick RC, Gorman RB, Burke D, and Gandevia SC. Postural proprioceptive reflexes in standing human subjects: bandwidth of response and transmission characteristics. *J Physiol* 458: 69-83, 1992.

Flanagan JR, and Wing AM. The role of internal models in motion planning and control: evidence from grip force adjustments during movements of hand-held loads. *J Neurosci* 17: 1519-1528, 1997.

Forssberg H, and Hirschfeld H. Postural adjustments in sitting humans following external perturbations: muscle activity and kinematics. *Exp Brain Res* 97: 515-527, 1994.

Gandolfo F, Mussa-Ivaldi FA, and Bizzi E. Motor learning by field approximation. *Proc Natl Acad Sci U S A* 93: 3843-3846, 1996.

Gatev P, Thomas S, Kepple T, and Hallett M. Feedforward ankle strategy of balance during quiet stance in adults. *J Physiol* 514 (Pt 3): 915-928, 1999.

Georgopoulos AP, Ashe J, Smyrnis N, and Taira M. The motor cortex and the coding of force. *Science* 256: 1692-1695, 1992.

Georgopoulos AP, Schwartz AB, and Kettner RE. Neuronal population coding of movement direction. *Science* 233: 1416-1419, 1986.

Getz EB, Cooke R, and Lehman SL. Phase transition in force during ramp stretches of skeletal muscle. *Biophys J* 75: 2971-2983, 1998.

Geurts AC, Mulder TW, Nienhuis B, and Rijken RA. Dual-task assessment of reorganization of postural control in persons with lower limb amputation. *Arch Phys Med Rehabil* 72: 1059-1064, 1991.

Gollhofer A, Horstmann GA, Berger W, and Dietz V. Compensation of translational and rotational perturbations in human posture: stabilization of the centre of gravity. *Neurosci Lett* 105: 73-78, 1989.

Goodbody SJ, and Wolpert DM. Temporal and amplitude generalization in motor learning. *J Neurophysiol* 79: 1825-1838, 1998.

Gottlieb GL, Chen CH, and Corcos DM. Relations between joint torque, motion, and electromyographic patterns at the human elbow. *Exp Brain Res* 103: 164-167, 1995.

Gregory JE, Brockett CL, Morgan DL, Whitehead NP, and Proske U. Effect of eccentric muscle contractions on Golgi tendon organ responses to passive and active tension in the cat. *J Physiol* 538: 209-218, 2002.

Hadders-Algra M, Brogren E, and Forssberg H. Ontogeny of postural adjustments during sitting in infancy: variation, selection and modulation. *J Physiol* 493 (Pt 1): 273-288, 1996.

Haftel VK, Bichler EK, Nichols TR, Pinter MJ, and Cope TC. Movement reduces the dynamic response of muscle spindle afferents and motoneuron synaptic potentials in rat. *J Neurophysiol* 91: 2164-2171, 2004.

Hanes DP, and Carpenter RH. Countermanding saccades in humans. *Vision Res* 39: 2777-2791, 1999.

Hansen PD, Woollacott MH, and Debu B. Postural responses to changing task conditions. *Exp Brain Res* 73: 627-636, 1988.

Hart S, and Gabbard C. Examining the stabilising characteristics of footedness. *Laterality* 2: 17-26, 1997.

He JP, Levine WS, and Loeb GE. Feedback gains for correcting small perturbations to standing posture. *IEEE Trans Autom Control* 36: 322-332, 1991.

Hedberg A, Carlberg EB, Forssberg H, and Hadders-Algra M. Development of postural adjustments in sitting position during the first half year of life. *Dev Med Child Neurol* 47: 312-320, 2005.

Hedberg A, Forssberg H, and Hadders-Algra M. Postural adjustments due to external perturbations during sitting in 1-month-old infants: evidence for the innate origin of direction specificity. *Exp Brain Res* 157: 10-17, 2004.

Henatsch HD. [Pro and contra on the acceleration sensitivity of muscle spindles]. *Bull Schweiz Akad Med Wiss* 27: 266-281, 1971.

Horak FB. Adaptation of automatic postural responses. In: *The Acquisition of Motor Behavior in Vertebrates*, edited by Bloedel JR, Ebner TJ, and Wise SP. Cambridge: The MIT Press, 1996, p. 57-85.

Horak FB, and Diener HC. Cerebellar control of postural scaling and central set in stance. *J Neurophysiol* 72: 479-493, 1994.

Horak FB, Diener HC, and Nashner LM. Influence of central set on human postural responses. *J Neurophysiol* 62: 841-853, 1989.

Horak FB, and Hlavacka F. Somatosensory loss increases vestibulospinal sensitivity. *J Neurophysiol* 86: 575-585, 2001.

Horak FB, and Macpherson JM. Postural orientation and equilibrium. In: *Handbook of Physiology, Section 12*. *Exercise: Regulation and Integration of Multiple Systems* New York: American Physiological Society, 1996, p. 255-292.

Horak FB, and Moore SP. The effect of prior leaning on human postural responses. *Gait Posture* 1: 203-210, 1993.

Horak FB, and Nashner LM. Central programming of postural movements: adaptation to altered support-surface configurations. *J Neurophysiol* 55: 1369-1381, 1986.

Houk J, and Simon W. Responses of Golgi tendon organs to forces applied to muscle tendon. *J Neurophysiol* 30: 1466-1481, 1967.

Hund-Georgiadis M, and von Cramon DY. Motor-learning-related changes in piano players and non-musicians revealed by functional magnetic-resonance signals. *Exp Brain Res* 125: 417-425, 1999.

Hwang EJ, and Shadmehr R. Internal models of limb dynamics and the encoding of limb state. *J Neural Eng* 2: S266-278, 2005.

Inglis JT, and Macpherson JM. Bilateral labyrinthectomy in the cat: effects on the postural response to translation. *J Neurophysiol* 73: 1181-1191, 1995.

Jansen JK, and Matthews PB. The central control of the dynamic response of muscle spindle receptors. *J Physiol* 161: 357-378, 1962.

Jeka JJ, and Lackner JR. Fingertip contact influences human postural control. *Exp Brain Res* 100: 495-502, 1994.

Jo S, and Massaquoi SG. A model of cerebellum stabilized and scheduled hybrid long-loop control of upright balance. *Biol Cybern* 91: 188-202, 2004.

Kagerer FA, Contreras-Vidal JL, and Stelmach GE. Adaptation to gradual as compared with sudden visuo-motor distortions. *Exp Brain Res* 115: 557-561, 1997.

Keshner EA. Head-trunk coordination during linear anterior-posterior translations. *J Neurophysiol* 89: 1891-1901, 2003.

Keshner EA, Allum JH, and Pfaltz CR. Postural coactivation and adaptation in the sway stabilizing responses of normals and patients with bilateral vestibular deficit. *Exp Brain Res* 69: 77-92, 1987.

Keshner EA, Woollacott MH, and Debu B. Neck, trunk and limb muscle responses during postural perturbations in humans. *Exp Brain Res* 71: 455-466, 1988.

Kiemel T, Oie KS, and Jeka JJ. Multisensory fusion and the stochastic structure of postural sway. *Biol Cybern* 87: 262-277, 2002.

Krishnamoorthy V, Latash ML, Scholz JP, and Zatsiorsky VM. Muscle synergies during shifts of the center of pressure by standing persons. *Exp Brain Res* 152: 281-292, 2003.

Kumar DK, Pah ND, and Bradley A. Wavelet analysis of surface electromyography to determine muscle fatigue. *IEEE Trans Neural Syst Rehabil Eng* 11: 400-406, 2003.

Kuo AD. An optimal control model for analyzing human postural balance. *IEEE Trans Biomed Eng* 42: 87-101, 1995.

Lackner JR, and Dizio P. Rapid adaptation to Coriolis force perturbations of arm trajectory. *J Neurophysiol* 72: 299-313, 1994.

Lappin JS, and Eriksen CW. Use of a delayed signal to stop a visual reaction-time response. *J Exp Psychol* 72: 803-811, 1966.

Lemay MA, and Grill WM. Modularity of motor output evoked by intraspinal microstimulation in cats. *J Neurophysiol* 91: 502-514, 2004.

Lennerstrand G, and Thoden U. Dynamic analysis of muscle spindle endings in the cat using length changes of different length-time relations. *Acta Physiol Scand* 73: 234-250, 1968.

Lisberger SG. The neural basis for learning of simple motor skills. *Science* 242: 728-735, 1988.

Lockhart DB, and Ting LH. Optimal sensorimotor transformations for balance. *Nat Neurosci* 10: 1329-1336, 2007.

Macpherson JM. Strategies that simplify the control of quadrupedal stance. II. Electromyographic activity. *J Neurophysiol* 60: 218-231, 1988.

Macpherson JM, Horak FB, Dunbar DC, and Dow RS. Stance dependence of automatic postural adjustments in humans. *Exp Brain Res* 78: 557-566, 1989.

Macpherson JM, Lywood DW, and Van Eyken A. A system for the analysis of posture and stance in quadrupeds. *J Neurosci Methods* 20: 73-82, 1987.

Maganaris CN, Baltzopoulos V, and Sargeant AJ. Changes in the tibialis anterior tendon moment arm from rest to maximum isometric dorsiflexion: in vivo observations in man. *Clin Biomech (Bristol, Avon)* 14: 661-666, 1999.

Maki BE, and Ostrovski G. Do postural responses to transient and continuous perturbations show similar vision and amplitude dependence? *J Biomech* 26: 1181-1190, 1993a.

Maki BE, and Ostrovski G. Scaling of postural responses to transient and continuous perturbations. *Gait Posture* 1: 93-104, 1993b.

McIlroy WE, and Maki BE. The 'deceleration response' to transient perturbation of upright stance. *Neurosci Lett* 175: 13-16, 1994.

Miall RC, Weir DJ, Wolpert DM, and Stein JF. Is the cerebellum a Smith Predictor? *J Mot Behav* 25: 203-216, 1993.

Morasso PG, Baratto L, Capra R, and Spada G. Internal models in the control of posture. *Neural Netw* 12: 1173-1180, 1999.

Morton SM, Lang CE, and Bastian AJ. Inter- and intra-limb generalization of adaptation during catching. *Exp Brain Res* 141: 438-445, 2001.

Mouchnino L, Mille ML, Cincera M, Bardot A, Delarque A, Pedotti A, and Massion J. Postural reorganization of weight-shifting in below-knee amputees during leg raising. *Exp Brain Res* 121: 205-214, 1998.

Myer GD, Paterno MV, Ford KR, Quatman CE, and Hewett TE. Rehabilitation after anterior cruciate ligament reconstruction: criteria-based progression through the return-to-sport phase. *J Orthop Sports Phys Ther* 36: 385-402, 2006.

Nardone A, Corra T, and Schieppati M. Different activations of the soleus and gastrocnemii muscles in response to various types of stance perturbation in man. *Exp Brain Res* 80: 323-332, 1990.

Nashner L, and Berthoz A. Visual contribution to rapid motor responses during postural control. *Brain Res* 150: 403-407, 1978.

Nashner LM. Adapting reflexes controlling the human posture. *Exp Brain Res* 26: 59-72, 1976.

Nashner LM. Fixed patterns of rapid postural responses among leg muscles during stance. *Exp Brain Res* 30: 13-24, 1977.

Ostlund N, Yu J, and Karlsson JS. Adaptive spatio-temporal filtering of multichannel surface EMG signals. *Med Biol Eng Comput* 44: 209-215, 2006.

Park S, Horak FB, and Kuo AD. Effect of initial lean on scaling of postural feedback responses. *On the Convergence of Bio-Information-, Environmental-, Energy-, Space- and Nano-Technologies, Pts 1 and 2* 277-279: 142-147, 2005.

Park S, Horak FB, and Kuo AD. Postural feedback responses scale with biomechanical constraints in human standing. *Exp Brain Res* 154: 417-427, 2004.

Peterka RJ. Postural control model interpretation of stabilogram diffusion analysis. *Biol Cybern* 82: 335-343, 2000.

Peterka RJ. Sensorimotor integration in human postural control. *J Neurophysiol* 88: 1097-1118, 2002.

Poppele RE, Bosco G, and Rankin AM. Independent representations of limb axis length and orientation in spinocerebellar response components. *J Neurophysiol* 87: 409-422, 2002.

Pratt CA, Fung J, and Macpherson JM. Stance control in the chronic spinal cat. *J Neurophysiol* 71: 1981-1985, 1994.

Qu X, Nussbaum MA, and Madigan ML. A balance control model of quiet upright stance based on an optimal control strategy. *J Biomech* 40: 3590-3597, 2007.

Ren X, Hu X, Wang Z, and Yan Z. MUAP extraction and classification based on wavelet transform and ICA for EMG decomposition. *Med Biol Eng Comput* 44: 371-382, 2006.

Runge CF, Shupert CL, Horak FB, and Zajac FE. Ankle and hip postural strategies defined by joint torques. *Gait Posture* 10: 161-170, 1999.

Runge CF, Zajac FE, III, Allum JH, Risher DW, Bryson AE, Jr., and Honegger F. Estimating net joint torques from kinesiological data using optimal linear system theory. *IEEE Trans Biomed Eng* 42: 1158-1164, 1995.

Sainburg RL, Ghez C, and Kalakanis D. Intersegmental dynamics are controlled by sequential anticipatory, error correction, and postural mechanisms. *J Neurophysiol* 81: 1045-1056, 1999.

Sainburg RL, and Kalakanis D. Differences in control of limb dynamics during dominant and nondominant arm reaching. *J Neurophysiol* 83: 2661-2675, 2000.

Schafer SS. The acceleration response of a primary muscle-spindle ending to ramp stretch of the extrafusal muscle. *Experientia* 23: 1026-1027, 1967.

Schafer SS, and Kijewski S. The dependency of the acceleration response of primary muscle spindle endings on the mechanical properties of the muscle. *Pflugers Arch* 350: 101-122, 1974.

Scheidt RA, Reinkensmeyer DJ, Conditt MA, Rymer WZ, and Mussa-Ivaldi FA. Persistence of motor adaptation during constrained, multi-joint, arm movements. *J Neurophysiol* 84: 853-862, 2000.

Schwabe A, Drepper J, Maschke M, Diener HC, and Timmann D. The role of the human cerebellum in short- and long-term habituation of postural responses. *Gait Posture* 19: 16-23, 2004.

Scott SH, and Kalaska JF. Reaching movements with similar hand paths but different arm orientations. I. Activity of individual cells in motor cortex. *J Neurophysiol* 77: 826-852, 1997.

Scrivens JE, Deweerth SP, and Ting LH. A robotic device for understanding neuromechanical interactions during standing balance control. *Bioinspir Biomim* 3: 26002, 2008.

Shadmehr R, and Moussavi ZM. Spatial generalization from learning dynamics of reaching movements. *J Neurosci* 20: 7807-7815, 2000.

Shadmehr R, and Mussa-Ivaldi FA. Adaptive representation of dynamics during learning of a motor task. *J Neurosci* 14: 3208-3224, 1994.

Shinha T, and Maki BE. Effect of forward lean on postural ankle dynamics. *IEEE Trans Rehab Eng* 4: 348-359, 1996.

Shumway-Cook A, Woollacott M, Kerns KA, and Baldwin M. The effects of two types of cognitive tasks on postural stability in older adults with and without a history of falls. *J Gerontol A Biol Sci Med Sci* 52: M232-240, 1997.

Shumway-Cook A, and Woollacott MH. Attentional demands and postural control: the effect of sensory context. *J Gerontol A Biol Sci Med Sci* 55: M10-16, 2000.

Siegmund GP. Gradation of neck muscle responses and head/neck kinematics to acceleration and speed change in rear-end collisions. *Stapp Car Crash Journal* 48: 419-430, 2004.

Siegmund GP, Sanderson DJ, and Inglis JT. The effect of perturbation acceleration and advance warning on the neck postural responses of seated subjects. *Exp Brain Res* 144: 314-321, 2002.

Soechting JF, and Lacquaniti F. Quantitative evaluation of the electromyographic responses to multidirectional load perturbations of the human arm. *J Neurophysiol* 59: 1296-1313, 1988.

Sparto PJ, Parnianpour M, Barria EA, and Jagadeesh JM. Wavelet and short-time Fourier transform analysis of electromyography for detection of back muscle fatigue. *IEEE Trans Rehabil Eng* 8: 433-436, 2000.

Stevens JA, Corso PS, Finkelstein EA, and Miller TR. The costs of fatal and non-fatal falls among older adults. *Inj Prev* 12: 290-295, 2006.

Surendran S, Welch TDJ, and Ting LH. Stability differences in right versus left-legged stance. In: *South East Biomechanics Conference*. Durham, NC: 2007.

Szturm T, and Fallang B. Effects of varying acceleration of platform translation and toes-up rotations on the pattern and magnitude of balance reactions in humans. *J Vestib Res* 8: 381-397, 1998.

Takahashi CD, Scheidt RA, and Reinkensmeyer DJ. Impedance control and internal model formation when reaching in a randomly varying dynamical environment. *J Neurophysiol* 86: 1047-1051, 2001.

Thoroughman KA, and Shadmehr R. Electromyographic correlates of learning an internal model of reaching movements. *J Neurosci* 19: 8573-8588, 1999.

Timmann D, and Horak FB. Prediction and set-dependent scaling of early postural responses in cerebellar patients. *Brain* 120 (Pt 2): 327-337, 1997.

Ting LH. Dimensional reduction in sensorimotor systems: a framework for understanding muscle coordination of posture. In: *Computational Neuroscience:*

Theoretical Insights into Brain Function, edited by Cisek P, Drew T, and Kalaska JF. *Progress in Brain Research* 165. Amsterdam: Elsevier, 2007, p. 301-325.

Ting LH, and Macpherson JM. A limited set of muscle synergies for force control during a postural task. *J Neurophysiol* 93: 609-613, 2005.

Ting LH, and Macpherson JM. Ratio of shear to load ground-reaction force may underlie the directional tuning of the automatic postural response to rotation and translation. *J Neurophysiol* 92: 808-823, 2004.

Todorov E. Optimality principles in sensorimotor control. *Nat Neurosci* 7: 907-915, 2004.

Tokuno CD, Carpenter MG, Thorstensson A, and Cresswell AG. The influence of natural body sway on neuromuscular responses to an unpredictable surface translation. *Exp Brain Res* 2006.

Torres-Oviedo G, Macpherson JM, and Ting LH. Muscle synergy organization is robust across a variety of postural perturbations. *J Neurophysiol* 96: 1530-1546, 2006.

Torres-Oviedo G, and Ting LH. Muscle synergies characterizing human postural responses. *J Neurophysiol* 98: 2144-2156, 2007.

Tseng Y, Scholz JP, and Schoner G. Goal-equivalent joint coordination in pointing: affect of vision and arm dominance. *Motor Control* 6: 183-207, 2002.

Unser M, and Aldroubi A. A review of wavelets in biomedical applications. *Proceedings of the Ieee* 84: 626-638, 1996.

van Antwerp KW, Burkholder TJ, and Ting LH. Inter-joint coupling effects on muscle contributions to endpoint force and acceleration in a musculoskeletal model of the cat hindlimb. *J Biomech* 40: 3570-3679, 2007.

van der Fits IB, Otten E, Klip AW, van Eykern LA, and Hadders-Algra M. The development of postural adjustments during reaching in 6- to 18-month-old infants. Evidence for two transitions. *Exp Brain Res* 126: 517-528, 1999.

van der Heide JC, Otten B, van Eykern LA, and Hadders-Algra M. Development of postural adjustments during reaching in sitting children. *Exp Brain Res* 151: 32-45, 2003.

van der Kooij H, Jacobs R, Koopman B, and Grootenboer H. A multisensory integration model of human stance control. *Biol Cybern* 80: 299-308, 1999.

Visser JE, and Bloem BR. Role of the basal ganglia in balance control. *Neural Plast* 12: 161-174; discussion 263-172, 2005.

Wakeling JM, Von Tscharner V, Nigg BM, and Stergiou P. Muscle activity in the leg is tuned in response to ground reaction forces. *J Appl Physiol* 91: 1307-1317, 2001.

Welch TDJ, and Ting LH. A feedback model explains the differential scaling of human postural responses to perturbation acceleration and velocity. *J Neurophysiol* in prep.

Welch TDJ, and Ting LH. A feedback model predicts muscle activity during human postural responses to support surface translations. *J Neurophysiol* 99: 1032-1038, 2008.

Wilson VJ, and Melvill Jones G. *Mammalian Vestibular Physiology*. New York: Plenum Press, 1979.

Winter DA. *Biomechanics and Motor Control of Human Movement*. Hoboken: John Wiley & Sons, 2005.

Woollacott MH, and Shumway-Cook A. Attention and the control of posture and gait: a review of an emerging area of research. *Gait Posture* 16: 1-14, 2002.

Zajac FE, and Gordon ME. Determining muscle's force and action in multi-articular movement. *Exerc Sport Sci Rev* 17: 187-230, 1989.

VITA

TORRENCE D.J. WELCH

Torrence David Jesse Welch was born to Carol and Carlyle Welch in Baton Rouge, Louisiana. He attended Catholic High School in Baton Rouge, Louisiana, graduating with honors in 1998. In 2003, he received B.S.E. and M.S.E. degrees in Biomedical Engineering from Tulane University (New Orleans, Louisiana) with the support of National Achievement and Tulane Deans Honor scholarships. For his Masters work, he validated a novel method for diagnosing osteoarthritis using ultrasound, before pursuing a doctorate in Biomedical Engineering in the joint PhD program at Georgia Institute of Technology and Emory University School of Medicine. During his PhD studies, Mr. Welch was recognized with a minority grant supplement from the National Institutes of Health and a National Science Foundation FACES fellowship. Upon completion of the PhD degree, he will work as an engineer for Exponent in Phoenix, AZ where he will provide expert witness testimony in personal injury and product liability cases. An avid lover of music, Mr. Welch plays thirteen musical instruments, including the entire woodwind family, and actively pursued performance opportunities in several music ensembles within the Atlanta community.